Expression and functional analysis of progranulin (GRN) in glial brain tumors

Inaugural-Dissertation

zur Erlangung des Doktorgrades
der mathematisch-naturwissenschaftlichen Fakultät
der Heinrich-Heine-Universität Düsseldorf

vorgelegt von

Julia Neß
aus Mainz

Düsseldorf, Mai 2012

TABLE OF CONTENTS

1 INTRODUCTION

1.1 Progranulin

Progranulin (GRN) is a secreted growth factor with functions in numerous physiological and pathological conditions. Synonymous names for this protein are granulin-epithelin precursor (Bhandari *et al.* 1996), proepithelin (Plowman *et al.* 1992), PC-cell-derived growth factor (Zhou *et al.* 1993), acrogranin (Baba *et al.* 1993), and epithelial transforming growth factor (Parnell *et al.* 1992). The human gene *GRN* is located on chromosome 17q21.32 and is translated into a 593 amino acid protein with a molecular weight of 68.5 kDa, which is subsequently highly glycosylated and secreted as a ~90 kDa protein (He & Bateman 2003). The GRN protein consists of 7.5 repeats of a 12-cysteine motif called granulins or epithelin domains, which are separated by linker regions (Fig. 1) (Bateman *et al.* 1990, Bhandari & Bateman 1992). Each granulin domain consists of four ß-hairpins stacked in a left-handed helix formation, with six disulfide bridges forming a central rod through the granulin fold and giving it a globular structure (He & Bateman 2003, Hrabal *et al.* 1996, Tolkatchev *et al.* 2008).

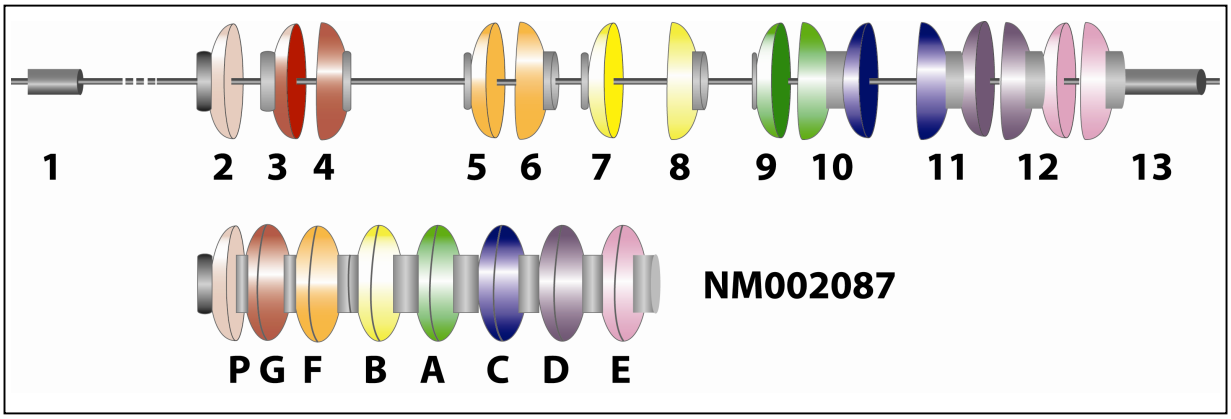

Figure 1: Structural organization of the GRN gene (top) and protein (bottom). The protein-coding region of the gene consists of 13 exons with intronic splice sites being positioned approximately in the middle of the granulin domains. N-terminal and C-terminal halves are represented by opposite halves of the disk. At the protein level, 7.5 repeats of the granulin motif separated by linker regions are present, in the order P-G-F-B-A-C-D-E, and granulin P being the half repeat (Cruts & Van Broeckhoven 2008).

The full-length GRN protein can be proteolytically cleaved by elastase and other proteases to release peptides of approximately 6 kDa corresponding to the individual granulin domains, which are believed to possess independent and possibly opposing biological activities to the full-length protein (Shoyab *et al.* 1990, Tolkatchev *et al.* 2008, Zhu *et al.* 2002). GRN is predominantly expressed in highly proliferative epithelia such as the skin, the gastrointestinal tract, and the reproductive tracts. Prominent expression has also been demonstrated in immunological tissues as the spleen and lymph nodes, and in cells of the innate immune

system. In the central nervous system, GRN expression has been detected in neurons of the neocortex, hippocampus, and hypothalamus, as well as in Purkinje cells of the cerebellum and in motor neurons. In addition, microglia representing the immune cells of the central nervous system displayed high expression of GRN (Daniel *et al.* 2000, Matsuwaki *et al.* 2011, Moisse *et al.* 2009, Petkau *et al.* 2010, Toh *et al.* 2011, Ryan *et al.* 2009).

1.2 Functions of progranulin

GRN has been shown to play a role in early development, tissue repair, inflammatory processes and tumorigenesis (Bateman & Bennett 2009).

GRN is expressed in preimplantation embryos with highest expression in the trophectoderm of blastocysts, the first lineage of epithelial cells that eventually gives rise to the fetal part of the placenta. In cultured eight-cell embryos, the onset of cavitation, rate of blastocoel expansion and growth of trophectoderm cells could be stimulated by exogenously added GRN, while depletion of endogenously secreted GRN with antisera resulted in dramatically delayed blastocyst formation (Diaz-Cueto *et al.* 2000). Moreover, a role for GRN in sexual determination during embryonic development has been reported (Suzuki & Nishiahara 2002). Embryonic GRN expression has been described in the epidermis, the developing brain and spinal cord, and the microvasculature (Daniel *et al.* 2003).

In adult tissues, GRN appears to play a role in the healing response to injury. In skin wounds, infiltrating inflammatory cells express GRN at high levels, and the early event of re-establishing the epidermal layer is accomplished by keratinocytes that also express GRN. Dermal fibroblasts and endothelial cells that proliferate and migrate into the wound to form the granulation tissue usually do not express GRN, but rapidly and strongly induce expression after the skin is damaged. Administering GRN to cutaneous wounds in rats resulted in increased accumulation of fibroblasts and blood vessels in the wound and prolonged inflammatory infiltration, particularly with neutrophils. *In vitro*, GRN directly promoted the proliferation of dermal fibroblasts and endothelial cells and their migration through type I collagen, and stimulated tubule formation of endothelial cells on matrigel suggesting direct angiogenic actions. However, a chemotactic effect on neutrophils has not been demonstrated. Furthermore, GRN accelerated wound closure in mice deficient for secretory leukocyte protease inhibitor (SLPI) that showed impaired healing capacity. SLPI is an inhibitor of proteases like neutrophil elastase and thus protects GRN from being digested into the smaller granulin peptides (He & Bateman 2003).

GRN has also been proposed to be a regulator of the innate immune response. The formation of antigen-antibody complexes (immune complexes, ICs) induces infiltration and

subsequent activation of neutrophils, which results in the generation of reactive oxygen species (ROS) and the release of intracellularly stored proteases, and leads to tissue damage and inflammation. In mice deficient for the two proteases proteinase 3 (PR3) and neutrophil elastase (NE), which both can degrade GRN into the granulin peptides, the response of isolated neutrophils to ICs was diminished. Interestingly, this defect was accompanied by the accumulation of full-length GRN, and exogenously administered GRN was also able to reduce ROS production of IC-activated neutrophils. Thus, the removal of GRN by proteolytic degradation into granulin peptides seems to be an important factor in the process of neutrophilic inflammation (Kessenbrock *et al.* 2008). Furthermore, GRN was shown to reduce the activation of neutrophils by the inflammatory cytokine tumor necrosis factor α (TNFα). Most recently, a direct interaction of GRN with TNF receptors has been demonstrated. In theses studies, GRN functioned as an antagonist of TNF receptors and was able to potently inhibit experimentally induced inflammatory arthritis in mouse models (Kessenbrock *et al.* 2008, Tang *et al.* 2011, Zhu *et al.* 2002).

Comparable to peripheral wounds, in the central nervous system (CNS) basal levels of GRN expression were upregulated in microglia cells upon activation in response to physical trauma like axotomy (Moisse *et al.* 2009) or spinal contusion (Naphade *et al.* 2010). In addition, GRN has recently been shown to be a chemoattractant for microglia and to increase their endocytic activity (Pickford *et al.* 2011). Elevated GRN mRNA levels have also been described in a number of neurodegenerative disorders that are associated with microglia activation including lysosomal storage disorders mucopolysaccharidoses type I and IIIB, amyotrophic lateral sclerosis, Alzheimer's disease, and in virally-induced neuroinflammation (Eriksen & Mackenzie 2008). In 2006, mutations in the GRN gene have been identified as the cause of chromosome 17-linked frontotemporal dementia with ubiquitin-positive inclusions (FTLD-U) (Baker *et al.* 2006, Cruts *et al.* 2006). These mutations inactivate one gene copy leading to haploinsufficiency. It has been hypothesized that dysregulation of neuroinflammation as a consequence of the partial loss of GRN plays a role in the course of this disease (Toh *et al.* 2011).

Despite its described roles in early development, GRN proved to be dispensable during embryogenesis of the mouse as GRN-deficient mice are healthy and fertile, and GRN-deficient pups are born at the expected Mendelian frequency from hemizygous parents (Kayasuga *et al.* 2007, Yin *et al.* 2010a). In contrast, the phenotype of the GRN-deficient mice supports the hypothesis that GRN is an important factor in the modulation of inflammatory processes during adulthood. GRN-deficient mice responded to bacterial infection with prolonged and exaggerated inflammation. In isolated macrophages, the absence of GRN led to overproduction of pro-inflammatory cytokines like TNFα and reduced expression of anti-inflammatory interleukin-10 (IL10) after stimulation with microbial products.

In addition, GRN-deficient macrophages and microglia became more cytotoxic towards hippocampal neurons in response to inflammatory stimuli as compared to wild type myeloid cells (Yin *et al.* 2010a). With age, GRN-deficient mice displayed excessive activation of astrocytes and microglia in the brain, and tissue vacuolation, focal neuronal loss in the hippocampus and behavioural deficits have been reported (Ahmed *et al.* 2010, Yin *et al.* 2010a, Yin *et al.* 2010b).

1.3 Progranulin in cancer

A growth-promoting activity of full-length GRN was initially identified in teratoma-derived cell lines. A highly tumorigenic cell line was selected by *in vivo* passaging of poorly tumorigenic teratoma cells, and it was found that the enhanced malignancy was accompanied by elevated levels of secreted GRN. In turn, downregulation of GRN expression by antisense cDNA transfection dramatically inhibited tumorigenicity of this cell line (Zhou *et al.* 1993, Zhang & Serrero 1998). Similarly, the adrenal small cell carcinoma cell line SW-13, which has only a low tumor-forming capacity, formed large tumors in nude mice when engineered to overexpress GRN (Fig. 2) (He & Bateman 1999).

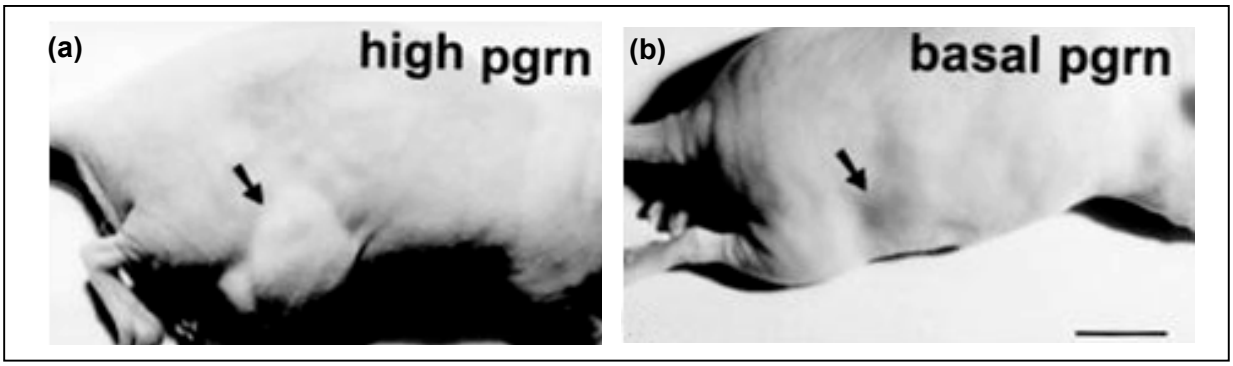

Figure 2: Tumor-promoting properties of GRN. SW-13 cells were engineered to overexpress GRN and injected subcutaneously into nude mice. Overexpressing cells **(a)** formed much larger tumors within 8 weeks as compared to control cells **(b)**. Arrows indicate the injection sites (He & Bateman 2003).

The GRN gene was found to be expressed by numerous primary cancers and derived cell lines. In particular, GRN expression has been linked to many epithelial cancers including carcinomas of the breast and ovaries, endometrium, liver, kidney, prostate and bladder, but also non-epithelial tumors such as leiomyosarcomas, multiple myelomas, mesotheliomas, and brain tumors including intracranial meningiomas and gliomas (Toh *et al.* 2011).

In a study that compared the transcriptome of 24 breast cancer cell lines against non-transformed mammary epithelia, GRN mRNA was overrepresented in the tumor cell lines

(Leerkes *et al.* 2002). A different study analyzed a pooled cDNA library, enriched with genes that encode membrane and secreted proteins, from four breast cancer cell lines, one prostate adenocarcinoma cell line, and one immortalized mammary epithelial cell line. The GRN mRNA was among the 15 most abundant transcripts after substraction with pooled RNA from normal brain, liver, lung, kidney, and skeletal muscle libraries to exclude ubiquitously expressed genes (Egland *et al.* 2003). Increased levels of GRN mRNA were found in human breast carcinoma cell lines compared to immortalized non-tumorigenic mammary epithelial cells, and increased expression levels correlated with increased tumorigenicity of the cell lines. Conversely, downregulation of GRN expression in breast cancer cell lines through antisense cDNA transfection resulted in a reduced proliferation rate, impaired anchorage-independent colony formation in soft agar, and lower tumorigenicity *in vivo* (Lu & Serrero 2000). Similarly, a study comparing cDNA libraries derived from micro-dissected low malignant potential (LMP) and invasive ovarian tumors showed that GRN was abundantly expressed in invasive ovarian cancer, whereas expression was not detected in the LMP libraries (Jones *et al.* 2003). Later studies also demonstrated a correlation of GRN expression with patient survival (Cuevas-Antonio *et al.* 2010), and a correlation with malignant phenotype of ovarian cancer cell lines (Liu *et al.* 2007). GRN was also found to be overexpressed in hepatocellular carcinomas (HCC) compared to non-tumor liver tissue with only minimal GRN expression, as demonstrated by cDNA microarray analysis, quantitative RT-PCR and immunohistochemistry (Cheung *et al.* 2004). Again, strong GRN expression was associated with larger and more aggressive tumors, and downregulation of GRN protein levels in tumor cell lines resulted in decreased cell proliferation, invasive ability, anchorage-independent growth in soft agar, and tumorigenicity in nude mice (Cheung *et al.* 2004). Furthermore, a systemically administrated anti-GRN antibody was able to dose-dependently inhibit growth of established HCC xenografts by reduction of tumor cell proliferation and tumor angiogenesis (Ho *et al.* 2008). In prostate cancer, a meta-analysis across six independent microarray studies revealed significantly upregulated GRN mRNA levels in primary prostate cancers compared to non-neoplastic samples, although there was no correlation between tumor stages and expression levels. In addition, prostate cancer cell lines responded to exogenous treatment with recombinant human GRN with enhanced migration, invasion and anchorage-independent growth, whereas depletion of endogenous GRN by siRNA transfection had the opposite effect (Monami *et al.* 2009).

GRN overexpression is not limited to epithelial cancers. A cDNA microarray analysis of uterine leiomyosarcoma and normal uterine smooth muscle cells with subsequent immunohistochemical verification revealed that the intensity of GRN overexpression correlated with histological grade and poor prognosis in this type of tumor. However, overexpression of GRN in *hTERT (*human telomerase reverse transcriptase)-immortalized

uterine smooth muscle cells had no effect on cell proliferation (Matsumura *et al.* 2006), although a proliferative effect of recombinant GRN had previously been shown for one of two examined leiomyosarcoma cell lines (Daniel *et al.* 2000). Whereas overexpression of GRN alone was not sufficient to transform the immortalized uterine smooth muscle cells, co-expression with *SV40 early region (SV40ER)* resulted in more extensive anchorage-independent growth and tumor formation in nude mice compared to *SV40ER* expression alone (Matsumura *et al.* 2006). For the clonal B-cell neoplasm multiple myeloma (MM), a study of 13 human bone marrow biopsy samples found GRN expression to be highly correlated with the presence of this disease. Exogenous GRN administration increased proliferation and survival of two MM cell lines approximately 2.5-fold, whereas anti-GRN neutralizing antibodies inhibited cell growth by 50% (Wang *et al.* 2003). In intracranial meningiomas, which mostly show benign pathology, GRN expression was detected in 29 of 79 samples by RT-PCR, and GRN expression correlated with increased tumor size and peritumoral brain edema volume (Kim *et al.* 2010). Finally, elevated expression of GRN was also identified in human gliomas. Higher expression levels (3-30 fold) were detected by cDNA microarrays in eight different glioma samples compared to normal brain tissue, and Northern blot analysis confirmed GRN expression in 18 of 21 gliomas but did not detect expression in 3 normal brain samples. An antibody raised against the 55 amino acid peptide granulin D dose-dependently inhibited growth of three early passage primary human glioblastoma cultures. Furthermore, recombinant granulin D modestly increased growth of glioblastoma cells in culture by 120-150% at high doses, and stimulated proliferation of primary rat astrocytes up to 300% (Liau *et al.* 2000). Overexpression of GRN in glioblastomas has been independently confirmed by cDNA microarray analysis (Markert *et al.* 2001). Most recently, a study reported a positive correlation between GRN overexpression and the pathological grading of the tumors in a series of 210 astrocytic gliomas analyzed by immunohistochemistry. This correlation was further supported by Western blot analysis of 35 astrocytoma samples. In addition, high GRN expression levels correlated with decreased survival times of glioblastoma patients in this study (Wang *et al.* 2011). In conclusion, GRN is overexpressed in many different malignancies and likely an important regulator of tumorigenesis.

1.4 Progranulin receptors and signal transduction

The intracellular signaling pathways that are stimulated by GRN are poorly understood but appear to involve typical growth factor signal transduction pathways. Primarily, the ERK1/2 (extracellular signal-regulated kinase) and PI3K (phosphoinositide 3-kinase) pathways were

activated in response to GRN in different cell types. In 3T3 mouse embryo fibroblasts deficient for the insulin-like growth factor I receptor (IGF-IR), both ERK and AKT (v-akt murine thymoma viral oncogene homolog 1) were activated by GRN treatment. So far, GRN is the only identified growth factor that can overcome the inability of these cells to proliferate in serum-free medium, possibly because of a more prolonged activation of these signaling pathways as compared to other growth factors (Zanocco-Marani *et al.* 1999, He & Bateman 2003). Similarly, both pathways have been found to be activated in response to GRN in the SW-13 adenocarcinoma cell line (He *et al.* 2002), multiple myeloma cell lines RPMI 8226 and ARP-1 (Wang *et al.* 2003), in the Hep3B hepatoma cell line (Ho *et al.* 2008), and in DU145 prostate cancer cells (Monami *et al.* 2009). Studies in MCF-7 breast cancer and NIH-OVCAR-3 ovarian cancer cell lines also reported phosphorylation of ERK after GRN stimulation, but did not evaluate PI3K signaling (Cuevas-Antonio *et al.* 2010, Lu & Serrero 2001). In contrast, in 5637 bladder cancer cells, no AKT phosphorylation was detected, whereas rapid ERK activation was demonstrated. In addition, the adaptor protein paxillin was found to be activated and to associate with focal adhesion kinase (FAK) and activated ERK upon GRN stimulation, thereby linking GRN with integrin signaling (Monami *et al.* 2006). Activation of FAK signal transduction has also been shown for SW-13 cells (He *et al.* 2002). In neurons derived from GRN-deficient mice, lower basal levels of phosphorylated AKT have been reported compared to wild type neurons, whereas there was no difference in levels of phosphorylated ERK. Stimulation of the GRN-deficient neurons with recombinant GRN resulted only in phosphorylation of AKT but not ERK, whereas both proteins were activated in GRN-deficient embryonic fibroblasts (Kleinberger *et al.* 2010). In contrast, a study in cortical neurons from wild type mice confirmed increased phosphorylation of AKT and its substrate glycogen synthase kinase-3β (GSK-3β) after stimulation with GRN, but also reported increased phosphorylation of ERK (Gao *et al.* 2010). PI3K dependent phosphorylation of GSK-3β in response to GRN stimulation has also been shown in neural progenitor cells (NPCs) from GRN-deficient mice but not in NPCs from wild type mice, and in this study phosphorylation of ERK was not detected in either cell type (Nedachi *et al.* 2011).

Recently, two different membrane proteins that bind GRN and could function as its receptor have been identified: Sortilin (SORT1) and tumor necrosis factor receptor (TNFR). SORT1 is a member of the vacuole protein sorting 10 protein (VPS10P)-domain receptor family that have originally been identified as regulators of lysosomal enzyme trafficking. It is expressed largely in neurons and has previously been shown to bind other growth factors like neurotensin and precursor forms of neutrophins like NGF (nerve growth factor) or BDNF (brain-derived neurotrophic factor) (Willnow *et al.* 2008, Bartkowska *et al.* 2011). A recent study demonstrated that SORT1 also binds GRN and promotes its endocytosis and delivery to lysosomes. This mechanism appears to regulate secreted levels of GRN, but functional

consequences of the GRN-SORT1 interaction in terms of signal transduction have not been evaluated yet (Hu *et al.* 2010, Carrasquillo *et al.* 2011). Another group recently reported that GRN binds directly to tumor necrosis factor receptors (TNFR). This interaction appears to prevent binding of the original ligand TNF-α to the TNFRs, which leads to reduced inflammatory signaling. This TNFα-antagonizing action of GRN was demonstrated to prevent or reverse inflammatory arthritis in multiple mouse models, and could also prove relevant for neuroinflammation in the central nervous system (Tang *et al.* 2011, Toh *et al.* 2011).

1.5 Brain tumors

Primary tumors of the central nervous system account for approximately 2-3% of all human cancers. The prevalence in the Western world has been estimated to about 69 patients per 100,000 individuals, with an incidence of approximately 15 new cases per 100,000 individuals per year (Riemenschneider & Reifenberger 2009b). Brain tumors are a heterogeneous group of benign and malignant neoplasms that are categorized in the World Health Organization (WHO) classification of tumors of the central nervous system (Louis *et al.* 2007). The most common brain tumors (70%) are tumors of glial origin, collectively referred to as gliomas (Riemenschneider & Reifenberger 2009a). In children below the age of 15 years, primary tumors of the CNS, most commonly pilocytic astrocytoma, medulloblastoma and ependymoma, comprise approximately 20% of cancers, making them the second most common form of childhood cancer after leukemia (Reifenberger & Collins 2004).

1.6 Gliomas

Gliomas are named according to the specific cell type they histologically resemble. The WHO classification of tumors of the central nervous system divides four main groups: astrocytic tumors, oligodendrocytic tumors, oligoastrocytic tumors and ependymal tumors. Additionally, gliomas are categorized according to their histological grade, which serves to predict the biological behavior of a neoplasm (Fig. 3). WHO grade I applies to benign tumors that grow slowly and well circumscribed and, therefore, can usually be cured by complete surgical resection. Gliomas of WHO grade II also grow slowly but tend to infiltrate into the surrounding brain tissue, making complete surgical resection difficult. Thus, patients with a WHO grade II glioma have a high risk for tumor recurrence and malignant progression. The estimated time of survival of these patients is more than 5 years after diagnosis. Examples

for WHO grade II gliomas are diffuse astrocytomas, oligodendrogliomas, oligoastrocytomas or ependymomas. WHO grade III is designated for tumors with histological evidence of malignancy, namely high cell density and increased mitotic activity, as well as nuclear and cellular atypia. Anaplastic astrocytomas, anaplastic oligodendrogliomas, anaplastic oligoastrocytomas or anaplastic ependymomas are examples for WHO grade III tumors. Patients with these types of tumors typically survive 2-3 years. In addition to the characteristics of malignancy, neoplasms of WHO grade IV exhibit endothelial and microvascular proliferation, areas of tumor necrosis, and in many cases widespread infiltration of the surrounding parenchyma (Louis *et al.* 2007). Glioblastoma multiforme (GBM) is a WHO grade IV glioma, and is the most common primary brain tumor in adults with an annual incidence of about 3/100,000 individuals. Glioblastomas can develop from lower grade gliomas through malignant progression. These are referred to as secondary glioblastomas and usually occur in younger patients (<45 years of age). However, the majority of glioblastomas develops *de novo* without a history of lower-grade lesions. For these primary glioblastomas, the median age of diagnosis is around 55-60 years. Although primary and secondary glioblastomas seem to be distinct disease entities that are associated with different patterns of genetic aberrations, they share histological features and a very poor prognosis. Patients with glioblastoma usually succumb to their disease within 1-2 years after diagnosis (Riemenschneider & Reifenberger 2009a).

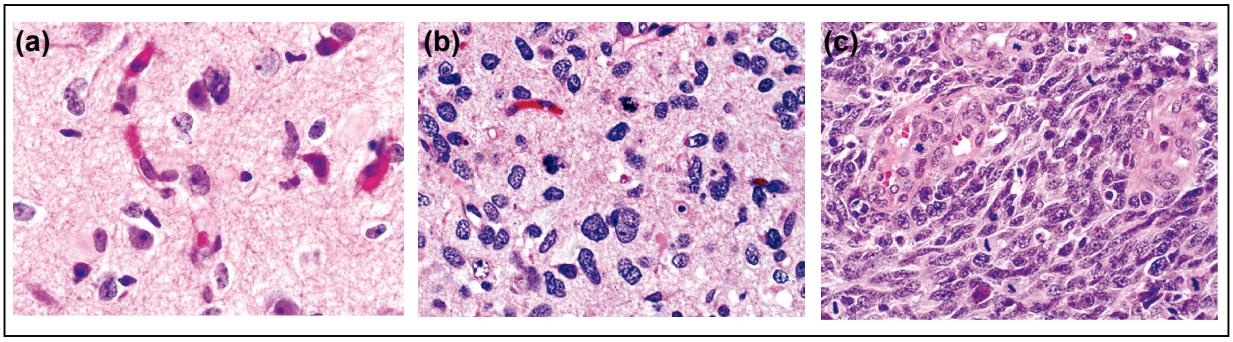

Figure 3: Histological classification of human gliomas. **(a)** Diffuse astrocytoma (WHO grade II). At the infiltrative edge, scattered individual or clustered, mildly enlarged, elongated, irregular and hyperchromatic nuclei (*arrowheads*) are visible, along with native non-neoplastic cells, such as cortical neurons (*arrows*). **(b)** Anaplastic astrocytoma (WHO grade III). Anaplastic astrocytomas are cytologically similar to WHO grade II astrocytomas, but show higher cell-density and mitotic figures (*arrows*). **(c)** Glioblastoma (WHO grade IV). The viable, non-necrotic portion of a glioblastoma displays very high cellularity, mitotic activity, and typical microvascular hyperplasia characterized by highly proliferative endothelial cells (Brat & Perry 2010).

Clinical symptoms of brain tumors generally depend on the location rather than the histology of the tumor. Neurological disturbances including weakness, somatosensory loss, visual loss or aphasia, and epileptic seizures, which can be focal or generalized, are common clinical

manifestations. In addition, intracranial hypertension (mass effect) can lead to headaches, nausea, vomiting, papilledema (optic disc swelling) or impaired consciousness. Diagnosis of gliomas is usually based on magnetic resonance imaging (MRI) and other tomographic techniques (Fig. 4). However, a histological verification of the diagnosis in tissue biopsies is recommended for all lesions suggestive of primary brain tumors before therapeutic decisions are made (Schneider *et al.* 2010, Weller 2011).

The primary treatment for low-grade gliomas that are symptomatic and surgically accessible is the total surgical resection. A positive effect of postoperative radiotherapy with respect to tumor progression that was initially reported did not translate into overall longer survival of patients. Therefore, a wait-and-see strategy is usually adopted after surgery (Schneider *et al.* 2010). The standard treatment strategy for newly diagnosed anaplastic gliomas (WHO grade III) includes resection of the tumor, followed by radiotherapy to the tumor region. Radiotherapy can be substituted by chemotherapy using either procarbazine/lomustine/vincristine (PCV) or temozolomide, but the combination of both strategies has no beneficial effect on overall survival of the patients. In the case of recurrent disease after radiotherapy as primary treatment, patients typically receive alkylating agent chemotherapy and vice versa. The standard care for newly diagnosed glioblastomas (WHO grade IV) includes surgical resection followed by combined treatment with radiotherapy and temozolomide (Weller 2011).

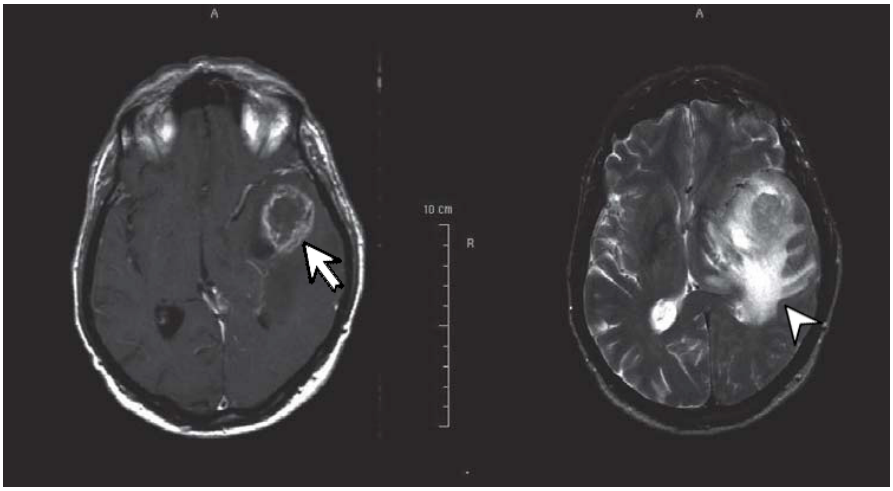

Figure 4: Magnetic resonance images of a glioblastoma showing a centrally necrotic mass with strong peripheral contrast enhancement (arrow) and marked perifocal edema (arrowhead). Left: T1-weighted image with contrast medium. Right: T2-weighted image clearly showing the perifocal edema (Schneider *et al.* 2010).

Recent advances in the understanding of molecular changes in gliomas have led to a variety of drugs and experimental therapies that are currently under investigation. For example, currently ongoing phase III trials evaluate the benefit of two inhibitors of angiogenesis, bevacizumab (Lai *et al.* 2011) and cilengitide (Stupp *et al.* 2010), and the local application of

antisense oligonucleotides directed against the immunosuppressive cytokine TGF-β2 (transforming growth factor beta 2) (Hau *et al.* 2007, Schneider *et al.* 2010) for treatment of glioblastomas and anaplastic astrocytomas. In addition to therapeutic approaches, symptomatic treatment is of central importance and may include corticosteroids for controlling tumor-associated brain edema, anti-thrombotic drugs as glioma patients are at high risk of thromboembolic complications, and anti-epileptic drugs for patients suffering from seizures (Weller 2011).

Unfortunately, current therapies only marginally extend survival of glioma patients, and despite the development of new techniques like MRI- or fluorescence-guided surgery and awake craniotomy that allow for more complete surgical resection, the early extensively infiltrative growth of gliomas still renders them incurable in most cases (Norden & Wen 2006).

1.7 Molecular pathology of gliomas

The development of malignant gliomas involves the stepwise progression of molecular genetic events, in general, the overexpression of proto-oncogenes and the loss of tumor supressor genes (Fig. 5). A diversity of genetic alterations has been identified to date, but many of them target the same key signaling pathways.

Inactivating mutations of the *TP53* gene, which encodes for the tumor supressor protein p53, and the overexpression of platelet-derived growth factor (PDGF) and PDGF receptor (PDGFR) are thought to be early events in the development of gliomas and occur in more than half of low-grade astrocytomas (Ichimura *et al.* 2000, Norden & Wen 2006). The transcription factor p53 regulates cell cycle progression and apoptosis in response to a variety of stress signals by driving the expression of cell cycle checkpoint proteins like $p21^{WAF1/CIP1}$ (Grzmil & Hemmings 2010). Tumors without *TP53* mutations frequently show hypermethylation of the $p14^{ARF}$ promoter leading to gene silencing. $p14^{ARF}$ inhibits the E3 ubiquitin ligase MDM2 (murine double minute 2), which mediates degradation of p53 (Watanabe *et al.* 2007). The overexpression of both PDGF and PDGFR enables autocrine growth stimulation of the tumor cells (Hermanson *et al.* 1992). Additionally, the *IDH1 (isocitrate dehydrogenase 1/2)* gene was mutated in about 70% of diffuse astrocytomas and was associated with longer patient survival. IDH1 is involved in lipid metabolism and glucose sensing and contributes to the cellular defense against reactive oxygen species, but the functional relevance for cancer cells remains elusive (Balss *et al.* 2008, Reitman & Yan 2010). Silencing of the *MGMT* gene *(O-6-methylguanine-DNA methyltransferase)* via promoter hypermethylation has been reported in more than 50% of cases (Watanabe *et al.*

2007). MGMT is a DNA repair enzyme that can counteract the effects of alkylating chemotherapy. Thus, epigenetic inactivation of this gene is a favorable prognostic marker (Riemenschneider *et al.* 2010). A characteristic molecular alteration that occurs early in the development of oligodendroglial tumors is the combined loss of chromosomes 1p and 19q in over 80% of the cases (Reifenberger *et al.* 1994).

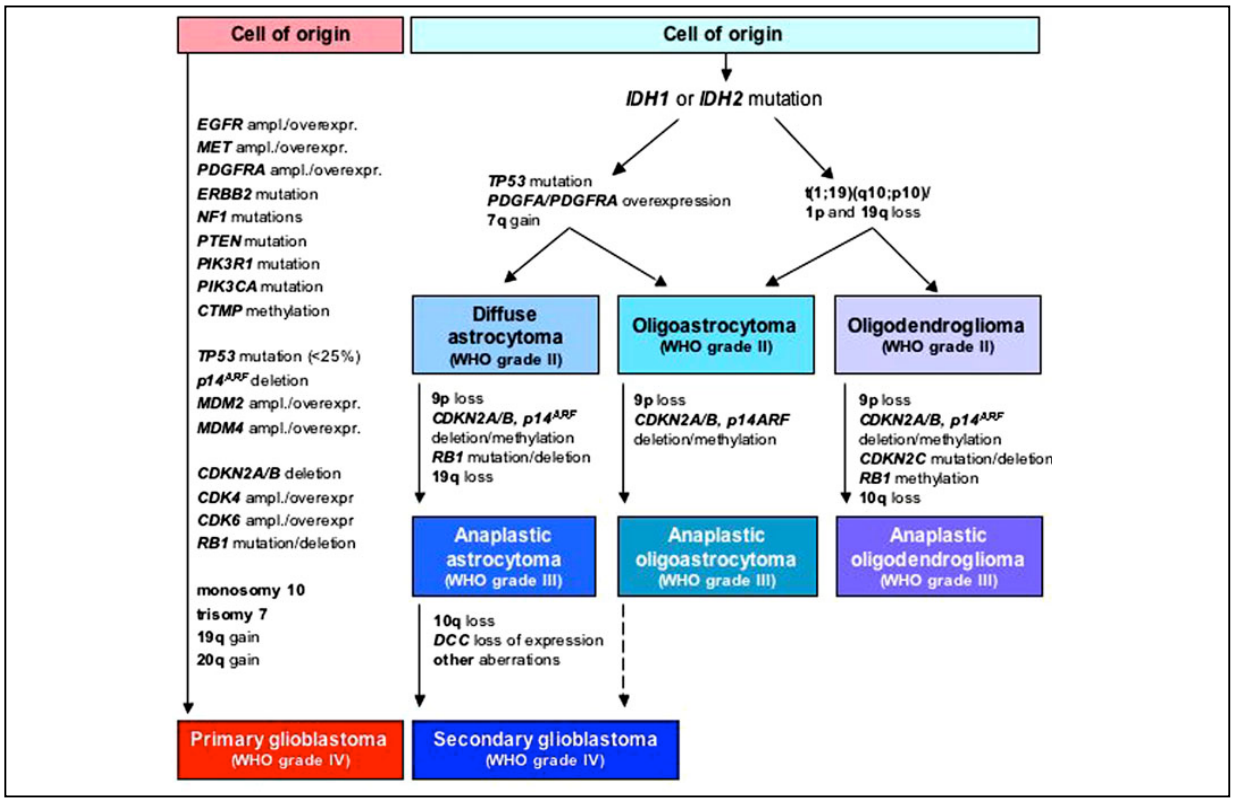

Figure 5: Summary of the most frequent molecular alterations found in astrocytic, oligodendroglial and mixed gliomas, and in secondary versus primary glioblastomas (Riemenschneider *et al.* 2010).

Progression to anaplastic gliomas is associated with inactivation of the p16 -cyclin-dependent kinase (CDK) – retinoblastoma tumor suppressor pathway (Norden & Wen 2006). The gene product of *CDKN2A (CDK inhibitor 2A)*, $p16^{INK4A}$, inhibits the cyclin D – CDK4/CDK6 complexes that phosphorylate the retinoblastoma tumor suppressor protein pRb. This phosphorylation event leads to the release of the E2F transciption factor that activates genes involved in the G_1/S transition (Grzmil & Hemmings 2010). About 25% of anaplastic astrocytomas carry mutations in the retinoblastoma gene (*RB1*), another 10% of these tumors show amplification and overexpression of the *CDK4* gene. In addition, the *CDKN2A* gene is located on chromosome 9p which is together with chromosomes 6, 11p, 19q and 22q among the most frequently lost chromosomal regions in these tumors (Riemenschneider & Reifenberger 2009b). The outcome of all these genetic alterations is increased expression of E2F target genes and enhanced cellular proliferation.

As secondary glioblastomas develop from their lower-grade precursor lesions, they also share genetic and epigenetic aberrations. Mutations in *TP53*, hypermethylation of *RB1* and overexpression of *PDGFRA (PDGFR alpha)* are common, and hypermethylation of *MGMT* and the putative tumor suppressor gene *EMP3 (epithelial membrane protein 3)* are present in 75% and 80% of tumors, respectively. An additional event associated with progression to secondary GBM is the loss of chromosome 10q. In primary glioblastomas that develop *de novo*, *TP53* mutations are found in only 30% of the cases. However, $p14^{ARF}$ alterations as well as *MDM2* or *MDM4* amplifications can serve as an alternative mechanism to bypass p53-regulated growth control in these tumors (Riemenschneider & Reifenberger 2009a). In addition, primary glioblastomas exhibit frequent *EGFR (epidermal growth factor receptor)* amplifications or mutations, and deletions or mutations of the tumor supressor gene *PTEN (phosphate and tensin homologue)* on chromosome 10 (Norden & Wen 2006).

Receptor tyrosine kinases (RTKs) like EGFR and PDGFR activate phosphatidylinositol-3-kinases (PI3Ks) upon ligand binding. In many cancers, RTKs are constitutively activated through mutations. Activated PI3Ks produce phosphatidylinositol-3,4,5 triphosphate (PIP_3) from its diphosphate-substrate (PIP_2), which eventually leads to recruitment, phosphorylation and activation of the kinase AKT. Activated AKT facilitates nuclear translocation of the transcription factor NFκB (nuclear factor of kappa light polypeptide gene enhancer in B-cells), which drives expression of genes that mediate cell survival and proliferation. Alternatively, activated AKT can act via mTOR (mechanistic target of rapamycin) to drive expression of cell cycle regulators like MYC (v-myc myelocytomatosis viral oncogene homolog), cyclin D1 or HIF1α (hypoxia inducible factor 1 alpha) leading to proliferation and angiogenesis. PTEN dephosphorylates PIP_3 to PIP_2 and thereby terminates PI3K signaling. Thus, inactivation of PTEN leads to hyperphosphorylation of AKT and further increases RTK signaling. Activation of RTKs can also initiate ERK signaling via the activation of the small GTPases Ras and Raf, which through transcription factors like IkB (inhibitor of NFκB)/NFκB and cyclic AMP response element binding protein (CREB) promotes glioma cell survival and proliferation (Krakstad & Chekenya 2010).

Taken together, numerous and complex genetic events underlie the formation and progression of malignant gliomas, but many different alterations eventually target the same key signaling pathways, namely p53, pRb1, PI3K/AKT and ERK (Fig. 6).

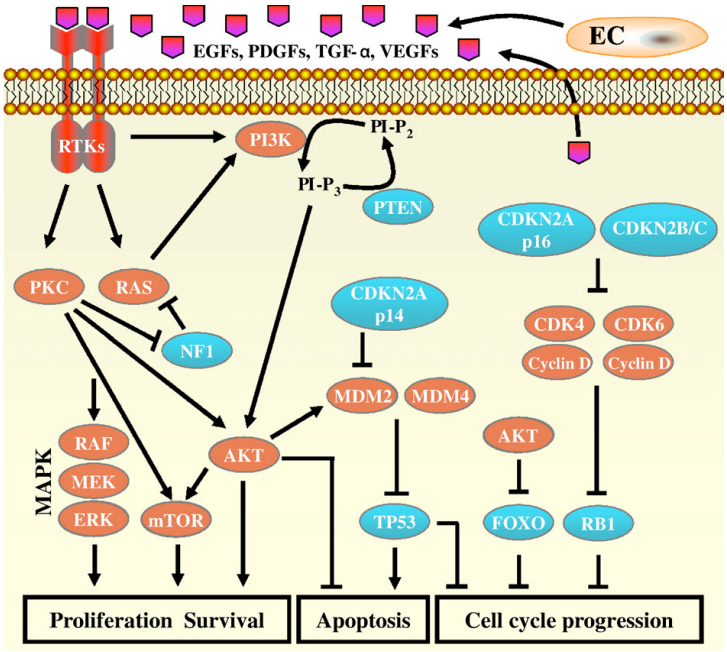

Figure 6: Key deregulated pathways in human gliomas. Although human GBMs are highly heterogenous, many genetic and molecular alterations lead to modifications of the same major signaling pathways that promote brain tumor growth and progression. Blue: Inactivated genes. Red: Hyperactivated genes (Grzmil & Hemmings 2010).

1.8 Brain tumor microenvironment

In addition to cancer cells, tumors contain a variety of non-transformed cells, referred to as the tumor microenvironment. An essential role for these stromal cells in disease progression but also as a target for prognostic and therapeutic strategies has been well documented for extracranial malignancies (Albini & Sporn 2007, Lorger 2012, Witkiewicz *et al.* 2009). In the brain, highly specialized brain resident cell populations and infiltrating cells from the periphery congregate to provide a unique microenvironment that is only poorly understood. Endothelial cells, microglia and peripheral immune cells, non-transformed astrocytes, pericytes and neural precursor cells are tumor-associated parenchymal cell types (Charles *et al.* 2012, Lorger 2012). Endothelial cells are essential for neovascularization, which promotes tumor growth by supplying nutrition and oxygen. Additionally, these cells can secrete inflammatory factors leading to vascular leakiness, and substances that support tumor stem-like cells in the perivascular niche. Pericytes and other mural cells facilitate blood vessel formation by supporting endothelial cells (Jones & Holland 2011). Microglia can contribute up to 30% of a brain tumor mass and, thus, are the most common tumor-associated cells (Charles *et al.* 2012). Glioma cells secrete chemoattractants to recruit microglia to the tumor environment, and concomitantly inhibit microglia activation and proliferation by anti-inflammatory factors like TGFβ. In addition, tumor stem-like cells produce cytokines that promote the immunosuppressive phenotype of microglia. A potential function of the recruited microglia is the secretion of matrix metalloproteinases to promote tumor growth and invasion

by destabilizing the extracellular matrix (Jones & Holland 2011). The importance of microglia to glioma formation has been demonstrated by *in vivo* studies that revealed that tumor growth is reduced in microglia deficent mice (Markovic *et al.* 2009). Another immune-related cell type found in gliomas is T-regulatory lymphocytes (Tregs). These cells are believed to promote a permissive tumor environment by suppressing the immune response, and depletion of Tregs in glioma mouse models was shown to prolong survival (El Andaloussi *et al.* 2006, Jones & Holland 2011). High infiltration of tumors with other peripheral T-lymphocytes, in contrast, was associated with better prognosis in patients with primary glioblastoma (Lohr *et al.* 2011). Suggested functions of tumor-associated astrocytes are the production of neurotrophic factors and the activation of metalloproteinases, both promoting cell invasion and tumor growth (Hoelzinger *et al.* 2007, Jones & Holland 2011, Le *et al.* 2003). Taken together, many different cell types appear to have important functions in maintenance and progression of gliomas, and understanding the interactions between cancer cells and stromal cells may provide new targets for therapeutic intervention strategies.

1.9 Objectives

High-grade gliomas belong to the most malignant human cancers. Despite substantial progress in the molecular understanding of glioma development, the prognosis of these tumors remains very poor with most glioblastoma patients dying within 1-2 years after diagnosis. Therefore, the establishment and functional characterization of novel therapeutic targets is urgently needed. Progranulin (GRN) is a secreted protein with growth factor-like properties that is upregulated in a variety of cancers and confers tumorigenic growth properties to cells *in vitro* and *in vivo*. At the beginning of this thesis project, very limited information was available about a potential role of GRN in human brain tumors. Two studies had suggested that GRN might be overexpressed in gliomas, and that peptides derived from GRN had growth-promoting effects on glioma cells *in vitro* (Liau *et al.* 2000, Markert *et al.* 2001). However, the conclusions in both of these studies were based exclusively on RNA transcript analysis in a small number of glioma cases and very limited functional analysis. Consequently, this thesis project had the following objectives:

(1) To validate the observation that GRN is overexpressed in gliomas in a much larger tumor collection, both on the RNA transcript and the protein level.

(2) To conduct functional studies in established human glioma cell lines to explore the phenotypic and molecular consequences of GRN overexpression.

(3) GRN is a secreted protein, and its predominant function in cancers might be to shape the tumor environment into a growth promoting tumor stroma. Such non-cell-autonomous effects are difficult to investigate in tissue culture models. Therefore, the third objective was to study the tumor-promoting effects of GRN in intracranial xenografts *in vivo* by transplantion of a GRN-overexpressing mouse glioma cell line into the brain of syngenic mice.

2 MATERIALS

2.1 Patients

Primary glioma samples were selected from the tumor tissue collection of the Department of Neuropathology, Heinrich-Heine-University, Düsseldorf, Germany, or were part of the Glioma Core Collection from the NGFN Brain Tumor Network, DKFZ Heidelberg. Samples were investigated according to protocols approved by the institutional review boards. All tumors were classified according to the criteria of the World Health Organization (WHO) classification of tumors of the nervous system (Louis *et al.* 2007). Parts of each tumor were snap-frozen immediately after operation and stored at -80°C. Only tissue samples with an estimated tumor cell content of 80 % or more were used for molecular analyses. RNA extracted by ultracentrifugation was used for RT-PCR and microarray studies, and paraffin-embedded material was used for immunohistochemistry. Non-neoplastic brain tissue samples from different individuals as well as commercially available RNA extracted from autopsy brain tissue (Bio Chain Institute, Inc and Stratagene) were used as reference.

2.2 Animals

VM/Dk mice were bred at the inhouse breeding facility of the German Cancer Research Center Heidelberg and used at 6-12 weeks of age. All animal work was approved by the governmental authorities (Regierungspraesidium Karlsruhe, Germany) and supervised by institutional animal protection.

2.3 Cell lines

Cell line	Origin /Description	*Reference*
A172	Human, glioblastoma multiforme	*Olopade et al., Cancer Res. 52: 2523-2529, 1992.*
GP2 293	Human embryionic kidney, expressing the MoMuLV Gag and Pol proteins	*Clontech (Retro-X™ Universal Packaging System)*
293FT	Human embryonic kidbey, expressing SV40 large T antigen	*Invitrogen (ViraPower™ Lentiviral Expression System)*
Hs683	Human, glioma	*Owens et al., J. Natl. Cancer Inst. 56: 843-849, 1976.*
SMA560	Mouse, spontaneous murine astrocytoma (SMA)	*Serano et al., Acta Neuropathol., 51(1):53-64, 1980.*

T98G	Human, glioblastoma multiforme	*Stein et al., J. Cell. Physiol. 99: 43-54, 1997.*
TP365	Human, glioblastoma multiforme	*James et al., Cancer Res. 53:3674-3676, 1993.*
U118	Human, glioblastoma / astrocytoma (grade III)	*Ponten J et al., Acta Pathol Microbiol Scand 74: 465-86, 1968.*
U138MG	Human, glioblastoma multiforme	*Beckman et al., Hum. Hered. 21: 234-241, 1971.*
U251MG	Human, glioblastoma / astrocytoma (grade III – IV)	*Ponten J et al., Acta Pathol Microbiol Scand 74: 465-86, 1968.*
U87MG	Human, glioblastoma / astrocytoma (grade III)	*Beckman et al., Hum. Hered. 21: 234-241, 1971.*

2.4 Bacteria, Plasmids and Primers

2.4.1 Bacteria

Escherichia coli	**Genotype**
DH5α	F$^-$ Φ80*lac*ZΔM15 Δ(*lac*ZYA-*arg*F)U169*rec*A1 *end* A1 *hsd*R17(r_K^-, m_K^+) *pho*A *sup*E44 *thi*-1 *gyr* A96 *rel*A1λ$^-$
TOP10	F- *mcr*A Δ(*mrr-hsd*RMS-*mcr*BC) φ80*lacZ*ΔM15 Δ*lac*X74 *rec*A1 *ara*D139 Δ(*ara-leu*)7697 *gal*U *gal*K *rps*L (StrR) *end*A1 *nup*G
Stbl3	F– *mcr*B *mrr hsd*S20(rB–, mB–) *rec*A13 *sup*E44 *ara*-14 *gal*K2 *lac*Y1 *pro*A2 *rps*L20(StrR) *xyl*-5 λ– *leu mtl*-1

2.4.2 Plasmids

Plasmid/Constructs	**Source**
pcDNA3-PGRN	Provided by A. Bateman, McGill University, Canada
pcDNA6.2-GW/EmGFP-miR	Invitrogen, Life Technologies, Darmstadt
pcDNA6.2-GW/EmGFP-miR-neg	Invitrogen, Life Technologies, Darmstadt
pCMV-ΔR8.9	Provided by S. Kins, ZMBH, Universität Heidelberg
pCMV-VSVg	Provided by S. Kins, ZMBH, Universität Heidelberg
pLenti6/V5-DEST	Invitrogen, Life Technologies, Darmstadt
pLHCX	Clontech Laboratories, Inc
pRetroX-Tet On-Advanced	Clontech Laboratories, Inc

pRetroX-Tight-Pur	Clontech Laboratories, Inc
pRetroX-Tight-Pur-Luc	Clontech Laboratories, Inc
pVSV-G	Clontech Laboratories, Inc

2.4.3 Oligonucleotides

Primer	**Sequence**
hmPGRN_fwd4	CGTCTCAGGGACTTCCAGTT
hmPGRN_rev4	GATCTTTGGAAGCAGGATCG
ARF1-F	GACCACGATCCTCTACAAGC
ARF1-R3	TCCCACACAGTGAAGCTGATG
miR GRN201_top	TGCTGTGTTAAGGCCACCCAGCTCACGTTTTGGCCACT GACTGACGTGAGCTGTGGCCTTAACA
miR GRN201_bottom	CCTGTGTTAAGGCCACAGCTCACGTCAGTCAGTGGCCA AAACGTGAGCTGGGTGGCCTTAACAC
miR GRN2140_top	TGCTGCAGGGAAGGCCTTAGATTGAGGTTTTGGCCACT GACTGACCTCAATCTGGCCTTCCCTG
miR GRN2140_bottom	CCTGCAGGGAAGGCCAGATTGAGGTCAGTCAGTGGCC AAAACCTCAATCTAAGGCCTTCCCTG
miR ctrl_top	Provided by Invitrogen
miR ctrl_bottom	Provided by Invitrogen
PGRN-HindIII_fwd	TTTTAAGCTTATGTGGACCCTGGTGAGCTGG
PGRN-ClaI_rev	TTTTATCGATTCACAGGAGCTGTCTCAAGGCTGG
Infusion-PGRN_NotI	GAAGGATCCGCGGCCGCATGTGGACCCTGGTGAGC
Infusion-PGRN-EcoRI_rev	CTACCCGGTAGAATTCTCACAGCAGCTGTCTCAA

2.5 Antibodies

2.5.1 Primary antibodies

Antigen	**Species**	**Type**	***Company/Reference***
CD44	Rabbit	Polyclonal	*Sigma (#HPA005785)*
Cd68 (clone KP-1)	Mouse	Monoclonal	*DakoCytomation (#M 0814)*
GFAP	Rabbit	Polyclonal	*DakoCytomation (#Z 0334)*
Progranulin (human)	Goat	Polyclonal	*R & D Systems (#AF2420)*

Progranulin (human)	Rabbit	Polyclonal	*Zymed (#40-3400)*
Progranulin (mouse)	Sheep	Polyclonal	*R & D Systems (#AF2557)*
α-Tubulin	Mouse	Monoclonal	*Sigma (#T 9026)*

2.5.2 Sekundary antibodies

Antigen	**Conjungate**	**Species**	***Company/Reference***
Mouse IgG	HRP	Goat	*Jackson Immuno Research*
Rabbit IgG	HRP	Goat	*Jackson Immuno Research*
Sheep IgG	HRP	Donkey	*Sigma*

2.6 Reagents

2.6.1 Chemicals

30 % Acrylamide 37.5 :1, Bis-Acrylamide	*National Diagnostics, USA*
Agar	*Carl Roth, Karlsruhe*
Agarose	*BioBudget, Krefeld*
Alamar blue	*Invitrogen, Carlsbad, CA*
Ammoniumpersulfate (APS)	*Sigma-Aldrich, Steinheim*
BisTris	*Calbiochem, Darmstadt*
Boric acid	*Sigma-Aldrich, Steinheim*
Bromphenolblue	*Carl Roth, Karlsruhe*
BSA	*Sigma-Aldrich, Steinheim*
ClearMount™ mounting solution	*Invitrogen, Carlsbad, CA*
Desoxynucleotide-tri-phosphate (dNTP)	*New England Biolabs, Ipswich*
Dimethylsulfoxide (DMSO)	*Sigma-Aldrich, Steinheim*
Dithiothreiotol (DTT)	*Sigma-Aldrich, Steinheim*
DMEM	*Invitrogen, Carlsbad, CA*
Dry-milk (fat-free)	*Oxoid, Hampshire, UK*
Ethanol	*Carl Roth, Karlsruhe*
Ethidiumbromide	*Sigma-Aldrich, Steinheim*
Fetal Calf Serum (FCS)	*Invitrogen, Carlsbad, CA*
Fetal Calf Serum (FCS), tet-system approved	*Clontech Technologies*
GeneJuice Transfection Reagent	*Merck, Darmstadt*
Glacial Acetic Acid	*Merck, Darmstadt*
Glycerine	*Carl Roth, Karlsruhe*

H33342	*Sigma-Aldrich, Steinheim*
Hydrochloric acid (HCl)	*Sigma-Aldrich, Steinheim*
Igepal (NP40)	*Sigma-Aldrich, Steinheim*
Immobilion™ Western HRP Substrate Luminol Reagent	*Millipore, Schwalbach*
Immobilion™ Western HRP Substrate Peroxidase	*Millipore, Schwalbach*
Isopropanol	*Carl Roth, Karlsruhe*
Magnesium-chloride ($MgCl_2$)	*Carl Roth, Karlsruhe*
Mayer's Hemalaun	*AppliChem, Darmstadt*
Methanol	*Carl Roth, Karlsruhe*
MTT	*Invitrogen, Carlsbad, CA*
Opti-MEM	*Invitrogen, Carlsbad, CA*
Paraformaldehyde	*Sigma-Aldrich, Steinheim*
PBS	*Invitrogen, Carlsbad, CA*
Polybrene	*Sigma-Aldrich, Steinheim*
Ponceau S	*Sigma-Aldrich, Steinheim*
Potassium chloride (KCl)	*Sigma-Aldrich, Steinheim*
Potassium dihydrogen phosphate (KH_2PO_4)	*Carl Roth, Karlsruhe*
Protease inhibitor cocktail tablets, EDTA-free	*Roche, Basel*
Random Hexamers	*Roche, Basel*
Sodium azide (NaN_3)	*Merck, Darmstadt*
Sodium chloride (NaCl)	*Carl Roth, Karlsruhe*
Sodium dihydrogen phosphate (NaH_2PO_4)	*Merck, Darmstadt*
Sodium dodecyl sulfate (SDS)	*Carl Roth, Karlsruhe*
Sodium hydroxide (NaOH)	*Merck, Darmstadt*
Sodium pyruvate	*Invitrogen, Carlsbad, CA*
TEMED (N,N,N+,N+-Tetramethylendiamine)	*Sigma-Aldrich, Steinheim*
Tris hydrochloride (HCL)	*Carl Roth, Karlsruhe*
Tris-Base	*Carl Roth, Karlsruhe*
TRIzol	*Invitrogen, Carlsbad, CA*
Trypan blue	*Invitrogen, Carlsbad, CA*
Trypsin/EDTA	*Invitrogen, Carlsbad, CA*
Tryptone	*Carl Roth, Karlsruhe*
Tween-20	*Carl Roth, Karlsruhe*
Xylol	*Carl Roth, Karlsruhe*
Yeast Extract	*Carl Roth, Karlsruhe*

2.6.2 Antibiotics

Ampicillin	*Sigma-Aldrich, Steinheim*
Blasticidin	*Invitrogen, Carlsbad, CA*
Chloramphenicol	*Sigma-Aldrich, Steinheim*
Doxycycline	*Sigma-Aldrich, Steinheim*
G418	*Sigma-Aldrich, Steinheim*
Kanamycin	*Sigma-Aldrich, Steinheim*
Penicillin/Streptomycin	*Invitrogen, Carlsbad, CA*
Puromycin	*Merck, Darmstadt*
Spectinomycin	*Sigma-Aldrich, Steinheim*

2.6.3 Size Standards

Biotinylated Protein Ladder	*New England Biolabs, Ipswich*
2-log DNA Ladder	*New England Biolabs, Ipswich*
Low molecular weight DNA ladder	*New England Biolabs, Ipswich*

2.7 General Enzymes und Restrictionendonucleases

2.7.1 General Enzymes

Enzyme	**Buffer**	***Company***
Phusion High-Fidelity DNA- Polymerase	5x Phusion HF Puffer $MgCl_2$	*Finnzymes*
T4-DNA-Ligase	10x Ligase Puffer 10 mM ATP	*NEB*
Antarctic Phosphatase	10x Antarctic Phosphatase Reaction Buffer	*NEB*
BP Clonase II Enzyme Mix	5x BP Clonase Reaction Buffer	*Invitrogen*
LR Clonase II Enzyme Mix	5x LR Clonase Reaction Buffer	*Invitrogen*
Superscript® II Reverse Transcriptase	5x First Strand Buffer + 0,1M DTT	*Invitrogen*

2.7.2 Restrictionendonucleases

Enzyme	Sequence	Buffer	Temperature	*Company*
ClaI	5´-AT↓CGAT-3´ 3´-TAGC↑TA-5´	NEB4 + BSA	37 °C	*NEB*
EcoRI	5´-G↓AATTC-3´ 3´-CTTAA↑G-5´	NEB EcoRI	37 °C	*NEB*
HindIII	5´-A↓AGCTT-3´ 3´-TTCGA↑A-5’	NEB 2	37 °C	*NEB*
NotI	5´-GC↓GGCCGC-3´ 3´-CGCCGG↑CG-5’	NEB 3 + BSA	37 °C	*NEB*

2.8 Kits

BCA Protein Assay Kit	*Pierce, Bonn*
Block-iT™ Pol II miR RNAi Expression Vector Kit	*Invitrogen, Carlsbad, CA*
DAKO REAL EnVision Detection System	*DAKO Cytomation,Hamburg*
Gateway® BP Clonase™ II Enzyme Mix	*Invitrogen, Carlsbad, CA*
Gateway® LR Clonase™ II Enzyme Mix	*Invitrogen, Carlsbad, CA*
GeneChip 3’IVT Express Kit	*Affymetrix, Santa Clara, CA*
GeneChip Hybridization Control Kit	*Affymetrix, Santa Clara, CA*
GeneChip Hybridization, Wash and Stain Kit	*Affymetrix, Santa Clara, CA*
Goat ABC Staining System	*Santa Cruz, Heidelberg*
In-Fusion® HD Cloning Kit	*Clontech Laboratories*
Jet Star Plasmid Maxi-Prep Kit	*Genomed, Löhne*
NucleoSpin Plasmid-Kit	*Macherey-Nagel, Düren*
ORIS Cell Migration Assay Kit	*Platypus Tech., Madison*
Platinum® SYBR® Green qPCR SuperMix-UDG	*Invitrogen, Carlsbad, CA*
QIAquick Gel Extraction Kit	*Qiagen, Hilden*
Retro-X™ Tet-On Advanced Inducible Expression System	*Clontech Laboratories*

2.9 Laboratory hardware

Autoclaves	*Systec, Wettenberg*
Block Thermostat	*HLC BioTech, Bovenden*
Centrifuges	*Eppendorf, Hamburg* *Hettich, Tuttingen*

Fluorescence microscope IX 50/ U-RFL-T	*Olympus GmbH, Münster*
Glassware	*Schott, Mainz*
Incubator	*Binder, Tuttlingen*
Laminar flow (Typ EF/S)	*CleanAir Techniek, Woerden*
Luminescent Image Analyzer LAS-3000 mini	*FULIFILM, Düsseldorf*
Microscope	*Nikon Instr., Düsseldorf*
Microtome Shandon® Finesse	*Thermo Scientific, Waltham*
Microwave pressure cooker ‚multi gourmet'	*Braun, Kronberg /Ts.*
Nanodrop ND1000	*Peqlab, Erlangen*
Paradigm Detection Platform	*Beckman Coulter, Krefeld*
pH meter	*WTW, Weilheim*
Photomicroscope	*Leica Microsystems, Wetzlar*
Pipettes	*Gilson, Middleton, WI*
Pipettors	*BRAND, Wertheim*
Power supplies	*Consort, Turnhout*
RunOne Electrophoresis Cell System	*EmbiTec, San Diego*
Scales	*Sartorius, Göttingen*
Semi-dry blotter	*Hoefer, USA*
StepONE Plus Real Time PCR System	*Applied Biosystems, CA*
T3 Thermocycler	*Biometra, Göttingen*
Tank Blotter	*CBS Scientific, USA*
ViCell XR Cell Viability Analyzer	*Beckman Coulter, Krefeld*

2.10 Consumables

Black 96-well plates with optical bottom	*Greiner, Frickenhausen*
Cell culture dishes / flasks	*Nunc, Wiesbaden*
Cover Slips	*Engelbrecht, Engermünde*
Cryotubes	*Nunc, Wiesbaden*
Disposable gloves	*Semperit, Wien*
Immobilion-P Transfer Membrane	*Millipore, Schwalbach*
Microscope slides	*Thermo Scientific, Waltham*
Multiwell plates (cell culture)	*Nunc, Wiesbaden*
Novex Gel Cassettes	*Invitrogen, Carlsbad, CA*
Pasteur pipettes	*Carl Roth, Karlsruhe*
PCR reaction tubes	*Thermo Scientific, Waltham*
Reaction tubes	*Sarstedt, Nümbrecht*

Petri dishes (bacteria)	*Sarstedt, Nümbrecht*
Pipet tips	*Starlab, Ahrensburg*
Pipettes (5 ml – 25 ml)	*Corning Inc., Corning, NY*
Real-time PCR plates	*Applied Biosystems, CA*
Whatman paper	*Whatman, Dassel*

2.6 Software

Adobe Design Standard CS3
Fuji Imaging Software
Microsoft Office 2003
Prism GraphPad 5.0
ImageJ
Gene Spring GX

3 METHODS

3.1 Tissue Culture

Routine cell culture was performed under sterile working conditions in S1 or S2 qualified laboratories. Pipettes, dishes, plates, filter tips, tubes, syringes and sterile filters were single-use plastic items and cell culture qualified. All solutions and media were stored at 4°C unless otherwise indicated by the manufacturer. Cells were cultured in DMEM complete medium supplemented with selection antibiotics as necessary and incubated at 37°C in 5% CO_2. Growth and morphology was checked on a daily basis and mycoplasm tests performed regularly.

DMEM complete: DMEM (high glucose, + L-glutamine)
10 % FCS
1 % Penicillin/Streptomycin (10000 U/ml Penicillin/10000 µg/ml Streptomycin)
1 mM Na-Pyruvate

Cell line	**Selection antibiotics**
293 FT	500µg/ml G418
A172	-
A172-miR	2 µg/ml Blasticidin
GP2 293	-
SMA560	-
SMA560 Tet-On	600 µg/ml G418
SMA560 Tet-On-GRN	600 µg/ml G418 1.25 µg/ml Puromycin
T98G	-
T98G Tet-On	400 µg/ml G418
T98G Tet-On-GRN	400 µg/ml G418 0.5 µg/ml Puromycin
T98G-pLHCX	300µg/ml Hygromycin
T98G-GRN	300µg/ml Hygromycin
TP365	-
TP365-miR	1 µg/ml Blasticidin
U138MG	-
U138MG-miR	1 µg/ml Blasticidin
U251MG	-

U251MG Tet-On	300 µg/ml G418
U251MG Tet-On-GRN	300 µg/ml G418 0.25 µg/ml Puromycin
U251MG-pLHCX	50µg/ml Hygromycin
U251MG-GRN	50µg/ml Hygromycin
U87MG	-
U87MG Tet-On	300 µg/ml G418
U87MG Tet-On-GRN	300 µg/ml G418 0.5 µg/ml Puromycin
U87MG-pLHCX	50µg/ml Hygromycin
U87MG-GRN	50µg/ml Hygromycin

3.1.1 Passaging of adherent cell lines

In general, adherent cell lines were cultured in 10 cm cell culture dishes. If cells were cultured in smaller or larger vessels the volumes were adjusted accordingly.

- Remove cell culture medium from dish.
- Wash cells with 5 ml 1 x PBS (Gibco, Invitrogen).
- Add 1 ml 1 x trypsin/EDTA (Gibco/Invitrogen) and sway dish, incubate for 1 min to 5 min at RT.
- Add 9 ml of the appropriate culture medium containing FCS and pipet up and down to achieve a single cell suspension.
- Transfer the desired amount of cell suspension into a fresh 10 cm dish, adjust volume to 10 ml with complete growth medium and add the appropriate selection antibiotic.

3.1.2 Cryopreservation of cells

For long-term storage and preservation cell lines were frozen and stored in liquid nitrogen.

- Trypsinize and resuspend cells as for passaging (3.1.1).
- Transfer cell suspension to a 15 ml tube and centrifuge at 1000 rcf for 5 min.
- Resuspend pellet in freezing media (90% FCS/10% DMSO), 1 ml per 10 cm dish.
- Aliquot cell suspension (1 ml) into 1.8 ml screw cap cryo-vials and place on ice.
- Transfer vials to -80°C quickly.
- For long-term storage transfer vials into liquid nitrogen tank.

3.1.3 Thawing of frozen cell stocks

- Prepare 15 ml tube with 10 ml pre-warmed complete growth medium.
- Place cryo-vial in 37°C water bath and thaw cells.
- Transfer cells into the medium and spin down at 1000 rcf for 5 min.
- Remove supernatant and resuspend cells in complete growth medium.
- Transfer cells onto a 10 cm dish and place in incubator.

3.1.4 Transient Transfection

- The day before transfection, seed target cells in 12-well dishes. Cell density should be adjusted so that cell lines reach 80-90% confluency 24 h later, approximately 300,000cells/well.
- Change medium on cells to 500 µl OptiMEM.
- Per well, pipet 100 µl OptiMEM to a sterile 1,5 ml tube and add 5 µl Lipofectamine 2000.
- Incubate for 5 min at RT.
- In a separate tube dilute 1.6 µg DNA in 100 µl OptiMEM and incubate for 5 min.
- Transfer DNA dilution to the tranfection reagent mixture and incubate for additional 20 min at RT.
- Add transfection mixture to cells.

3.1.5 Generation of retroviral particles

When working with retroviral particles, adhere to biosafety level 2 (S2) rules, these include (but are not limited to):

- Work only in S2 qualified rooms and at S2 qualified cell culture benches.
- Wear lab-coat at all times.
- Double-glove with nitril gloves.
- Wear arm protection.
- Keep disinfectant ready at hand.
- Use plastic pipettes and filtered pipette tips; no glassware!
- Inactivate liquid waste by incubation with 70% ethanol or disinfectant before autoclaving.
- Double-bag solid waste and autoclave on a regular basis.

Day 1:

- Split a confluent plate of GP2-293 cells 1:4 T75 flasks.

Day 2:

- Cell density should be 70 – 80%.
- Prepare transfection mixture for each plate:
  - Add 800 µl Optimem (Invitrogen) to a sterile 1.5 ml tube.
  - Add 45 µl Gene Juice and incubate for 5 min at RT.
  - Add 7.5 µg retroviral shuttle plasmid (e.g. pLPCX, pLHCX, etc.), containing gene of interest, and 7.5 µg pVSVG plasmid to the transfection mixture. The total volume of the DNA should not exceed 100 µl.
  - Incubate for 15 – 20 min at RT.
  - Carefully change medium on the GP2-293 cells.
  - Add the transfection mix in a dropwise manner onto the cells and carefully sway the plate.
  - Place in incubator.

Day 4:

- Take off supernatant and inactivate with disinfectant.
- Carefully add 5 ml fresh medium and place cells in incubator.

Day 5:

- Draw supernatant containing the retroviral particles into a 10 ml syringe.
- Place a sterile filter (0.45 µm) on the syringe and filter supernatant into a 50 ml tube to remove cells and debris.
- Aliquot filtered supernatant into screw cap cryovials (1 ml per vial).
- Store virus particles at -80°C.
- Inactivate and discard cells.

3.1.6 Generation of lentiviral particles

When working with lentiviral particles, adhere to biosafety level 2 (S2) rules, see ‘Generation of retroviral particles’.

Day 1:

- Split a confluent plate of 293FT cells 1:2 T75 flasks.

Day 2:

- Cell density should be 90-100%.
- Change medium to 5 ml Optimem 1 h before transfection.
- Prepare transfection mixture for each plate:
  - Add 640 µl Optimem (Invitrogen) to a sterile 1.5 ml tube.
  - Add 27 µl Lipofectamine 2000 and incubate for 5 min at RT.
  - In a separate tube, add 5.5 µg lentiviral shuttle plasmid (e.g. pLenti6/V5-DEST) containing gene of interest, 4 µg pCMV-dR8.9 plasmid and 3 µg pCMV-VSVg plasmid to Optimem to obtain a final volume of 667 µl. Incubate for 5 min at RT.
  - Combine both mixtures and incubate for another 20 min at RT.
  - Add the transfection mix in a dropwise manner onto the cells and carefully sway the plate.
  - Place in incubator.
  - After 8-14 h change medium to 6ml normal growth medium without antibiotics.

Day 4:

- Draw supernatant containing the retroviral particles into a 10 ml syringe.
- Place a sterile filter (0.45 µm) on the syringe and filter supernatant into a 50 ml tube to remove cells and debris.
- Aliquot filtered supernatant into screw cap cryovials (1 ml per vial).
- Store virus particles at -80°C.
- Inactivate and discard cells.

3.1.7 Infection with viral particles

To produce cell lines with stable expression of transgenes, cells were infected with retro- or lentiviral particles and then subjected to selection with the appropriate antibiotic depending on the resistance gene encoded on the plasmid.

Day 1:

- Seed target cells in T25 flasks. Cell density should be adjusted so that cell lines reach confluency about 48 – 72 h later, approximately 500,000 cells/T25 flask.

Day 2:

- Aspirate medium, replace by 1 ml fresh complete growth medium and add 2 µl polybrene stock solution (5 mg/ml).
- Thaw viral particles quickly in a 37°C waterbath.

- Add 1 ml viral particles to cells and incubate for 24 h.

Day 3:

- Remove medium containing viral particles and inactivate.
- Wash cells with 1 x PBS and add fresh medium.
- Incubate for 24 h.

Day 4:

- Trypsinize the infected cells and resuspend in 10 ml medium containing the appropriate concentration of selection antibiotic.
- Plate cells on a 10 cm dish. For fast growing cells split cells 1:10.

- Change media every 2 – 3 days and add selection antibiotic until stable cell clones appear. Make sure the control cells are all dead.
- Check expression of transgene by Western Blot analysis.
- Do not remove selection antibiotic until stable clones are frozen for long-term storage.

3.1.8 Killing curve

To evaluate the concentration of selection antibiotic needed to select for transfected cells, cell lines without expression of the transgene were subjected to treatment with different concentrations of the selection antibiotic. The concentration range was dependent on the cell line and the antibiotic used:

Hygromycin	100 µg/ml to 800 µg/ml
Puromycin	0.25 µg/ml to 6 µg/ml
Geneticin	100 µg/ml to 800 µg/ml
Blasticidin	1 µg/ml to 8 µg/ml

- Seed cells at low density in 12-well plates.
- After 24 h change medium to medium containing the selection antibiotic and keep 1 well in regular medium.
- Exchange medium every 2 – 3 days and add fresh selection antibiotic.
- Depending on the cell line selection takes 1 – 2 weeks. Check cells regularly and note at which concentration all cells are dead.

For selection of cell lines with transgenes use the concentration at which all cells were dead and in addition one lower concentration at which approximately 80% of all cells were dead or dying. Sometimes selection at lower concentrations yields higher expression levels.

3.1.9 Subcloning of cell lines

- Trypsinize mass culture and count cells in a Neubauer chamber or ViCell.
- Dilute cells in media containing the selection antibiotic to a density of 0.5-1 cells/ 100 µl.
- Plate cells on 96-well plates, add 100 µl of the dilution per well.
- Observe growth on plate on a regular basis and mark wells with single clones.
- When the single clones have reached confluency in the 96-well, transfer the cells into one well of a 24-well plate.
- Expand the single clones and check for expression.
- Keep selection antibiotic on the cells at all times!

3.1.10 Viabilityassay

AlamarBlue® was used as an indicator for cell viability. This compound (resazurin) is membrane permeable and upon entering cells is reduced to resorufin by viable cells only, leading to a coulor change and the production of red fluorescence.

- Seed cells at low density in 100 µl complete medium in 96well plates (~5000cells/well)
- After 24 h, prepare 2x stocks of the compounds and treat cells by adding 100µl/well (=1:2 dilution)
- After additional 24 h add 20 µl alamar blue and incubate at 37°C until color change can be seen, usually several hours up to over night.
- Measure absorbance at 560 nm and use 600 nm as reference wavelength.

3.1.11 Proliferationassay

To assess differences in proliferation of cell lines, growth rates were evaluated by counting cell numbers for six adjacent days.

- Seed cells at low density (e.g. 50000cells/well) in 12-well plates.
- The next day, wash the cells once with PBS and change to serum free medium or add compounds if necessary.
- At the desired timepoints, trypsinize cells and count in a Neubauer chamber or ViCell.

3.1.12 Soft Agar Colony Formation Assay

Clonogenicity of cell lines was assessed by the evaluation of achorage-independent growth capacity in semi-solid medium.

- Prepare 3% Agar in MilliQ water, autoclave and store at 4°C.
- Melt 3% agar in a microwave and let cool to ~40°C. Dilute melted agar 1:5 (→0.6%) in prewarmed complete growth medium and immediately pour 1ml/well into 6-well plates. Be sure that the bottom of the well is completely covered.
- Incubate at RT until agar is solidified.
- Prepare a cell suspension with 100000 cells (→ 25000 cells/well) in 3.6 ml prewarmed complete growth medium and add compounds if necessary.
- Add 400 µl (→ 0.3%) melted agar, mix and immediately pour 1 ml/well on top of the solidified bottom agar layer.
- Incubate in a cell culture incubator for 3 weeks and feed cells every 3-5 days with 200 µl complete growth medium, supplemented with compound if necessary.
- To assess colony formation, stain viable cells with MTT (500µl/well) over night and count colonies.

3.1.13 Migrationassay

Cell migration assays were performed using the Oris™ Cell Migration Assay Kit from Platypus Technologies, LLC. Silicone stoppers were washed in 70% Ethanol after each assay and reused on separate 96well plate with optical bottom from Greiner.

- Place silicone stoppers in all wells of a black 96well plate with optical bottom
- Seed 25,000 cells in 100 µl complete growth medium per well
- Incubate for 24 h in cell culture incubator
- Remove silicone stoppers to create migration zone and change medium if necessary; for negative control don't remove stoppers or use Cytochalasin D to inhibit migration of cells
- At the desired timepoint, fix cells for 10 min in 4% paraformaldehyde
- Stain cell nuclei with 5 µg/ml H33342 in PBS for 10 min
- Place detection mask underneath the assay plate to cover all non-migration zone areas and photograph each well under fluorescence microscope
- Count migrated cells or analyze pictures with ImageJ software

3.2 Proteinbiochemistry

3.2.1 Harvesting of secreted proteins

To investigate secreted proteins, cell culture supernatants were harvested. Supernatants were stored at -80°C.

- Prepare and label two sets of 1.5 ml tubes for each sample.
- Add 25 x complete protease inhibitor stock solution to one set of tubes. 20 µl per 500 µl of supernatant.
- Place cell culture dish or plate on ice.
- Pipet supernatant into the set of tubes containing the protease inhibitor.
- Spin samples for 3 min at 13000 rcf.
- Transfer supernatant to fresh tubes and store at -80°C.

25 x Complete Protease Inhibitor: dissolve one tablet in 2 ml Milli-Q water (EDTA-free; Roche)

3.2.2 Harvesting of cellular lysates

To investigate intracellular proteins, cells were lysed in NP40-buffer. Lysates were stored at – 20°C.

- Prepare and label two sets of 1.5 ml tubes for all samples.
- Dilute the Complete protease inhibitor stock in NP40 lysis buffer to a final concentration of 1 x.
- Place cell culture dishes or plates on ice.
- Remove supernatant and wash cells once with cold 1 x PBS.
- Add 1 ml 1 x PBS onto the cells and scrape them off the plate.
- Transfer cells into 1.5 ml tube and centrifuge for 3 min at 13000 rcf.
- Discard supernatant and add appropriate amount of NP40 lysis-buffer with protease inhibitor.
- Incubate for 20 min on ice and vortex every 5 min.
- Centrifuge for 15 min at 13000 rcf.
- Transfer supernatant into fresh tube.
- Store at -20°C.

NP40 Lysis Buffer:	50 mM Tris-HCl, pH 7.8	
	150 mM	NaCl
	1 %	NP40
	Store at 4°C.	
10 x PBS, pH 7.4:	137 mM	NaCl
	2.7 mM	KCl
	10 mM	Na_2HPO_4
	10 mM	KH_2PO_4
	Store at RT.	
25 x Complete Protease Inhibitor:	Dissolve one tablet in 2 ml Milli-Q water. (EDTA-free; Roche) , Store at -20°C.	

3.2.3 Bicinchonic acid protein assay (BCA)

To load equal amount of protein on gels or use equal amounts of protein for experiments, the concentration of the samples was determined by a bicinchonic acid (BCA) protein assay. Protein concentrations were measured using the BCA Protein Assay Kit (Pierce) according to the manufacturer's protocol.

- Pre-heat heating-block to 60 °C.
- Dilute BSA standard (1 mg/ml) for the standard curve:

Final concentration [µg/ml]	Volume NP40 buffer [µl]	Volume BSA standard [µl]
0	50	0
100	45	5
200	40	10
300	35	15
400	30	20
500	25	25
600	20	30

- Add 45 µl NP40 buffer into 1.5 ml tubes and add 5 µl samples.
- Mix BCA Reagent A and B in a 50:1 ratio.
- Add 500µl of BCA reagent mix to each sample and standard.

- Incubate for 30 min at 60 °C.
- Load samples and standard in duplicates onto a clear 96-well microtiterplate.
- Measure OD at 540 nm and calculate sample concentration.

NP40 Lysis Buffer: 50 mM Tris-HCl, pH 7.8
150 mM NaCl
1 % NP40
Store at 4 °C.

BSA and BCA reagents are supplied with the kit.

3.2.4 SDS-Polyacrylamide gelelectrophoresis (SDS-PAGE)

SDS-Polyacrylamide gelelectrophoresis allows the separation of denatured proteins according to their molecular weight. The loading buffer for the proteins contains SDS which results in an overall negative charge of the proteins, therefore their separation is not influenced by any intrinsic charges.

- Prepare resolving gel mixture:

	10 %	12 %
30% Acrylamide 37.5 :1	2.20 ml	2.64 ml
1.6 M Bis-Tris, pH 6.4	1.65 ml	1.65 ml
MilliQ-water	2.70 ml	2.26 ml
10% APS stock solution	33 µl	33 µl
Temed	11 µl	11 µl

- Gently mix the resolving gel mixture and fill 3/4 of the Novex gel cassette.
- Carefully overlay the gel mixture with isopropanol and wait until the polymerization is complete (~ 15 min).
- Pour off the isopropanol and wash the gel surface with MilliQ water. Carefully drain all the water out of the gel cassette
- Prepare the stacking gel mixture:

	4 %
30% Acrylamide 37.5 :1	260 µl
1.6 M Bis-Tris buffer	500 µl
MilliQ-water	1.23 ml
10% APS stock solution	20 µl
Temed	5 µl

- Gently mix the stacking gel mixture and pour it onto the gel cassette up to the top.
- Add the comb and wait until the gel is polymerized.
- Gels can be used immediately or stored at 4 °C if wrapped in wet paper towels and cling wrap.
- Remove comb and wash each slot with MilliQ water to remove unpolymerized acrylamide.
- Place gel in running chamber and fill with 1 x MES running buffer.
- Load samples and run gel at 180 V for approximately 45 min.

Bis-Tris gel-buffer:	1.6 M Bis-Tris, pH 6.4 Store at RT.
10 % APS:	10 % Ammoniumpersulfate in MilliQ water Store at -20°C.
20 x MES:	1 M MES 1 M Tris-Base 69.3 mM SDS 20.5 mM EDTA Store at RT.
4 x SDS sample buffer:	1.44 M Bis-Tris 0.64 M Bicine 4 % SDS 100 mM DTT 0.05 % Bromphenoleblue Store at -20°C.

3.2.5 Western-Blot

After separation in SDS-PAGE gels, the proteins were blotted on PVDF-membranes.

- Soak one pieces of Whatman paper in blotting buffer A, one in buffer B, and two in buffer C.
- Soak PVDF membrane in Methanol.
- Build blotting stack as follows:

- Blot for 1 h at 50 mA per gel.

Blotting buffer A: 210 mM Tris-Base
30 % v/v Methanol
pH 10,4
Store at 4°C.

Blotting buffer B: 25 mM Tris-Base
30 % v/v Methanol
pH 10,4
Store at 4°C.

Blotting buffer C: 25 mM Tris-Base
0,025 % SDS
pH 9,0 mit Borsäure (0,5 M)
Store at 4°C.

3.2.6 PonceauS staining of membranes

Correct and equal blotting of proteins was confirmed by staining the membranes with PonceauS, which unspecifically and reversibly visualizes all proteins.

- Place membrane in PonceauS solution and incubate for ~ 1 min.
- Transfer membrane into MilliQ water and gently swirl until bands are clearly visible.

Ponceau S solution: 0.2 % PonceauS
3 % Glacial acetic acid

3.2.7 Immunostaining of membranes

To visualize specific proteins the membranes were subjected to immunostaining with specific antibodies.

- Block membrane in 5% dry-milk/TBST, 3% BSA/ TBST, or TBST alone, for 1 h at RT while shaking. Blocking conditions depend on the antibody used.
- Wash blocking solution off the membrane to avoid contamination of the primary antibody. 3 x 5 min with 1 x TBST.
- Dilute primary antibody in 1x TBST and add 0.02% NaN_3. Incubate for 2 h at RT or 4°C over night with gentle shaking. Dilution and optimal incubation time depends on the antibody.
- Wash the membrane at least 3 x 10 min or longer with TBST while shaking.
- Incubate membrane with HRP-coupled secondary antibody for 1 h at RT with gentle shaking. Antibody is diluted in TBST or blocking solution.
- Wash the membrane at least 3 x 10 min or longer with TBST while shaking.
- Wash the membrane once with TBS.
- Visualize proteins with enhanced chemiluminescence and expose to film or CCD camera.

10 x TBS, pH 7.4:	1.37 M NaCl 27 mM KCl 0.25 M Tris-Base
TBS:	1:10 dilution of 10 x TBS
TBST:	1:10 dilution of 10 x TBS 0.01 % Tween-20

3.3 Immunohistochemistry

3.3.1 GRN in human tissue

Stainings were performed on paraffin-embedded tissue samples and components of the Dako REAL EnVision Detection System and Santa Cruz goat ABC Staining System were used. Tissue slices of 2 – 3 µm thickness on glass slides were treated as follows:

- Dry slices at 40°C over night.
- Incubate slices for 15 min in xylol, then rehydrate samples by immersing them in 100% → 70% → 50% Ethanol → deionized water.
- For target retrieval cook slices for 20 min in citrate buffer pH 6 using a microwave pressure cooker, then rinse in deionized water and transfer to TBST buffer.
- Incubate 10 min in Peroxidase Blockin Solution (DAKO-Kit).
- Rinse 3x in TBST.
- Block samples for 1h in 1.5% Blockin Solution (Santa Cruz-Kit) diluted in PBS.
- Incubate samples over night with primary antibody goat-anti-human Progranulin (R&D Systems), 1:250 in PBS/ 1.5% Blocking Serum, 4°C.
- Rinse 3x in TBST.
- Incubate for 30 min with biotinylated secondary antibody donkey-anti-goat (Santa Cruz-Kit), 1:2000 in PBS/ 1.5 Blocking Serum, RT.
- Rinse 3x in TBST.
- Incubate for 30 min with AB enzyme reagent (Santa Cruz-Kit), Avidin/ biotinylated HRP/ PBS 1:1:50, RT.
- Rinse 3x in TBST.
- Stain samples 1-5 min with DAB+ (DAKO-Kit), then rinse in tap water
- Stain 5 sec in Mayer's hemalaun solution, then rinse in tap water.
- Dehydrate samples by immersion in 50% → 70% → 100% Etahnol → Xylol and mount in ClearMount™ mounting solution.

3.3.2 Cd68 and GFAP in human tissue

Stainings were performed on paraffin-embedded tissue samples using the Dako REAL EnVision Detection System according to the manufacturer's instructions on an automated staining platform. Tissue slices were of 2 – 3 µm thickness and antibodies diluted as follows:

Cd68 (KP1)	1:6000
GFAP	1:4000

3.4 Molecular Biology

3.4.1 DNA preparation

Plasmid DNA from bacteria was isolated using a combination of alkaline lysis and ion-exchange columns which are the basis for almost all commercially available DNA extraction kits. For large scale DNA extraction from 250 ml bacterial cultures the JETstar plasmid

purification system from Genomed, for small scale DNA extraction from 4 ml of bacterial culture the NucleoSpin Plasmid kit from Macherey-Nagel was used. Both kits contained all the necessary buffers and solutions and the DNA extraction was performed according to the manufacturer's protocol.

3.4.2 Agarose gelelectrophoresis

To analyse DNA fragments they are separated depending on their size in an electric field on an agarose-gel matrix.

- Boil agarose in 1 x TAE buffer. The percentage of agarose depends on the size of the DNA fragments that are analyzed. 1 % agarose in 1 x TAE is most commonly used.
- Swirl the dissolved agarose and let it cool down to approximately 65°C.
- Pour agarose in gel cassette and place comb in the gel.
- Wait until the gel is solid.
- Remove comb and place gel in running chamber filled with 1 x TAE.
- Load samples and size standard and run at 100 V.
- Place gel in ethidiumbromide bath to stain DNA and incubate for 15 min.
- Wash gel once in 1 x TAE and place on UV table to take picture or excise fragments.

10 x TAE:	0.80 M Tris-Base 20 mM EDTA 1 % glacial acetic acid
1 x TAE:	1:10 dilution of 10 x TAE in MilliQ water.
Ethidiumbromide bath:	1 x TAE 10 µl Ethidiumbromide solution (10 mg/ml).

3.4.3 Gelelution

To purify PCR products from the plasmid template DNA or to remove the vector backbone after restriction digests, the DNA was loaded onto an agarose gel and the respective band excised with a razor blade. The DNA was eluted from the gel slice using the Qiagen Gel Extraction Kit according to the manufacturer's protocol. DNA was eluted in 30 µl sterile filtered MilliQ water pH 8.0.

3.4.4 Restriction-enzyme digest

For an analytic digest 1 µg DNA was digested in a final volume of 20 µl with either one or two enzymes at the same time. The analytic digests were incubated at 37°C or the respective optimal temperature for the enzyme, for 1 h. For preparative digests the volume was increased due to the larger amounts of enzyme and DNA used. Preparative digests were incubated for 3 – 4 h at 37°C or, in the case of PCR-product double-digests, over night at 37°C.

Analytic digest:

DNA	1 µg	
Enzyme	0.5 µl	(at least 1 U)
100 x BSA stock	0.2 µl	
10 x Enzyme buffer	2 µl	
Water	x µl	(adjust total volume to 20 µl)

Preparative digest:

DNA	5 – 8 µg	
Enzyme	2 µl	
100 x BSA stock	0.5 µl	
10 x Enzyme buffer	5 µl	
Water	x µl	(adjust total volume to 50 µl)

3.4.5 Dephosphorylation of DNA

To avoid re-ligation of a vector after digestion with restriction enzymes it was treated with a phosphatase which removed the 5' phosphoryl groups from DNA.

Example reaction:

Digest	50 µl
10 x Antarctic phosph. buffer	6 µl
Antarctic phosphatase	1 µl
Water	3 µl

- Incubate reaction for 1 h at 37°C.
- Heat inactivate enzyme for 20 min at 65°C.
- Purify reaction via gelelution.

3.4.6 Ligation of DNA

The ligation of cohesive ended DNA was performed in a total volume of 20 µl. Plasmid and insert were mixed in a 1:1 molar ratio. With the notably smaller size of the insert fragment this translated into an approximately 1:3 mixture of plasmid to insert. The concentration of the fragments was estimated from their signal on an agarose gel. The enzyme used for the ligation was the T4 DNA ligase which catalyzes the formation of a phosphodiester-bond between two juxtaposed 5' phosphate and 3' hydroxyl termini in duplex DNA.

- Thaw 10 x ligase buffer on ice. Contains ATP! Avoid storage at RT or 4°C.
- Prepare ligation mixture in a small volume, preferably 20 µl or less.

Plasmid DNA	x µl
Insert DNA	x µl
10 x buffer	2 µl
Ligase	1 µl
Water	x µl to a final volume of 20 µl

- Also prepare a ligation control containing water instead of the insert DNA to assess possible religation of the vector.
- Incubate over night at 16°C and then transform into bacteria.

3.4.7 Transformation

To propagate plasmids, the DNA was transformed into bacteria, positive clones confirmed, and DNA preparations performed.

- Thaw competent bacteria on ice.
- Add DNA (plasmid or ligation) and incubate for 30 min on ice.
- Heat shock for 90 sec in a 42 °C waterbath.
- Place on ice for 2 min.
- Add 1 ml pre-warmed (37°C) SOC.
- Incubate at 37°C for 1 h.
- Pellet bacteria by centrifugation at 1000 rcf for 3 min.
- Resuspend pellet in 100 µl SOC and spread on agar plate with appropriate selection antibiotic.
- Incubate over night at 37 °C.

SOB medium:	8 g tryptone
	2 g yeast extract
	0.2 g NaCl
	400 ml de-ionized water
	Autoclave and store at 4°C.

SOC medium:	10 ml SOB medium
	200 µl 2 M Glucose (sterile filtered)
	Store at 4°C.

LB medium:	1 % Trypton
	0.5 % Yeast extract
	1 % NaCl
	Store at 4°C.

LB-agar:	1 % Trypton
	0.5 % Yeast extract
	1 % NaCl
	1.5 % Agar
	Store at 4°C.

Ampicillin Stock:	50 mg/ml Ampicillin
	Sterile filter and store at -20°C.

3.4.8 Polymerase chain reaction (PCR)

PCR facilitates in vitro amplification of specific DNA sequences using a thermostable DNA polymerase. During the PCR the DNA becomes thermally denatured and hybridizes with short oligonucleotides that are subsequently elongated by a DNA polymerase. These steps, denaturation, hybridization/annealing and elongation are repeated several times and result in amplification of the DNA stretch that was flanked by the primer sequences.

PCR protocols vary, depending on the template DNA, the oligonucleotide sequence, the polymerase and the length of the amplified DNA fragment.

3.4.9 Cloning with Infusion® Technology

To insert the GRN cDNA into the pRetroX-Tight-Pur vector Infusion® technology was used according to the manufacturer's instructions. The ClaI and EcoRI restriction sites of the vector were chosen as insertion site.

3.4.10 Cloning with Gateway® Technology

Gateway technology (site-directed recombination) was used to transfer pre-miRNA expression cassettes from pcDNA6.2-GW/EmGFP-miR vectors into the lentiviral expression vector pLenti6/V5-DEST.

- Set up BP reaction:

15-150 ng	pcDNA6.2-GW/EmGFP-miR-x
150 ng	pDONR221
ad 8 µl	TE buffer, pH 8
2 µl	BP Clonase™ II enzyme mix

- Incubate for 1 h at 25°C.
- Add 1µl Proteinase K and incubate 10 min at 37°C.
- Transform competent *E. coli* DH5α and select for kanamycin-resistant entry clones.
- Extract DNA and confirm vector integrity by analytic digests.
- Set up LR reaction:

50-150 ng	entry clone (pDONR221-miR-x)
150 ng	pLenti6/V5-DEST
ad 8 µl	TE buffer, pH 8
2 µl	LR Clonase™ II enzyme mix

- Incubate for 1 h at 25°C.
- Add 1 µl Proteinase K and incubate for 10 min at 37°C.
- Transform competent *E.coli* Stbl3 and select for ampicillin-resistant destination clones.
- Extract DNA and confirm vector integrity by analytic digests.

3.4.11 DNA-Sequencing

All DNA constructs were sequenced at Genterprise GmbH in Mainz.

3.4.12 RNA isolation

Total RNA from cells was isolated via Guanidinium thiocyanate-phenol-chloroform extraction.

- Add 1 ml TRIzol per well (6well). Pass cell lysate several times through pipette and transfer to 1,5 ml tube.
- Incubate for 5 min at RT.
- Add 0.2 ml of chloroform and shake vigorously by hand for 15 sec.
- Incubate for 2-3 min at RT.
- Centrifuge at 12000 rcf for 15 min at 4°C.
- Transfer the aqueous (=upper) phase to a fresh tube and precipitate RNA by adding 0.5ml isopropanol, incubate for 10 min at RT.
- Centrifuge at 12000 rcf for 10 min at 4°C.
- Remove supernatant and wash RNA pellet once with 1 ml 75% ethanol, vortex.
- Centrifuge at 7500 rcf for 5 min at 4°C.
- Briefly air-dry pellet (5-10 min) and dissolve RNA in RNase-free water by passing through pipette and incubating for 10 min at 55 – 60°C.

3.4.13 cDNA Synthesis

cDNA synthesis was performed using 3 µg RNA, random hexamer primers and SuperScript™ II Reverse Transcriptase (Invitrogen) according to the manufacturer's protocol.

- Dilute 3 µg RNA in 10 µl H_2O
- Add 1 µl dNTPs (10 mM each) and 1 µl $pd(N)_6$ primers (25 µM)
- Incubate for 5 min at 65°C in a thermocycler
- Add 4 µl 5x First Strand buffer and 2 µl DTT (0.1M)
- Incubate for 2 min at RT
- Add 1 µl SuperScript™ II Reverse Transcriptase
- Incubate for 10 min at 25°C, followed by 50 min at 40°C and 15 min at 70°C in a thermocycler
- Store cDNA at -20°C

3.4.14 Realtime RT-PCR

Realtime RT-PCR was performed on a StepOnePlus™ platform (Applied Biosystems) using Platinum® SYBR® Green qPCR SuperMix-UDG. The samples were analyzed using the ddCt method.

- Prepare Mastermix as needed and aliquot 20 µl/well into an appropriate 96-well plate (MicroAmp Fast Optical 96-Well Reaction Plate).

  1x: 6,0 µl H2O
  12,5 µl SYBR-Green
  0,75 µl forward Primer
  0,75 µl reverse Primer

- Add 5 µl sample cDNA to each well. Depending on expression level of the target gene, the used cDNA is usually diluted 1:25 or 1:50. Always include a H_2O control!
- Seal plate with appropriate adhesive film (MicroAmp Optical Adhesive Film) and run PCR.

3.4.15 Microarray Expression Profiling

Microarray experiments from cell lines were performed in collaboration with the 'Biologisch-Medizinisches Forschungszentrum (BMFZ)', a core facility of the Heinrich-Heine-University. Samples were prepared using the Gene Chip® 3' IVT Express Kit (Affymetrix) according to the manufacturer's instructions. Hybridization on GeneChip® Human Genome U133 Plus 2.0 Arrays (Affymetrix) was performed by the BMFZ. Data was analyzed with Gene Spring GX software.

Microarray experiments from tumor samples constituing the 'Glioma Core Collection' of the NGFN2 Brain Tumor Network were performed at the German Cancer Research Center (DKFZ) in Heidelberg. For this purpose, a 35,035 oligonucleotide microarray representing approximately 25,100 unique genes and 39,600 transcripts was generated for the analyses of brain tumors. The microarray was complemented by 500 additional 70mer probes, which are specific for genes in the commonly deleted chromosomal regions 10q24-qter and 22q (http://www.science.ngfn.de/6_120.htm).

3.5 *In vivo* experiments

In vivo experiments were performed by Dr. Philipp Pfenning at the German Cancer Research Center (DKFZ)/ Universitätsklinikum Heidelberg (Abt. Neuroonkologie). All animal work was approved by the governmental authorities (Regierungspraesidium Karlsruhe, Germany) and supervised by institutional animal protection. A total of 5,000 murine SMA560 glioma cells suspended in PBS were stereotactically implanted into the right striatum of 6-12 week old VM/Dk mice (inhouse breeding facility, German Cancer Research Center, Heidelberg, Germany) at a depth of 3 mm.

Tumor volume was assessed in five mice per group on day 14 and 21 after tumor cell inoculation by magnetic resonance imaging (MRI). MRI was performed using a 1.5 tesla whole-body MR-scanner (Siemens Symphony, Munich, Germany) in combination with a custom-made radio-frequency coil for excitation and signal reception. Brain tumors were located on T2w turbo spins echo images (TE, 109 ms; TR, 4000; FoV, 40 x 30 mm; matrix, 128; voxel size, 0.3 x 0.3 x 1 mm^3). T1w imaging was performed using a high resolution spinecho sequence (TE, 600ms; TR, 14 ms; field of view, 40 x 40; matrix, 192; voxel size, 0.2 x 0.2 x 1 mm^3) three minutes after intraperitoneal administration of Gd-DTPA contrast agent (Magnevist, Bayer Schering Pharma, 0.5 mmol/ml). Statistical significance in tumor volumes was assessed by two-sided Student's t-Test. Values of $p < 0.05$ were considered significant and asterisked. MR-Imaging was performed by Dr. Manfred Jugold at the 'Small Animal Imaging Center' of the German Cancer Research Center, Heidelberg, Germany.

For the histological assessment of tumor growth, two mice per group were sacrificed at postoperative day 21, brains were isolated and cryosectioned (9 µm) for further histological analysis.

At least 11 mice per group were used for survival analysis according to the Kaplan-Meier method. Mice were sacrificed by an overdose of anaesthetic at the onset of grade 2 neurological symptoms. Neurological symptoms were assessed daily according to modified neurological scores. Grade 0: normal; Grade 1: tail weakness or tail paralysis; Grade 2: hind leg paraparesis or hemiparesis; Grade 3: hind leg paralysis or hemiparalysis; Grade 4: tetraplegia, moribund stage or dead.

4 RESULTS

4.1 Progranulin expression in normal brain tissue

Initial studies using Northern blot analysis in rat brain homogenates reported relatively low levels of GRN expression in the brain (Bhandari *et al.* 1993). However, in adult rodent brains analyzed by *in situ* hybridization, GRN mRNA has been shown to be abundant in neuronal cells of the cerebral cortex, pyramidal neurons in the hippocampus and Purkinje and granule cells in the cerebellum. In contrast, no expression of GRN transcripts was observed in mesenchymal and glial cells (Daniel *et al.* 2000). Several immunohistochemistry studies in human brain tissue confirmed that GRN immunoreactivity is restricted to neuronal and microglial populations (Ahmed *et al.* 2007, Baker *et al.* 2006, Mackenzie *et al.* 2006, Mukherjee *et al.* 2006). Consistent with the published data, we found that in normal brain GRN is predominantly expressed in neurons and microglia cells, while expression in other cell populations was completely absent or very weak. In the cortex,

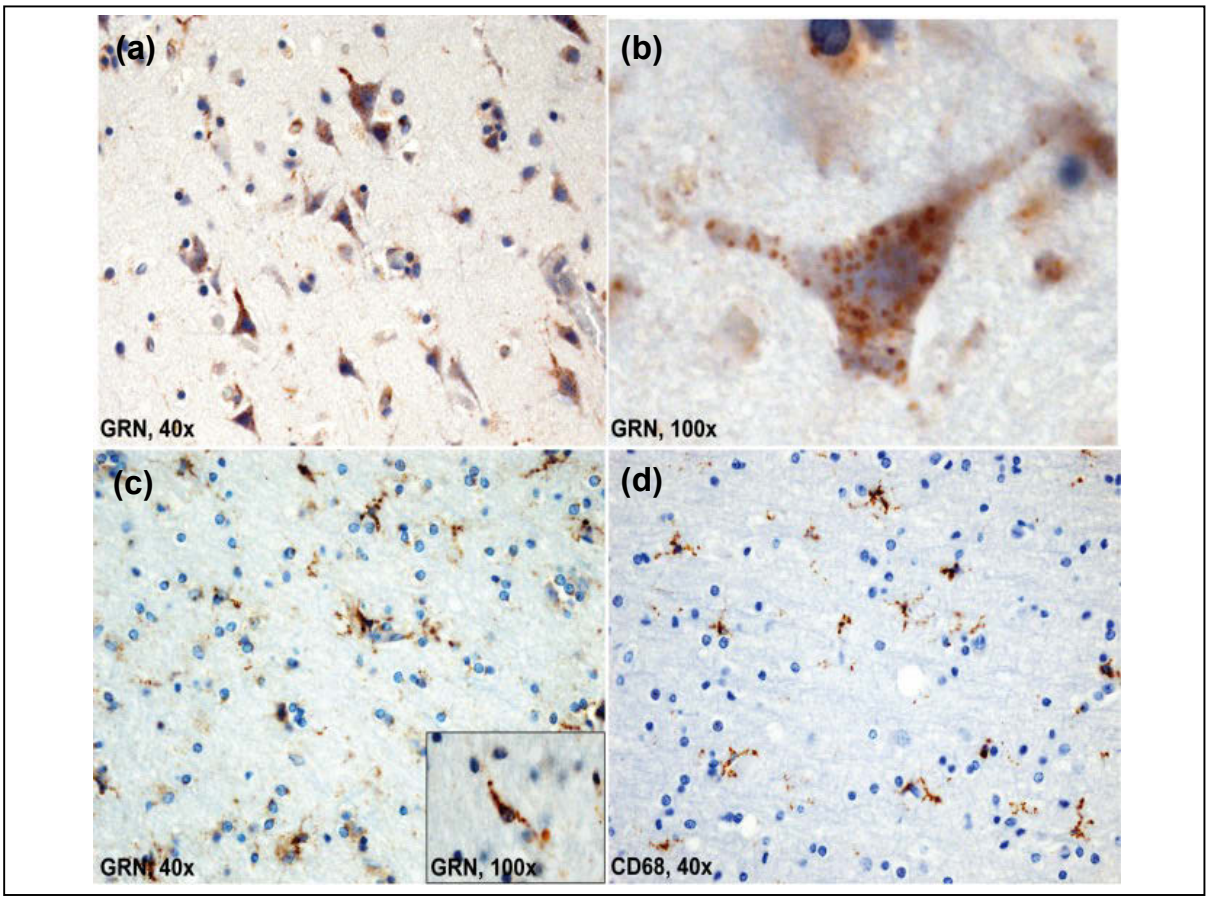

Figure 7: Immunohistochemistry in normal brain tissue samples. Samples were stained with a polyclonal antibody directed against human progranulin (R&D Systems). **(a)** In cortex, large neurons stained intensely for GRN. **(b)** Higher magnification of a single neuron demonstrated punctate vesicular staining indicative of GRN expression in the secretory pathway. **(c)** In white matter, only weak GRN expression was observed. Staining was restricted to microglia cells, whereas astrocytes displayed no GRN expression. Inset: Higher magnification of a single microglia cell expressing GRN. **(d)** Immunostaining for the microglial marker CD68 showed a comparable staining pattern in the white matter. (Original magnifications 400x and 1000x)

staining with an antibody against human GRN (R&D Systems) revealed highly restricted expression only in neuronal cells (Fig. 7a). In accordance with GRN being a secreted protein, we found a vesicular staining pattern indicative of GRN expression in the secretory pathway (Fig. 7b). Within the white matter, GRN expression was observed only in microglial cells, whereas no distinct staining could be found in astrocytic or oligodendroglial cells (Fig. 7c). Immunostaining with an antibody against the microglial marker protein CD68 demonstrated a comparable staining pattern in the white matter, indicating that the immunoreactivity with the GRN antibody was indeed due to GRN expression in microglia cells (Fig. 7d).

In addition, immunostaining in serial brain sections of an individual with massive astrogliosis due to a pathology unrelated to cancer was performed. This demonstrated that even in highly activated astrocytes there is no detectable expression of the progranulin protein. Antibodies against the astroglial marker protein GFAP resulted in very prominent staining of numerous astrocytes (Fig. 8a). In contrast, immunostaining for CD68 showed that microgliosis was not present at this lesion (Fig. 8b). With the antibody against progranulin, no labelling of reactive astrocytes could be detected, supporting the restriction of GRN expression to cells of neuronal and microglial origin (Fig. 8c).

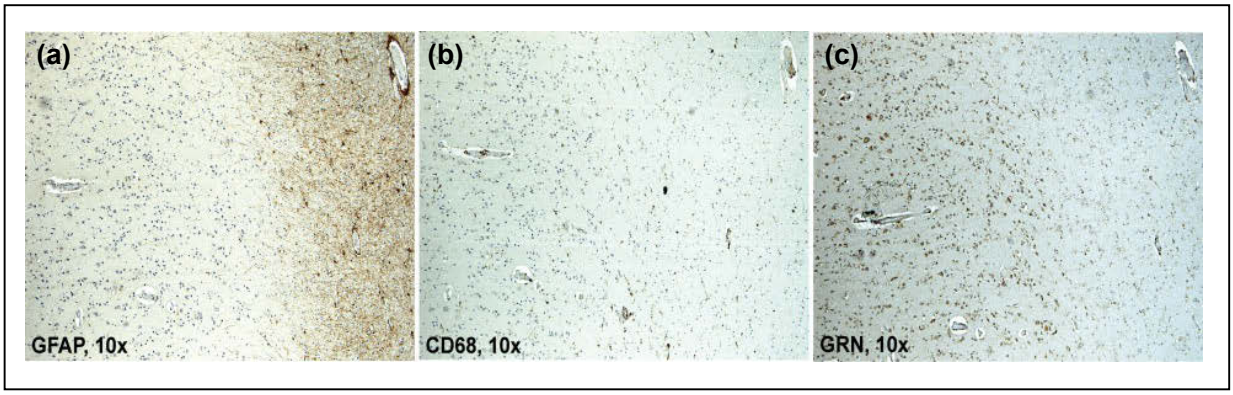

Figure 8: Immunohistochemistry in serial sections of a brain area with astrogliosis. Samples were stained with antibodies against GFAP, CD68 and GRN. **(a)** GFAP staining revealed massive astrogliosis in the right part of the tissue section. **(b)** Distribution of microglia was normal. **(c)** Anti-GRN antibodies did not stain reactive astrocytes, but expression in neurons and microglia was observed. (Original magnification 100x)

4.2 Progranulin expression in glial brain tumors

In contrast to non-transformed glial cells, glioma cells were shown to express GRN. Elevated expression of GRN in brain tumors over normal brain tissue was first identified in a microarray study of eight glioma samples, which showed 3-30 fold overexpression compared to two normal brain specimens. The differential expression was confirmed by Northern blotting, with GRN transcripts detectable in 18 of 21 tumor samples (11 of 12 glioblastomas (WHO grade IV), 5 of 6 anaplastic astrocytomas (WHO grade III), 2 of 2 anaplastic

oligodendroglioma (WHO grade III), and 0 of 1 oligodendroglioma (WHO grade II)), but not in 3 normal brain samples. In the same study, quantification of *in situ* hybridization data with a GRN antisense riboprobe in 10 tumor samples (3 pilocytic astrocytomas (WHO grade II), 2 oligodendrogliomas WHO grade II, 2 anaplastic astrocytomas (WHO grade III), and 2 glioblastomas (WHO grade IV)) compared to 2 normal brain samples revealed significantly higher expression of GRN in high grade gliomas (Liau *et al.* 2000). A second study independently reported differential expression of GRN in 4 glioblastoma tumors versus 3 temporal lobe normal brain samples by gene expression profiling, but the authors did not conduct any further experiments to verify these observations (Markert *et al.* 2001).

These previous studies suggested that GRN might be upregulated in glioma cells during tumorigenesis. However, both studies included only a small number of samples from a heterogenous group of glial brain tumors. Furthermore, expression of GRN was only measured at the mRNA transcript level and no studies to confirm differential protein expression were reported. Consequently, in this thesis, expression levels of GRN were analyzed in much larger tumor collectives both on the mRNA and protein level. Initially, GRN expression was studied in a total of 48 tumor samples (4 astrocytomas, 6 oligodendrogliomas, and 3 oligoastrocytomas (WHO grade II), 5 anaplastic astrocytomas, 9 anaplastic oligodendrogliomas, and 8 anaplastic oligoastrocytomas (WHO grade III), and 13 primary glioblastomas (WHO grade IV)) by quantitative real-time reverse transcription PCR. Compared to cDNA reverse transcribed from commercially available normal brain RNA (Bio Chain) all tumors except one oligoastrocytoma WHO grade II showed 1.5 to 22.5 fold increased expression of GRN. To assess whether GRN expression levels correlated with the malignancy of the tumors, the samples were grouped according to their WHO grade (Fig. 9a). Statistical analysis using one-way ANOVA with Tukey's post tests revealed that all three groups, WHO grade II, III, and IV, displayed significantly elevated GRN expression over normal brain samples (cDNA reverse transcribed from commercially available RNAs of frontal lobe, temporal lobe, parietal lobe, and occipital lobe (Stratagene), plus 3 surgically resected normal brain tissue samples). There was no significant difference between the groups of WHO grade II and WHO grade III tumors, indicating that GRN expression is unlikely associated with the progression to higher grade tumors, but rather with tumor initiation or early tumorigenesis. However, in WHO grade IV samples, which in this series comprised only primary glioblastomas that develop *de novo* in a relatively short time period, GRN expression levels were significantly higher as compared to WHO grade III samples.

The differential expression of GRN was also confirmed in a second independent set of tumors, the Glioma Core Collection of the NGFN Brain Tumor Network. This set consisted of 7 normal brain samples, 8 astrocytomas (WHO grade II), 13 anaplastic astrocytomas (WHO grade III), 11 secondary and 42 primary glioblastomas (WHO grade IV) (Fig 9b). Microarray

gene expression profiling in these tumors detected significantly elevated GRN expression levels in all tumor subgroups over normal brain samples. Entirely consistent with our qPCR results in the first set of tumors, tumor progression from low-grade astrocytomas to anaplastic astrocytomas and secondary glioblastomas was not associated with further elevation of GRN expression. However, primary glioblastoma samples again displayed a significantly higher expression of GRN compared to anaplastic astrocytomas of WHO grade III.

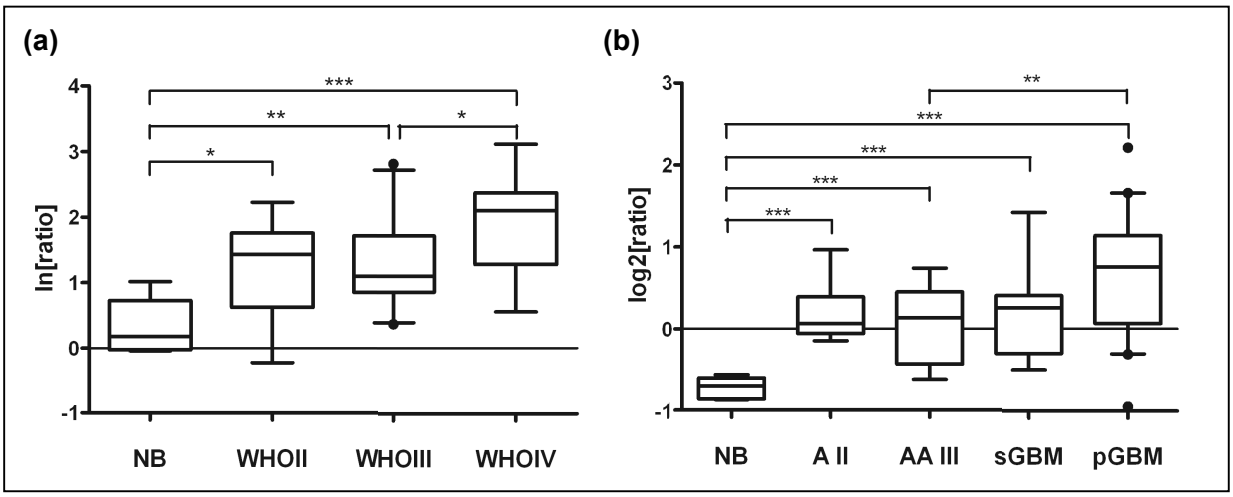

Figure 9: GRN expression in human gliomas. **(a)** GRN transcript levels in reverse transcribed RNA extracted from 48 human gliomas were measured by quantitative real-time PCR. The samples were grouped according to their WHO grade, and GRN levels were found to be significantly upregulated in all three groups as compared to normal brain samples (NB). In addition, expression levels in WHO grade IV glioblastomas were significantly higher than in the group of WHO grade III tumors. Statistical analysis: One-way ANOVA followed by Tukey's multiple comparison tests; * $p<0.05$, ** $p<0.01$, *** $p<0.001$. **(b)** GRN gene expression levels were analyzed in the microarray gene expression profiles of the Glioma Core Collection, consisting of 74 tumor samples. GRN expression levels were significantly upregulated in all tumor subgroups versus normal brain samples. In addition, primary glioblastomas displayed significantly higher expression levels compared to anaplastic astrocytomas. NB, normal brain; AII, astrocytomas (WHO grade II); AAIII, anaplastic astrocytomas (WHO grade III); sGBM, secondary glioblastomas (WHO grade IV); pGBM, primary glioblastomas (WHO grade IV). Statistical analysis: Mann-Whitney test, * $p<0.05$, ** $p<0.01$, *** $p<0.001$.

To confirm the overexpression of GRN on the protein level, a tissue microarray of paraffin embedded tumor samples was analyzed by immunohistochemistry (Fig. 10). The samples included 7 astrocytomas (WHO grade II), 13 anaplastic astrocytomas (WHO grade III), and 36 glioblastomas (WHO grade IV) and were stained with a polyclonal antibody against human GRN (R&D systems). The protein expression levels were semiquantitatively scored (0-3) based on staining intensity and percentage of positively stained cells, and stainings in normal brain tissue samples being defined as score 1. GRN protein expression was detected in all tumor samples except one glioblastoma with a sarcomatous component. The staining

was localized predominantly to the cytoplasm of tumor cells and was frequently also present in endothelial cells. Furthermore, a trend towards higher staining intensity in high-grade glioblastomas compared to lower-grade astrocytomas was observed with 30/36 (83%) WHO grade IV glioblastomas scoring 2 or 3.

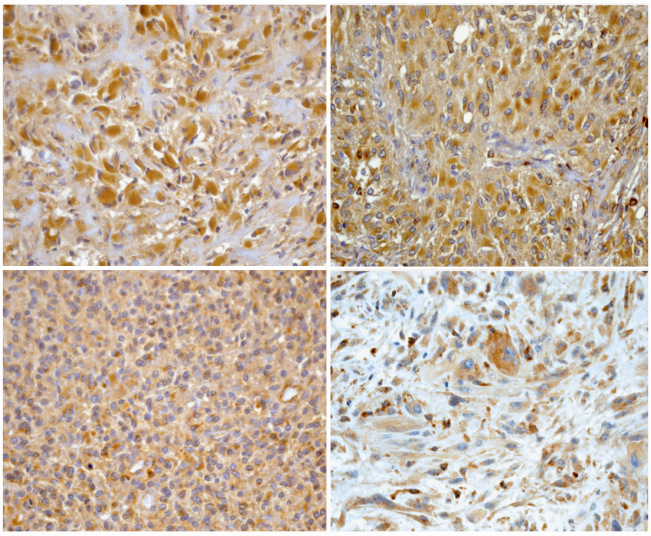

	0	1	2	3	total
A II	0	2	4	1	7
AA III	0	6	3	4	13
GBM IV	1	5	19	11	36

Figure 10: Tissue microarray of paraffin embedded glioma tumor samples. Samples were stained with a polyclonal antibody directed against human progranulin (R&D Systems). 7 astrocytomas (AII, WHO grade II), 13 anaplastic astrocytomas (AAIII, WHO grade III) and 36 glioblastomas (GBM IV, WHO grade IV) were included. GRN expression was detected in all tumors with the exception of one glioblastoma with a sarcomatous component. Four exemplary stainings are shown. Semiquantitative scoring of protein expression (0-3) was based on percentage and staining intensity of positively stained cells. Stainings in normal brain tissue samples were defined as score 1. Generally, highly malignant glioblastomas displayed more abundant and more intense GRN staining as compared to lower grade astrocytomas.

In addition, Western blot analysis confirmed elevated GRN protein expression in tumor samples compared to normal brain tissue (Fig. 11a). Lysates of snap-frozen glioblastoma and normal brain tissue samples were subjected to SDS-PAGE electrophoresis and Western blotting with a polyclonal antibody directed against human GRN (Zymed). GRN protein expression was clearly present in all tumor samples, whereas expression could not be detected in 2 normal brain samples. The GRN protein runs at approximately 90 kDa and, depending on its glycosylation status, is detected as a rather diffuse band. Tissue culture supernatants from a GRN overexpressing cell line (see below) were used as a positive control. Furthermore, in established glioma cell lines, variable but robust GRN expression could be detected by Western blot analysis of cell lysates (Fig. 11b).

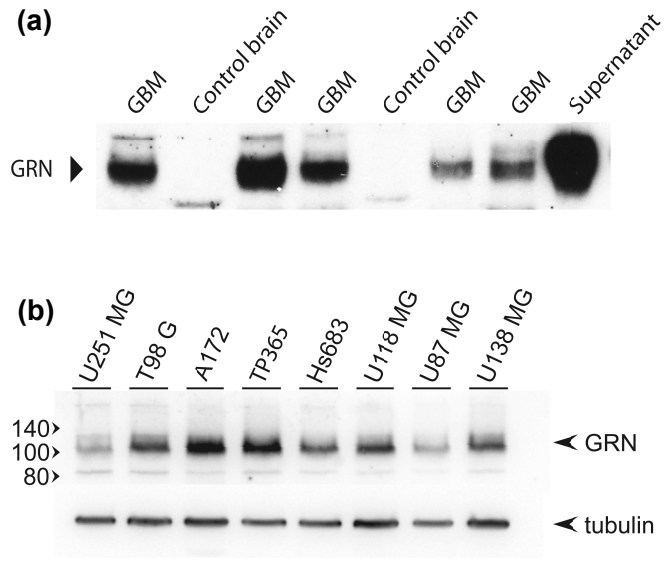

Figure 11: Western blot analysis of GRN protein levels in human gliomas and established glioma cell lines. **(a)** Lysates of frozen tumor and normal brain tissue samples were subjected to SDS-PAGE electrophoresis followed by immunoblotting with an antibody directed against human GRN (Zymed). GRN protein was clearly present in tumor samples, whereas expression could not be detected in normal brain tissue. **(b)** Lysates of established glioma cell lines were analysed as in (a). Variable but robust expression was detected in all tested cell lines.

4.3 Generation of cell lines with elevated or reduced GRN expression

As tools to investigate the functional role of GRN in glial tumors, a number of stable cell lines with modified GRN expression levels were generated based on established glioma cell lines. Cell lines with low basal GRN expression levels were chosen to generate cells with overexpression of GRN. Vice versa, cell lines with higher basal expression were chosen for GRN knock down studies.

To obtain cell lines with inducible overexpression of GRN, the retroviral Retro-X™ Tet-On Advanced® Inducible Expression System (Clontech Laboratories) was used. This vector system consists of two plasmids that need to be introduced in two steps into a cell line to achieve inducible expression of a cDNA of interest. First, the human glioma cell lines U251MG, T98G, and U87MG and the murine glioma cell line SMA560 were infected with the pRetro-X Tet-On Advanced vector, which constitutively expressed the tetracycline-controlled transactivator rtTA-Advanced. Stable cell lines were generated by selection with G418. Subsequently, resulting mass cultures were subcloned to obtain single clone cultures, and the quality of these subclones was assessed using a luciferase assay. In these experiments, cells were infected with the pRetroX-Tight-Pur-Luc control vector and the induction of luciferase activity after treatment with doxycycline was measured (Fig. 12a). Subclones with high inducibility and low background of luminescence were chosen for subsequent studies. The GRN cDNA was cloned into the pRetro-X-Tight-Pur vector. In this vector, GRN expression is under the control of the inducible response promoter P_{Tight}. Thus, upon induction in the presence of doxycycline, the rtTA-Advanced transactivator binds to the P_{Tight}

promoter on the response vector and activates transcription of the downstream gene GRN. Double-stable cell lines were generated by infection of transactivator-expressing single clones and selection with puromycin. The human cell lines U251MG Tet-On-GRN, T98G Tet-On-GRN, and U87MG Tet-On-GRN were used as mass cultures, whereas the murine cell line SMA560 Tet-On-GRN was again subcloned to obtain a single clone culture. To check proper expression of the GRN gene in response to doxycycline induction, all inducible cell lines and their respective parental cell lines were treated over night with complete medium with or without the supplement of 100ng/ml doxycyline. Cell lysates were generated and GRN expression was analysed by SDS-PAGE and Western blot analysis with a GRN antibody (Zymed). As shown in Figure 12b, all inducible cell lines exhibited robust overexpression of GRN upon induction with doxycycline. However, some leakage of GRN expression in the non-induced state of the cell lines as compared to the parental cell lines was also observed.

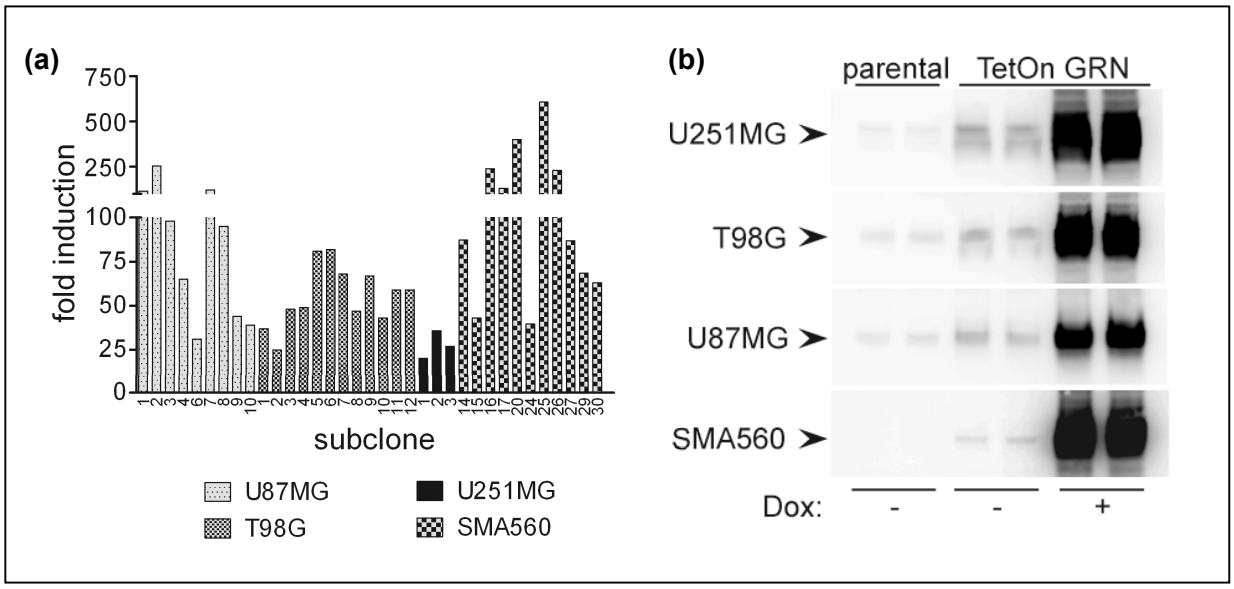

Figure 12: Generation of glioma cell lines with inducible overexpression of GRN. **(a)** Cell lines stably infected with the tetracycline-controlled transactivator were subloned and tested for inducibility using a luciferase assay. Subclones were transiently infected with the pRetroX-Tight-Pur-Luc vector and cultured with or without doxycycline. Fold induction of luciferase activity after treatment was measured. **(b)** Subclones stably infected with the pRetroX-Tight-Pur-GRN vector. Inducibility of GRN overexpression by doxycyline treatment (100ng/ml doxycyclin for 24h) was verified by Western blot analysis of cell lysates with an antibody directed against human GRN (Zymed). All cell lines showed robust overexpression after treatment with doxycycline. Slightly increased expression levels were also observed in the non-induced state as compared to the respective parental cell lines.

In addition to the inducible cell lines, stable cell lines with constitutive overexpression of GRN were generated. The GRN cDNA was cloned into the retroviral shuttle vector pLHCX, and

the same cell lines, U251MG, T98G, U87MG, and SMA560 were transduced with retroviral vector preparations. GRN overexpressing cells were selected with hygromycin, and overexpression was verified by Western blot analysis (Fig. 13a). To exclude the possibility that changes in the stable cell lines were caused by the hygromycin selection rather than the GRN overexpression, control cell lines with stable expression of the empty pLHCX vector were established.

Since all human glioma cell lines examined expressed basal amounts of GRN that might be sufficient to exert its putative function (see Fig. 11b), we considered the possibility that further elevation of GRN expression might not have a detectable effect on the growth properties of these cell lines. Therefore, additional cell lines with reduced GRN expression were generated. For this approach, the Block-iT™ Pol II miR RNAi Expression System (Invitrogen) was used. Different miRNA sequences were cloned into the entry vector pcDNA6.2-GW/EmGFP-miR, and the pre-miRNA expression cassette was subsequently shuttled into a lentiviral expression vector using Gateway Technology. The human glioma cell lines TP365, A172, and U138 were transduced with lentiviral preparations of the vectors pLenti6/V5-DEST_EmGFP-miR-control, pLenti6/V5-DEST_EmGFP-miR-GRN201, or pLenti6/V5-DEST_EmGFP-miR-GRN2140. The selected miRNA sequences target the GRN mRNA in the coding region or in the 3'UTR, whereas the control vector contains a scrambled sequence that is predicted not to target any known vertebrate gene. Stable cell lines were selected with blasticidin and the knockdown efficiency of the two miRNAs as compared to the scrambled control miRNA was evaluated by Western blot analysis. This confirmed strongly reduced GRN expression with both miRNA sequences (Fig. 13b).

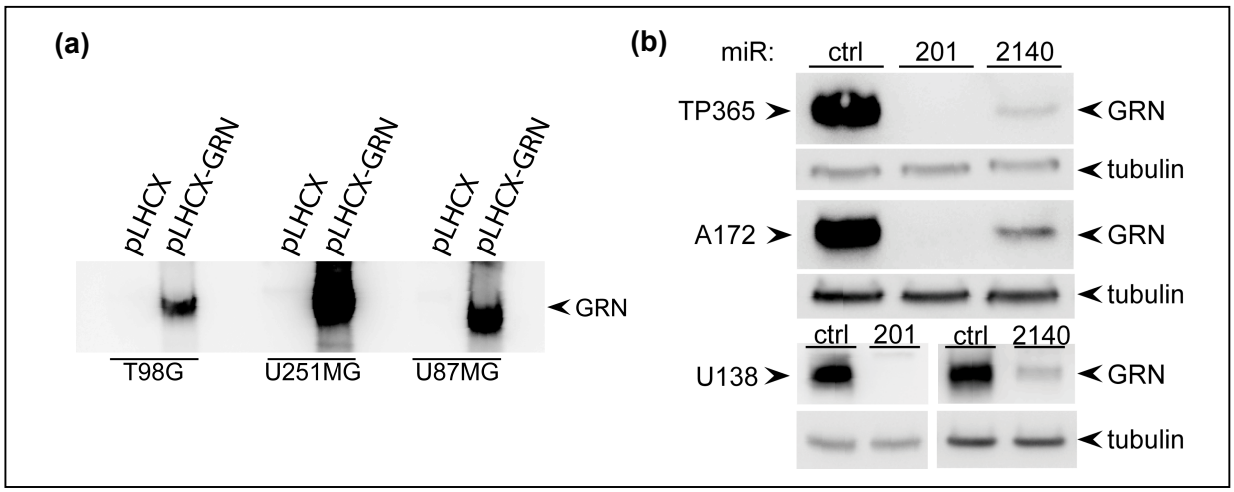

Figure 13: Glioma cell lines with elevated or reduced GRN expression levels. Western blot analysis using an antibody directed against human GRN (Zymed) of **(a)** Cell lysates from cell lines with constitutive overexpression of a retroviral GRN construct. Strong overexpression of GRN was detected compared to the respective empty vector control cell lines. **(b)** Cell lysates from cell lines expressing miRNA constructs targeting the GRN mRNA (201/2140) or a scrambled control miRNA (ctrl). Excellent knockdown efficiency was achieved with both miRNA contructs. Tubulin protein levels are shown as a loading control.

4.4 Functional characterization of GRN cell lines

4.4.1 Microarray gene expression profiling

By microarray gene expression profiling, we aimed to identify target genes that might be regulated by GRN in human glioma cell lines. To analyze gene expression profiles of cell lines with either GRN overexpression or miRNA-mediated knockdown of GRN expression, total RNA was extracted using TRIzol reagent. cDNA synthesis, *in vitro* transcription and the synthesis of fragmented, labelled aRNA for array hybridization was performed using the Gene Chip® 3' IVT Express Kit (Affymetrix). Hybridization on Affimetrix GeneChip® Human Genome U133 Plus 2.0 arrays was performed by the core facility of the Heinrich-Heine-University Düsseldorf (BMFZ), and resulting data was analyzed with the software GeneSpring.

In a first set of experiments, we analyzed the gene expression profiles of the T98G Tet-On-GRN, U251MG Tet-On-GRN, and U87MG Tet-On-GRN cell lines after induction of GRN expression with 100ng/ml doxycycline for 48 hours in serumfree medium as compared to the non-induced condition. Statistical analysis of the resulting data sets by a paired t-test with subsequent correction for multiple testing did not reveal any differentially expressed genes between the two groups. Analysis without correction (fold change ≥ 1.5, p-value ≤ 0.05) resulted in a list of 13 known genes that were differentially regulated (Table 1). However, none of these genes could reproducibly be validated by RT-PCR (Fig. 14). Note that GRN was overexpressed in these cell lines from a cDNA construct. Therefore, as expected, GRN itself was not detected by the Affymetrix probes that target sequences of the 3' untranslated regions.

Table 1

Probe Set ID	p-value	regulation	Gene Symbol	Gene
1567224_at	0,001	down	HMGA2	high mobility group AT-hook 2
224563_at	0,003	down	WASF2	WAS protein family, member 2
242762_s_at	0,004	down	FAM171B	family with sequence similarity 171B
213125_at	0,008	down	OLFML2B	olfactomedin-like 2B
219387_at	0,018	down	CCDC88A	coiled-coil domain containing 88A
232238_at	0,024	down	ASPM	asp (abnormal spindle) homolog, microcephaly associated (Drosophila)
235577_at	0,024	down	ZNF652	zink finger protein 652
242918_at	0,043	down	NASP	nuclear autoantigenic sperm protein (histone-binding)
230417_at	0,02	up	GALNTL1	UDP-N-acetyl-alpha-D-galactosamine:polypeptide N-acetylgalactosaminyltransferase-like 1
221841_s_at	0,021	up	KLF4	Krüppel-like factor 4 (gut)
1556340_at	0,035	up	MAPK12	mitogen-activated protein kinase 12
242918_s_at	0,036	up	GALNTL1	UDP-N-acetyl-alpha-D-galactosamine:polypeptide N-acetylgalactosaminyltransferase-like 1
209114_at	0,043	up	TSPAN1	tetraspanin 1

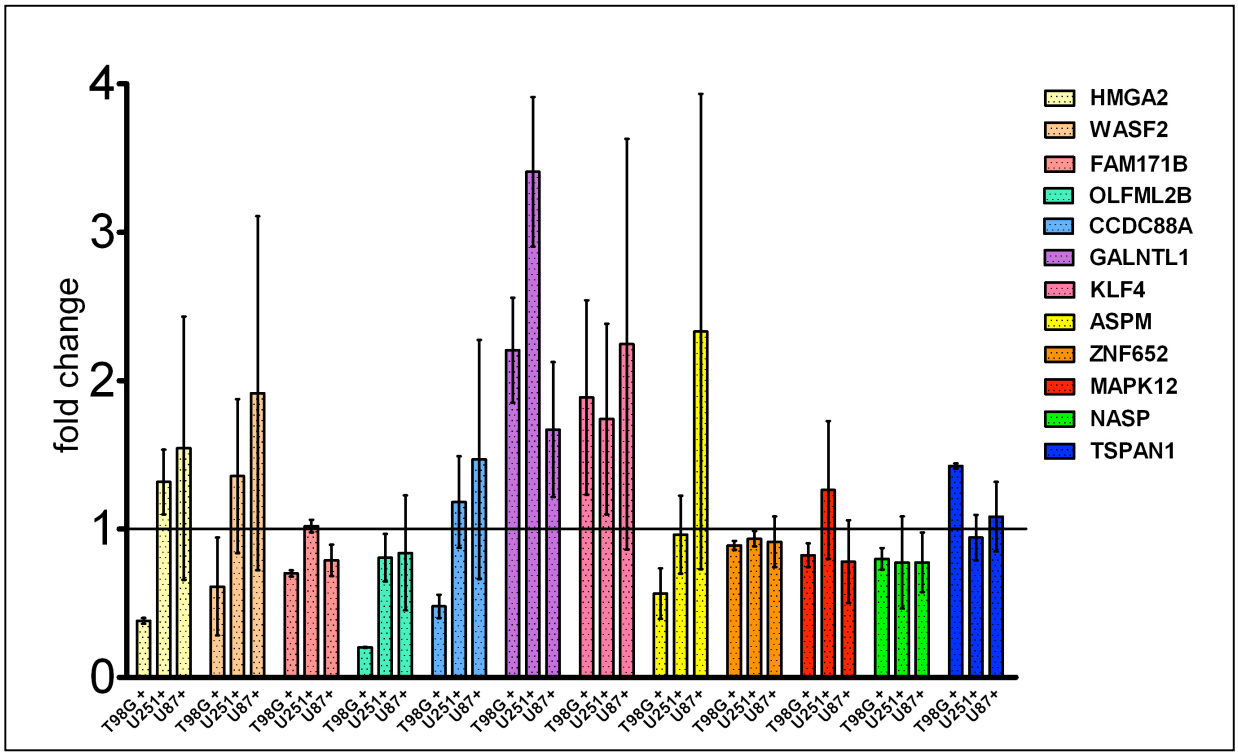

Figure 14: Validation of microarray data by real time RT-PCR (Tet-On-GRN cell lines). Differentially expressed genes listed in Table 1 were analyzed by real time RT-PCR using samples from two independent RNA preparations. Differential expression could not be reproducibly validated for any of the genes. Data is shown as fold change compared to the respective control sample (non-induced state of the cell lines).

A second microarray experiment was performed with the TP365, A172 and U138 cell lines expressing the miR-GRN201 construct as compared to the corresponding control cell lines expressing the scrambled control miRNA. Consistent with the results from the GRN overexpressing cell lines, statistical analysis of the obtained data with a paired t-test and subsequent correction for multiple testing revealed no differentially expressed genes between the two groups. When the data was analyzed without correction (fold change ≥ 2.0, p-value ≤ 0.01) (Table 2), GRN itself was found to be significantly down regulated in the miR-GRN201 expressing cell lines as expected. In addition, CD44 was the most prominently regulated gene. Validation experiments by RT-PCR and Western blotting confirmed the down regulation of both GRN and CD44 in the knockdown cell lines (data not shown). However, the reduction in CD44 expression could not be reproduced in cells expressing the second GRN-targeting miRNA (miR-GRN2140) or after GRN knockdown by siRNA (Fig. 15). Thus, the down regulation of CD44 was evidently an off-target effect of the miRNA-GRN201. Other differentially regulated genes that were identified with less stringent data analysis could also not be validated by RT-PCR. In summary, these experiments did not reveal any substantial effect of GRN on the global gene expression pattern in established human glioma cell lines.

Table 2

Probe Set ID	p-value	regulation	Gene Symbol	Gene
200678_x_at	0,0054	down	GRN	Progranulin
216041_x_at	0,0094	down	GRN	Progranulin
212014_x_at	0,0061	down	CD44	CD44 molecule (Indian blood group)
204490_s_at	0,0025	down	CD44	CD44 molecule (Indian blood group)
204489_s_at	0,009	down	CD44	CD44 molecule (Indian blood group)
228885_at	0,0033	down	MAMDC2	MAM domain containing 2
209835_x_at	0,0056	down	CD44	CD44 molecule (Indian blood group)
210916_s_at	0,0039	down	CD44	CD44 molecule (Indian blood group)
205547_s_at	0,0004	up	TAGLN	transgelin
1555724_s_at	0,0038	up	TAGLN	transgelin

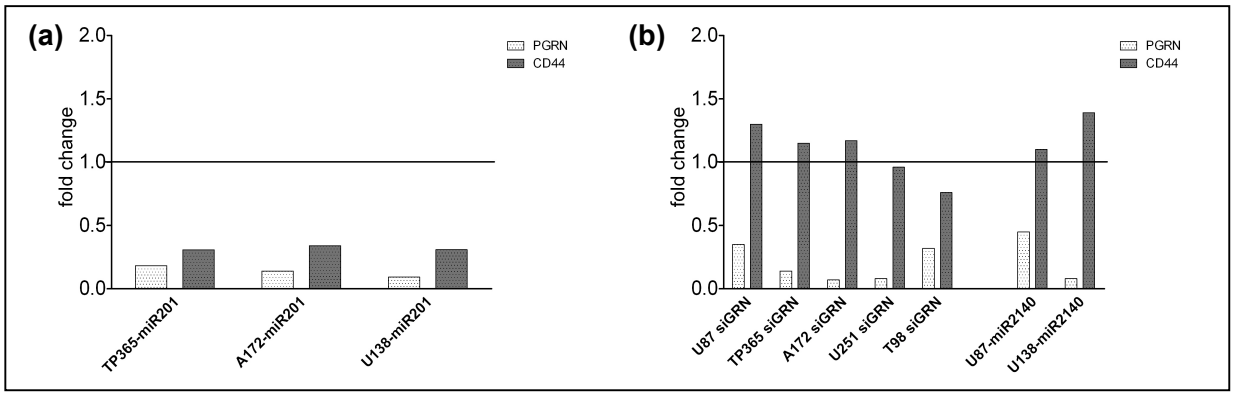

Figure 15: Validation of microarray data by real time RT-PCR (GRN knock down cell lines). **(a)** Differential expression of GRN and CD44 after knockdown of GRN by miRNA GRN201 was confirmed by real time RT-PCR analysis. **(b)** Down regulation of CD44 expression was not observed after knock down of GRN by siRNA or miRNA GRN2140. CD44 regulation was thus considered an off-target effect of miRNA GRN201. Data is shown as fold change compared to the respective control (scrambled miRNA or siRNA sequence).

4.4.2 Proliferation

GRN has been demonstrated to function as a mitogen for several cancer cell lines. For example, constitutive overexpression of GRN increased proliferation in the adrenal small cell carcinoma cell line SW-13 and the canine renal epithelial cell line DU145 (He & Bateman 1999). Conversely, expression of antisense GRN cDNA was shown to inhibit cell growth in a breast carcinoma (MCF-7), ovarian carcinoma (SW626 and A2780), and hepatocellular carcinoma (Hep3B) cell lines (Lu & Serrero 2000, Liu *et al.* 2007, Cheung *et al.* 2004). GRN might also be a mitogen for glial cells as exogenous stimulation of primary rat astrocytes with a synthetic granulin D peptide resulted in increased cell growth. Notably, in early-passage primary human glioblastoma cell cultures, treatment with granulin D had only minimal effects but proliferation could be suppressed with an antibody directed against granulin D (Liau *et al.* 2000).

Here, the effects of increased or reduced expression of GRN on the growth of glioma cell lines were evaluated. To quantify the proliferation rate in the different cell lines, cells were seeded in 12-well plates ($5x10^4$/well). For the following six days, duplicate wells were trypsinized every day and viable cells were counted using the ViCell Cell Counter. First, the influence of GRN overexpression on the proliferation rate was analyzed in the doxycycline-inducible cell lines SMA560 Tet-On-GRN, U251MG Tet-On-GRN, U87MG Tet-On-GRN, and T98G Tet-On-GRN cultured under serum-containing (10%) conditions. Because some leakage of the Tet-On system leading to slightly increased GRN expression even in the non-induced state was observed in these cell lines (see Fig. 12b), the corresponding parental cell lines with endogenous GRN expression were also included in these assays. As shown in Figure 16a-d, overexpression of GRN did not result in increased cell proliferation in any of these cell lines. Slight reductions in cell growth were observed after treatment with doxycyline suggesting minor toxic effects of this compound. In addition, the growth rates of the constitutively overexpressing cell lines SMA560-GRN, U251MG-GRN, U87MG-GRN, and T98G-GRN were compared to their corresponding empty vector control cell lines. No differences in growth rates were detected confirming the results with the inducible cell lines (Fig. 16e-h).

To investigate potential effects of decreased endogenous GRN expression on cell growth, the proliferation assays were repeated with the GRN knockdown cell lines A172-miR-GRN201/2140, TP365-miR-GRN201/2140, and U138-miR-GRN201/2140, and their respective control cell lines. Again, only minor changes in the proliferation rates could be observed for both miRNAs targeting GRN as compared to the scrambled control as shown in Figure 17a-c.

To exclude any interfering effects of serum proteins, all assays were repeated under serum-free conditions. For this, cells were challenged with serum depletion 24h after seeding, and cells of duplicate wells were counted for the following six days. All cell lines showed greatly reduced proliferation rates in serum-free medium. However, the levels of GRN expression did not influence cell growth. As an example, the cell lines with constitutive overexpression of GRN are shown here (Fig. 17d-f). In conclusion, neither overexpression of GRN nor depletion of endogenous GRN expression affected the growth rates of glioma cell lines under serum-containing or serum-free conditions.

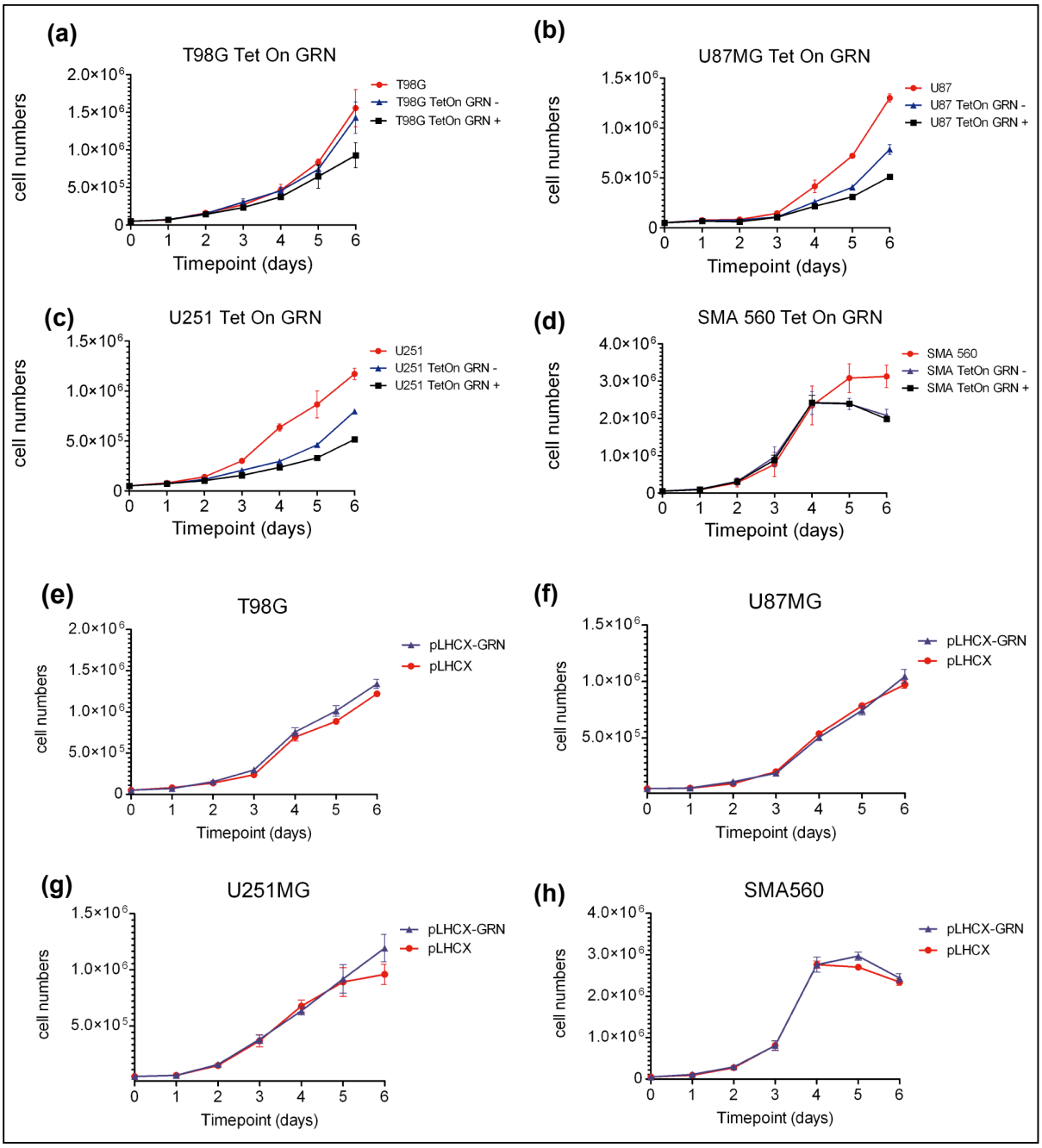

Figure 16: Proliferation assays of glioma cell lines with GRN overexpression. **(a-d)** Cell lines with tet-inducible overexpression of GRN were cultured with or without 100ng/ml doxycycline and proliferation rates were compared. Overexpression of GRN did not result in increased cell proliferation in any of these cell lines (n=3). **(e-h)** Cell lines with constitutive GRN overexpression were compared to their respective empty vector control cell lines. No differences in proliferation rates were observed (n=3).

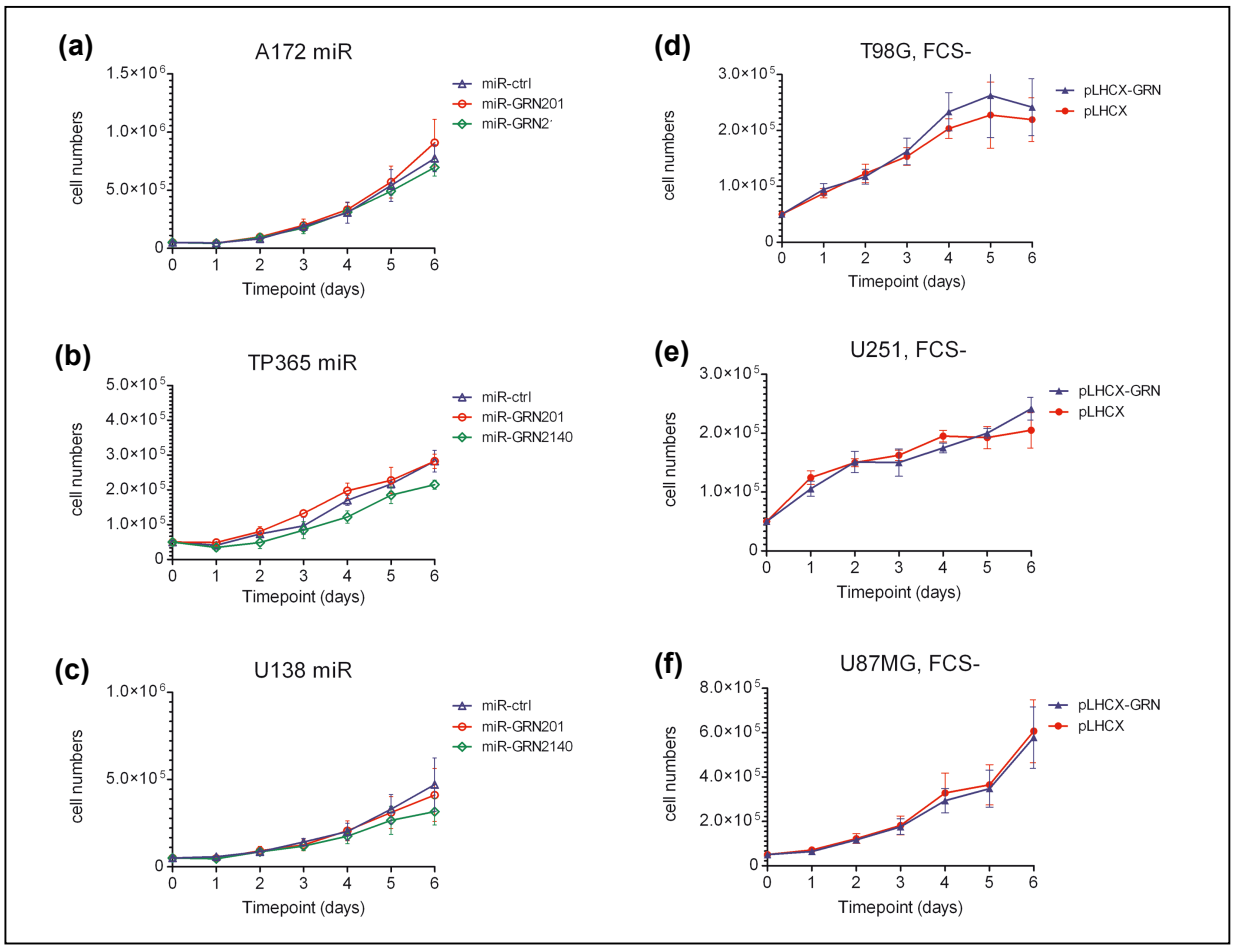

Figure 17: **(a-c)** Proliferation assays of glioma cell lines with reduced endogenous GRN expression. Proliferation rates of cell lines with stable expression of miRNA contructs targeting GRN (miR201 or miR2140) were compared to the respective control cell lines expressing a non-targeting scrambled sequence. No consistent differences were observed (n=3). **(d-f)** Representative proliferation assays under serum-free conditions. Proliferation rates of cell lines with constitutive overexpression of GRN were compared to proliferation rates of the respective empty vector control cell lines. No reproducible differences were observed (n=3).

4.4.3 Migration

The ability of cancer cells to migrate and invade through the extracellular matrix is critical for invasive growth and tumor metastasis. GRN has been proposed to promote cell motility in several studies (Monami *et al.* 2009, Monami *et al.* 2006). Gliomas usually do not metastasize but infiltrative growth into the surrounding brain parenchyma is a key biological and clinical characteristic of these tumors. Therefore, the influence of GRN on the migratory behaviour of glioma cell lines was investigated in this study. Cell migration was analyzed using the Oris™ Cell Migration Assay (Platypus Technologies). In this assay, cells were

seeded in 96-well plates around circular migration zones in the center of each well. At appropriate time points, the seeding area was masked and cells that had migrated into the migration zones were quantified. Because most glioma cell lines did not migrate at all under serum-free conditions, all experiments were carried out using complete medium (10% serum).

In a first set of experiments, it was investigated whether down-regulation of endogenous GRN expression would influence cell migration by comparing the three cell lines A172, TP365, and U138 with stable expression of miR-GRN201 and the corresponding control cell lines. In this assay, the cells were allowed to migrate for 48 hours. As shown in Figure 18a-c, reduced endogenous GRN expression did not change the migration rates of the cell lines. In addition, cell migration in response to induction of GRN overexpression in the Tet-inducible glioma cell lines was investigated. T98G Tet-On-GRN, U251MG Tet-On-GRN, and U87MG Tet-On-GRN cells were seeded with or without 100ng/ml doxycycline in complete medium, and allowed to attach for 24 hours before the migration zone was cleared. 48 hours later, cells that had migrated were quantified. No significant changes in the migration rates were observed when doxycycline-induced and non-induced cell lines were compared (Fig. 18d). Taken together, GRN expression levels did not affect the migratory behaviour of the investigated glioma cell lines.

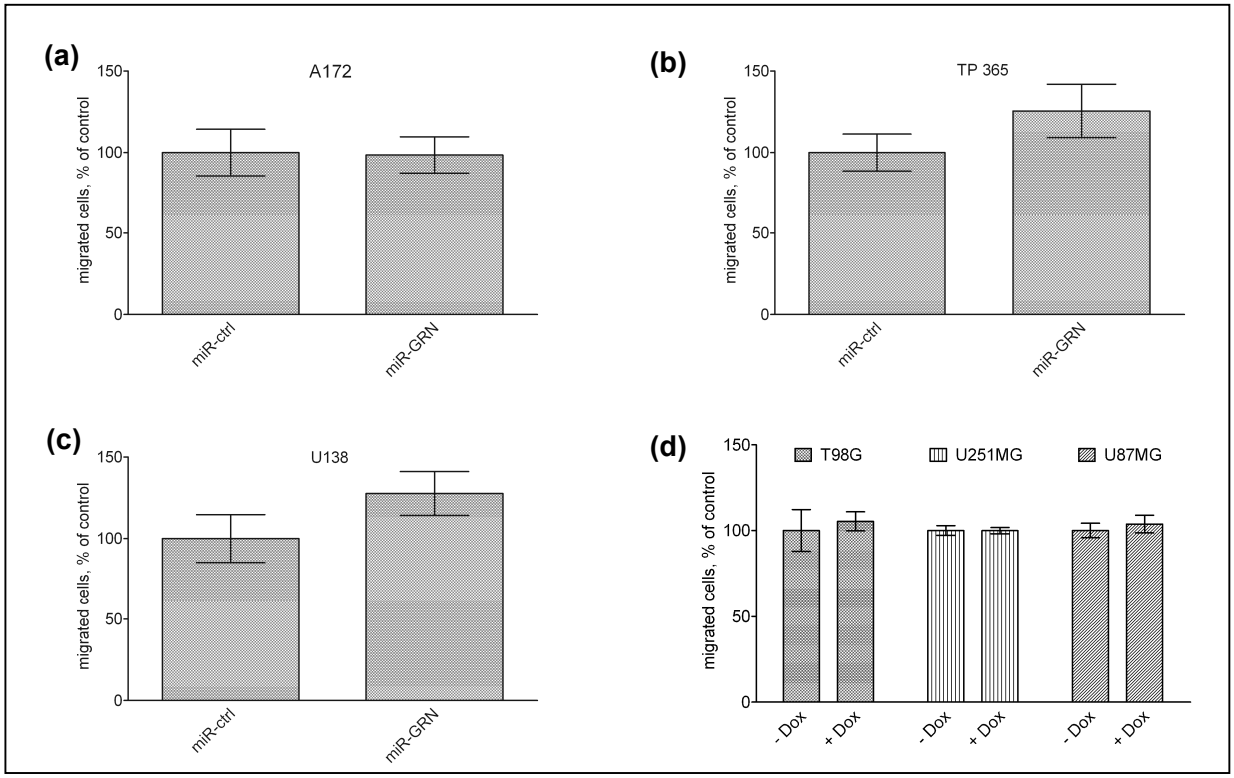

Figure 18: Modulation of GRN expression did not affect the migration of human glioma cell lines. **(a-c)** Cell lines with stable expression of miRNA GRN201 were compared to their respective control cell lines with stable expression of a scrambled control miRNA. Knock down of endogenous GRN expression did not influence the migration of these cells (n=5). **(d)** Tet-inducible cell lines were examined for their ability to migrate with or without induction of GRN expression with 100ng/ml doxycycline. No differences were observed (n=1).

4.4.4 Sensitivity to apoptosis-inducing and chemotherapeutic agents

Acquired resistance to apoptosis is a hallmark in the development of cancers, and programmed cell death is one of multiple defense mechanisms of cells against malignant growth (Hanahan & Weinberg 2000). Evasion of apoptosis also contributes to the occurrence of drug resistance during chemotherapeutic treatment (Raguz & Yague 2008). To test whether GRN expression might protect glioma cells from apoptosis, we evaluated the sensitivity of glioma cell lines with GRN overexpression or reduced endogenous GRN expression levels to different apoptosis-inducing agents. Cisplatin is an inorganic heavy metal complex and alkylating agent that causes intra- and inter-strand DNA cross-links leading to disruption of DNA replication and transcription. Vincristine is a natural compound that binds to tubulin dimers and blocks polymerization of microtubules, which results in impaired mitotic spindle formation during the cell cycle. Both compounds are commonly used for chemotherapeutic treatments (Himes *et al.* 1976, Siddik 2003). Thapsigargin is a natural product that disrupts the Ca^{2+} homeostastis of cells by depleting Ca^{2+} stores of the endoplasmatic reticulum (ER). Consequently, cytoplasmic Ca^{2+} levels are elevated, which eventually results in the induction of apoptosis (Denmeade & Isaacs 2005). Staurosporine is a bacterial toxin that functions as a potent inhibitor of protein kinases, and thus interferes with multiple signaling pathways leading to apoptosis (D'Alimonte *et al.* 2007).

To assess the toxicity of these compounds on glioma cell lines with variable GRN expression levels, the cells were seeded at low density ($5x10^3$ cells/well) in 96-well plates, and treated with the respective compounds one day later. Cell viability was measured using alamar blue reagent after either 24h or 72h and compared to vehicle treated control cells. The cell lines U251MG Tet-On-GRN, and SMA560 Tet-On-GRN cultured with or without 100ng/ml doxycycline were used to evaluate the influence of GRN overexpression on cell survival after compound treatment. In addition, the miRNA expressing cell lines U138-miR-GRN201 and TP365-miR-GRN201 and their corresponding control cell lines were used to investigate whether reduced endogenous GRN expression had any influence on cell viability after compound treatment. Although minor differences in cell viability were observed in some cases, there were no consistent effects of GRN expression levels on the survival of these cells (Fig. 19). Thus, we concluded that elevation or down-regulation of GRN expression in glioma cell lines did not influence their sensitivity to apoptosis-inducing or chemotherapeutic agents.

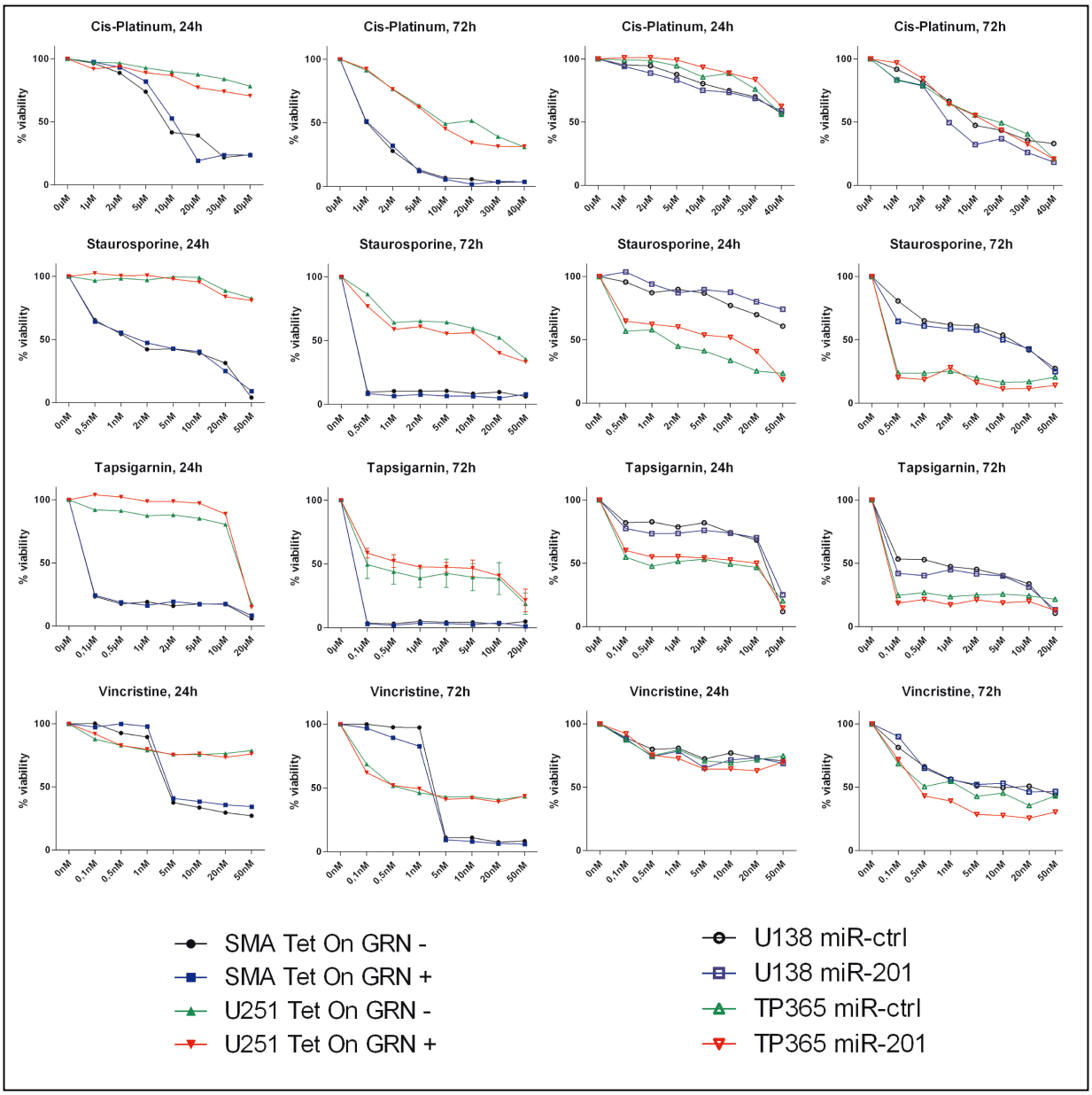

Figure 19: Sensitivity of glioma cell lines to apoptosis-inducing and chemotherapeutic agents. The Tet-inducible cell lines SMA Tet-On-GRN and U251 Tet-On-GRN with or without induction of GRN expression (left part), and the GRN knock down cell lines U138-miR-GRN201, TP365-miR-GRN201 and their respective control cell lines (right part) were treated with different concentrations of compounds as indicated. Viability of the cells was assessed after 24h and 72h.

4.4.5 Anchorage-independent growth

A characteristic of cellular transformation is the capacity for anchorage-independent growth. Normal cells are typically not capable to grow in semi-solid media, but cancer cells are able to evade attachment-regulated apoptosis (anoikis) leading to uncontrolled proliferation. *In vitro*, colony formation in soft agar is used as a measure of malignancy of cancer cells (Anderson *et al.* 2007). Several studies have demonstrated an influence of GRN on the capacity for anchorage-independent growth (Cheung *et al.* 2004, Jones *et al.* 2003, Monami *et al.* 2009, Lu & Serrero 2000, Matsumura *et al.* 2006, Tangkeangsirisin & Serrero 2004, He & Bateman 1999).

To investigate putative effects of GRN on the clonogenicity of glioma cells, the cell lines SMA560-GRN, U251MG-GRN, U87MG-GRN and T98G-GRN with stable overexpression of GRN and their corresponding empty vector control cell lines were seeded in soft agar ($5x10^4$ cells/well) and allowed to grow for 14 days. Viable colonies were then stained with MTT reagent and counted. Three independent experiments, each with triplicate wells were performed. As shown in Figure 20, no significant differences in colony numbers could be detected. Similar results were obtained with the Tet-inducible cell lines SMA560 Tet-On-GRN, U251MG Tet-On-GRN, U87MG Tet-On-GRN, and T98G Tet-On-GRN when doxycycline-induced and non-induced conditions were compared (data not shown). In summary, GRN overexpression did not influence the capacity for anchorage-independent growth in human glioma cell lines.

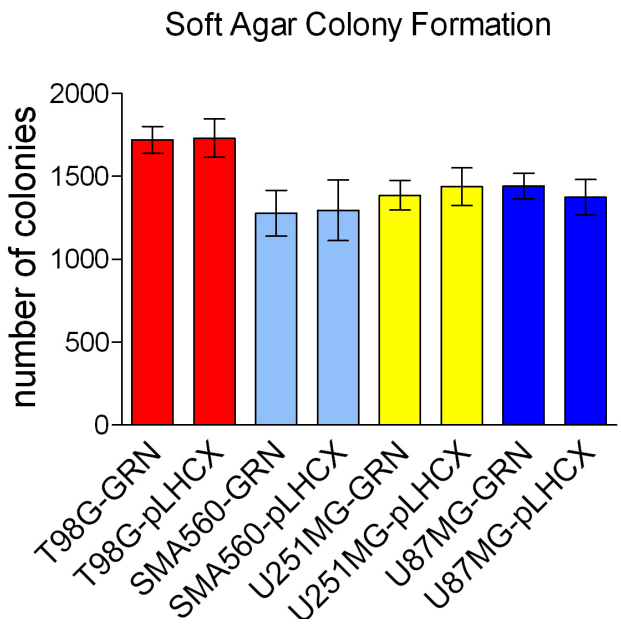

Figure 20: Anchorage-independent growth of glioma cell lines. Cell lines with stable overexpression of GRN and empty vector controls were seeded in semisolid agar. The number of viable colonies was counted after 14 days of cultivation.

4.4.6 Xenograft formation

The results described above indicated that GRN expression levels had no substantial effects on gene expression, proliferation, migration, apoptosis resistance or anchorage-independent growth of glioma cell lines. These intrinsic properties of tumor cell lines could be adequately addressed by the performed *in vitro* assays. However, it remained possible that GRN as a secreted protein could have non-cell-autonomous effects on stroma cells in the vicinity of the tumor mass. Shaping of the tumor stroma by GRN might, in turn, promote tumor growth or malignancy. Specifically, GRN appears to be a chemoatractant for microglia cells, and microglia were shown to support glioma growth *in vivo*. Increased tumorigenicity of cancer cell lines with overexpression of GRN has been demonstrated in several studies using skin xenografts (He & Bateman 1999, Lu & Serrero 2000, Pickford *et al.* 2011). However, while skin xenografts are an accepted model to quantify tumor growth *in vivo*, they do not account for the interaction of tumor cells with their physiological stromal environment, particularly in the case of gliomas that interact with cell types that do not occur in the periphery such as microglia cells. In addition, skin xenografts of human tumor cells require the use of immunosuppressed or nude mice to avoid rejection of the tumor cells by the host immune system. Therefore, we chose to study the role of GRN in intracranial xenografts of the SMA560 mouse glioma cell line in syngenic mice. This cell line was established from a primary glioma that arose spontaneously in the immunocompetent inbred mouse strain VM/Dk and has been demonstrated to form tumors with a high-grade glioma histology after intracranial transplantation (Ashley *et al.* 1998, Roth *et al.* 2010).

A total of 5,000 SMA560 cells with inducible overexpression of GRN (SMA560 Tet-On-GRN) suspended in PBS were stereotactically implanted into the right striatum of 6-12 week old VM/Dk mice at a depth of 3 mm. To induce GRN overexpression, the drinking water was supplemented with doxycyline starting two days prior to operation. The control group did not receive doxycycline treatment. A third group was injected with the parental cell line SMA560 Tet-On that expressed the rtTA-Advanced transactivator but lacked the plasmid encoding for GRN. This group also received doxycycline to additionally control for effects of this treatment. 14 mice were operated per group. Tumor volume was assessed in 4-5 mice per group on day 14 and 21 after tumor cell inoculation by magnetic resonance imaging (MRI). Brain tumors were located on T2-weighted turbo spins echo images. T1-weighted imaging was performed using a high-resolution spinecho sequence three minutes after intraperitoneal administration of Gd-DTPA contrast agent. The intracranial injections were performed by Dr. Philipp Pfenning, the MRIs were recorded by Dr. Manfred Jugold (both at the German Cancer Research Center, Heidelberg, Germany). At postoperative day 14, the tumors formed in animals injected with the SMA560 Tet-On-GRN cells and treated with doxycycline were 1.6 fold larger compared to tumors in animals injected with SMA560 Tet-On-GRN cells but

without doxycycline treatment, and 2.3 fold larger than tumors that formed in animals injected with the parental cells and treated with doxycycline. At this time point, the differences in tumor size were not statistically significant. At postoperative day 21, tumors that had formed in animals injected with the SMA560 Tet-On-GRN cells and treated with doxycycline were significantly larger (2.5 fold) compared to the non-induced control group (p=0.002). The size difference to tumors formed in animals injected with the parental cells but treated with doxycline was smaller (1.5 fold) but still statistically significant (p=0.048) (Fig. 21). Two mice per group were sacrificed at postoperative day 21 after the MRI recordings, and brains were isolated, cryosectioned and stained with hematoxylin and eosin stain to visualize the tumor masses (Fig. 22). The tumors were highly cellular and, unlike human gliomas, well circumscribed. Small areas of necrosis could be observed. The tumor cells were pleiomorph and had an epitheloid shape. Pale eosinophilic cytoplasm and irregular hyperchromatic nuclei were visible in the H & E staining. No obvious differences between the tumors of the three different groups could be detected.

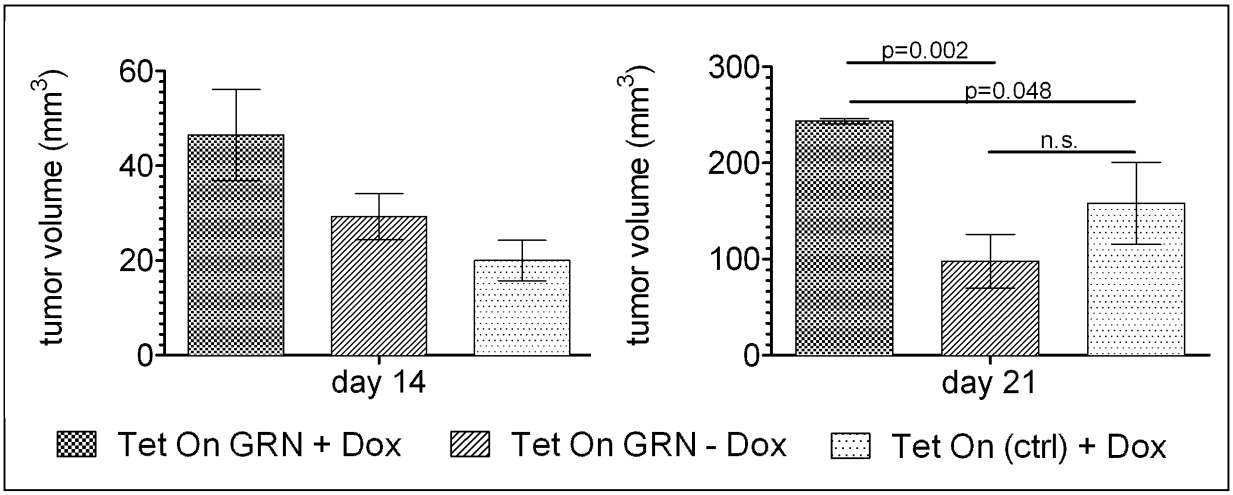

Figure 21: Tumor volumes of intracranial xenografts were assessed by T1-weighted MR imaging after administration of contrast agent. 14 days after tumor cell injection, no significant differences were observed although the largest tumor volumes were found in mice that had received doxycyline to induce GRN expression in SMA Tet-On-GRN cells. At day 21 post operation, tumors formed in animals injected with SMA Tet-On-GRN cells and treated with doxycycline (Tet On GRN + Dox) were significantly larger than those formed in the non-induced (Tet On GRN – Dox) or the parental cell (Tet On (ctrl) + Dox) control groups (p=0.002 and p=0.048, respectively; n=4-5; two-sided Student's t-Test).

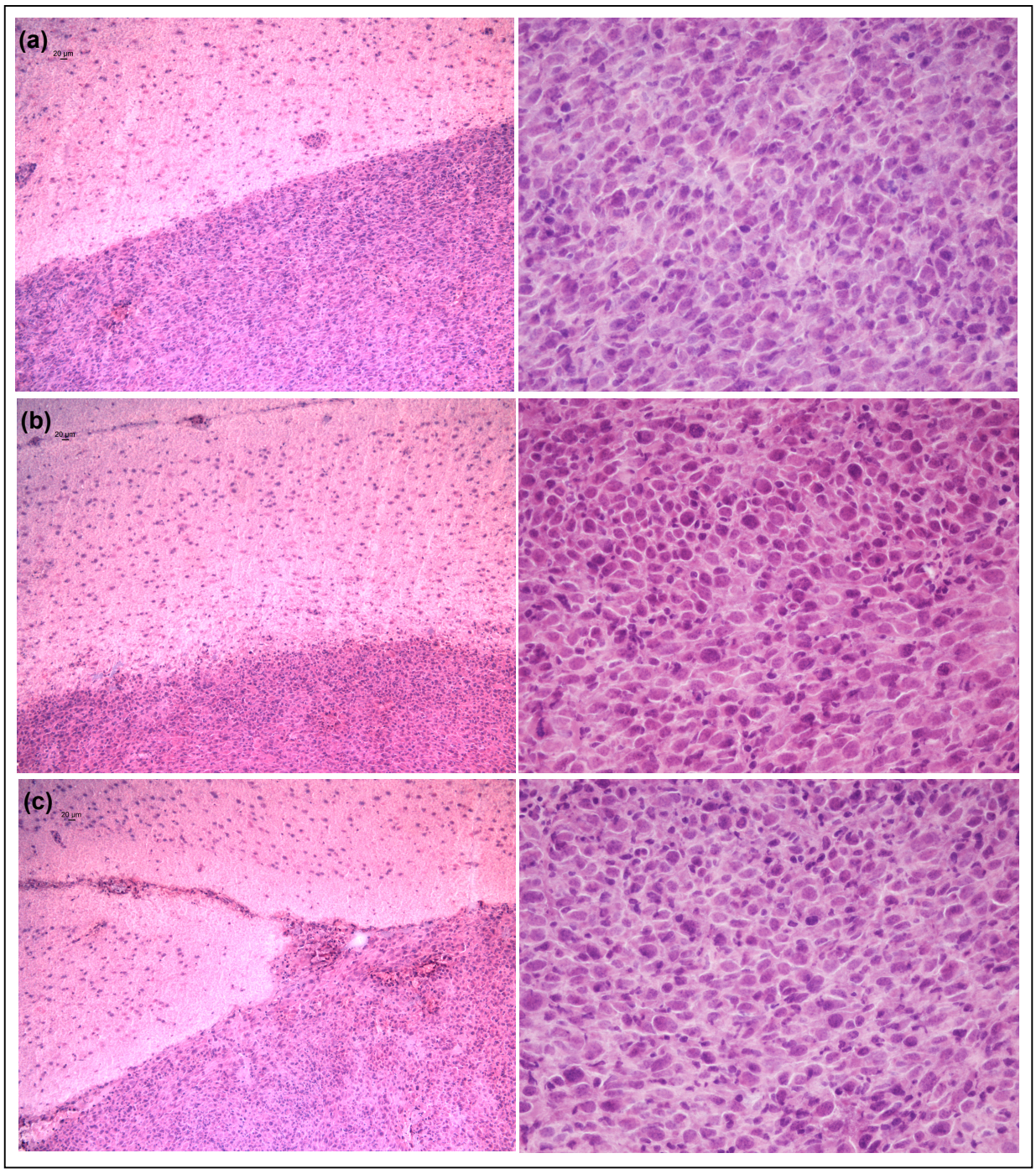

Figure 22: Cryosections of brains from mice sacrificed 21 days post operation were stained with H & E stain. Well circumscribed, highly cellular tumors formed by the injected cells are clearly visible.The pleiomorphic cells display an epitheloid shape with pale eosinophilic cytoplasm and irregular hyperchromatic nuclei. **(a)** SMA560 Tet-On-GRN + Dox, **(b)** SMA560 Tet-On-GRN – Dox, **(c)** SMA560 Tet-On (ctrl) + Dox. (original magnifications: 25x (left) and 400x (right))

5 DISCUSSION

GRN overexpression has been reported in many types of human cancers, including carcinomas of the breast, ovaries, endometrium, liver, kidney, prostate and bladder, in uterine leiomyosarcomas, multiple myelomas, mesotheliomas and brain tumors like intracranial meningiomas and gliomas (Toh *et al.* 2011). In some cases, the intensity of GRN overexpression could be correlated with the malignancy of the tumors. In ovarian cancer, GRN overexpression has been reported in malignant invasive tumors but not in benign tumors, and correlated with patient survival (Cuevas-Antonio *et al.* 2010). In hepatocellular carcinomas, strong GRN expression was associated with larger and more aggressive tumors (Cheung *et al.* 2004). In uterine leiomyosarcomas, the intensity of GRN expression corresponded to the histological grade, and high GRN expression was associated with a poor prognosis of the investigated tumors (Matsumura *et al.* 2006). A correlation with increased tumor size and peritumoral brain edema volume has been shown for intracranial meningiomas (Kim *et al.* 2010). In contrast, in a meta-analysis across six independent microarray studies in primary prostate carcinomas, a correlation between GRN expression levels and the grade of malignancy was not observed (Monami *et al.* 2009).

For glial brain tumors, GRN overexpression in tumor tissue as compared to normal brain tissue has been reported in two independent studies, both with only a limited number of tumor samples and only on the RNA transcript level. Liau *et al.* identified GRN as a 'glioma-associated growth factor' in a cDNA microarray analysis of eight glioma samples compared to normal brain tissue. Validation by Northern blot analysis confirmed GRN expression in 18 of 21 tested glioma samples, whereas GRN expression could not be detected in normal brain samples. In addition, *in situ* hybridization demonstrated higher expression of GRN in five high-grade primary brain tumors (2 anaplastic astrocytomas and 3 glioblastomas) as compared to non-transformed brain tissue (Liau *et al.* 2000). Markert *et al.* confirmed the overrepresentation of GRN in four glioblastoma samples compared to normal brain samples in an independent cDNA microarray study (Markert *et al.* 2001).

In this study, a set of 48 glioma samples was analyzed by quantitative real time RT-PCR and significantly elevated levels of GRN expression were observed for low- and high-grade gliomas as compared to normal brain control samples. In addition, the analysis of cDNA microarray data of the Glioma Core Collection consisting of 74 astrocytic glioma samples confirmed significantly increased GRN expression levels in gliomas as compared to normal brain samples. In both studies, the highest GRN expression levels were found in the most aggressive tumors of WHO grade IV, specifically in primary glioblastomas that develop *de novo* without a history of lower-grade gliomas. Interestingly, no significant differences in GRN levels were detected between WHO grade II and WHO grade III samples in the first study, and diffuse astrocytomas (WHO grade II), anaplastic astrocytomas (WHO grade III) and

secondary glioblastomas (WHO grade IV) in the second study. This indicates that the progression from low-grade gliomas to anaplastic gliomas and secondary glioblastomas is not associated with further elevation of GRN overexpression, and suggests an important function of GRN in the early development and establishment of gliomas rather than in the progression of these tumors. We could also demonstrate overexpression of GRN in gliomas on the protein level. In normal brain samples, GRN expression was found to be restricted to neurons and microglia, as reported previously (Ahmed *et al.* 2007, Baker *et al.* 2006, Mackenzie *et al.* 2006, Mukherjee *et al.* 2006). In contrast, ubiquitous GRN expression was found in all tumor samples with one exception, when a tissue microarray consisting of 56 glioma samples was examined by immunohistochemistry. Similar results were found by Western blot analysis. Robust GRN expression could be shown in all five glioblastoma samples for which frozen tissue was available. In sharp contrast, GRN expression in normal brain samples was undetectable by this method. In addition, prominent GRN expression was observed in all eight investigated established glioma cell lines. In summary, in accordance with previous publications and findings in other types of cancer, we observed that GRN is overexpressed in the majority of gliomas as compared to normal brain tissue, both on the transcriptional and the protein level. A very recent study has confirmed our data to a large extent (Wang *et al.* 2011). Wang *et al* have investigated GRN expression in a series of 210 astrocytic tumors by immunohistochemistry, and reported positively stained tumor cells in 96% of the samples. In this study, an increase in GRN expression levels correlated with higher grading of the tumors. However, statistical significance was only demonstrated for grade II, III and IV astrocytomas versus grade I astrocytomas. In addition, 35 astrocytoma samples were analyzed by semi-quantitative RT-PCR and Western blotting, and GRN overexpression in the tumor samples compared to normal brain tissue was validated by both methods (Wang *et al.* 2011). In contrast, our data do not support the hypothesis that the level of GRN overexpression correlates with the grade of malignancy in gliomas. It cannot be excluded that a correlation between GRN expression and glioma grade can only be observed on the protein rather than the transcriptional level. However, the interpretation by Wang et al was largely based on the subjective scoring of immunohistochemical GRN stainings, a method that does not allow an accurate quantifying of expression of proteins. Nevertheless, our analysis of two independent tumor sets demonstrated the highest mRNA expression levels of GRN in primary glioblastomas, which are a genetically distinct entity. This might suggest that upregulation of GRN expression is particularly important in the development of these highly malignant tumors with a fast and fatal disease course.

Exactly how GRN expression contributes to the development or progression of tumors is still unresolved. However, several possibilities have been proposed that relate to different stages of tumor genesis: (i) stimulation of proliferation and/or inhibition of apoptosis to support tumor

growth, (ii) enhancement of cell motility and anchorage-independent survival required for metastasis, and (iii) the induction and maintenance of a tumor stroma that supports the growth and survival of tumor cells (Toh *et al.* 2011).

A mitogenic effect of GRN has been reported in many studies. Increased proliferation in response to GRN overexpression or exogenous treatment with recombinant GRN has been shown for cell lines representing adrenal small cell carcinoma (SW-13), prostate cancer (DU145), multiple myeloma (ARP-1, RPMI 8226), lung adenocarcinoma (A549), guinea pig colonic cancer (GPC16), and canine renal epithelium (MDCK) (He & Bateman 1999, Monami *et al.* 2009, Wang *et al.* 2003). Conversely, the depletion of GRN expression using antisense cDNA or the depletion of secreted GRN using anti-GRN antibodies resulted in reduced cell growth of breast carcinoma cell line MDA-MB468, ovarian carcinoma cell lines SW262 and A2780, and hepatocellular carcinoma cell lines Hep3B and HepG2 (Cheung *et al.* 2004, Ho *et al.* 2008, Liu *et al.* 2007, Lu & Serrero 2000). Not only stimulation of proliferation but also inhibition of apoptosis can contribute to the growth of a tumor, and many chemotherapeutic agents induce apoptosis of cancer cells. However, tumor cells often develop resistance to chemotherapeutic drugs and several studies have implicated GRN in this process. For example, overexpression of GRN was shown to increase the survival of ovarian cancer cells in the presence of cisplatin and to mediate tamoxifen resistance of breast cancer cells (Pizarro *et al.* 2007, Tangkeangsirisin & Serrero 2004). In hepatocellular carcinoma cells, overexpression of GRN mitigated apoptosis in response to doxorubicin or cisplatin, whereas suppression of GRN expression sensitized the cells to these chemotherapeutic agents (Cheung *et al.* 2011). So far, the only function that has been proposed for GRN in gliomas is stimulation of tumor cell proliferation. Liau *et al.* reported that a synthetic granulin D peptide was able to dose-dependently stimulate the proliferation of rat astrocytes *in vitro* (Liau *et al.* 2000). Cultured primary glioblastoma cells showed only modest effects in response to the synthetic peptide, but their proliferation could be inhibited by the addition of an antibody raised against the granulin D peptide.

In this study, we performed extensive experiments to investigate cell growth promoting effects of GRN using established glioma cell lines, and we were not able to confirm the findings reported by Liau *et al.* (Liau *et al.* 2000). Stable or inducible overexpression of GRN did not accelerate the proliferation of the investigated glioma cell lines T98G, U251MG, and U87MG. Similarly, miRNA-mediated knockdown of endogenous GRN expression did not slow the proliferation of the cell lines TP365, U138, and A172. In addition, we have assessed the sensitivity of glioma cell lines to different apoptosis-inducing agents, namely cisplatin, vincristine, tapsigarnin and staurosporine. Neither overexpression nor suppression of endogenous GRN expression had a significant influence on cell viability in the presence of these compounds. We thus concluded that GRN did not modulate cell proliferation or

apoptosis resistance of established glioma cell lines. All of the investigated glioma cell lines displayed substantial endogenous levels of GRN protein expression. Therefore, additional ectopic overexpression might not be able to promote further cell growth, particularly when taking into account that GRN levels did not seem to increase during the progression of human gliomas. The suppression of endogenous GRN expression might therefore be more informative and might more likely lead to an observable phenotype. However, in this study the same results were obtained with both GRN overexpression and miRNA-mediated knockdown of endogenous GRN expression. An additional issue may be the usage of established glioma cell lines, which have been cultured under artificial conditions for undefined periods of time. It has been demonstrated that the cellular and genetic features of glioblastoma cell lines change progressively over time in culture, and this is especially pronounced when the cells are exposed to serum. Thus, the representation of primary tumors by established glioma cell lines may be limited (De Witt Hamer *et al.* 2008, Fael Al-Mayhani *et al.* 2009, Lee *et al.* 2006). Furthermore, frequent co-alterations of the *TP53*, *p16/CDKN2A*, $p14^{ARF}$, and *PTEN* tumor suppressor genes, which are part of key signaling pathways that control cellular proliferation and apoptosis resistance, have been described in many glioma cell lines. Mutations in PTEN that lead to hyperactivation of the PI3K/AKT pathway have been detected in the glioma cell lines U87MG, U138MG, U251MG, T98G, and A172 (Ishii *et al.* 1999, Krakstad & Chekenya 2010). The same PI3K/AKT signaling pathway has been suggested to mediate at least some of the biological effects of GRN including promotion of cell proliferation (He *et al.* 2002, Ho *et al.* 2008, Monami *et al.* 2009, Wang *et al.* 2003). Therefore, growth promoting effects mediated by GRN via this signaling pathway may not be visible in glioma cell lines with PTEN mutations. Similarly, p53 regulates cell cycle progression and apoptosis in response to stress signals (Grzmil & Hemmings 2010). The encoding gene, *TP53,* is mutated in at least three of our investigated cell lines (U138MG, U251MG, and T98G) (Ishii *et al.* 1999). Mutations in *CDKN2A* encoding for $p14^{ARF}$ also lead to destabilization of p53 and have been found in the cell lines U87MG, U138MG, U251MG, T98G, and A172. An alternative gene product of *CDKN2A,* p16, prevents the phosphorylation of pRB (retinoblastoma protein) by inhibiting cyclin dependent kinases. Mutations in *CDKN2A* and loss of p16 enhance pRb phosphorylation, also driving uncontrolled proliferation (Ishii *et al.* 1999). Because of these genetic alterations, GRN may not be able to substantially influence the already highly deregulated growth properties of established glioma cell lines. Further studies using early passage primary glioma cell lines cultured under defined serum-free conditions could be performed to exclude that the highly transformed phenotype of the established glioma cell lines is the reason for their lack of response to GRN. On the other hand, although a proliferative effect of GRN has been demonstrated for a variety of tumor cell lines, this response clearly does not apply to all tumor entities and cell lines. Notably,

several cell lines have been reported not to respond to GRN with increased proliferation. For example, the epidermoid carcinoma cell line A431, mouse embryonic fibroblasts NIH3T3 and the bladder cancer cell line 5637 did not proliferate in response to recombinant GRN (He & Bateman 1999, Monami *et al.* 2006). Likewise, uterine leiomyosarcoma cells SK-UT-1, neuroblastoma cells SK-N-DZ, promyelocitic leukemia cells HL-60, and histiocytic lymphoma cells U937 did not respond to treatment with recombinant GRN (Daniel *et al.* 2000). Thus, the mitogenic effect of GRN is dependent on the cell type and the specific cell line, and may not apply to glioma cells.

Other functions that have been attributed to GRN in cancers are the stimulation of migration and invasive behavior. The breast cancer cell line MCF-7 displayed an invasive phenotype after treatment with recombinant GRN or overexpression of GRN (Tangkeangsirisin & Serrero 2004). Conversely, a reduced ability to migrate through matrigel was observed after expression of antisense GRN cDNA in hepatocellular Hep3B cells and the ovarian carcinoma cell lines SW626 and A2780 (Cheung *et al.* 2004, Liu *et al.* 2007). Because infiltrative growth is a key feature of gliomas, we investigated whether modulation of GRN expression would influence the motility of glioma cell lines. We did not observe reduced migration of the glioma cell lines A172, TP365, and U138 after suppression of GRN expression. The capacity to migrate into a cell free area of a culture dish, which was analyzed in our experiments, is a measure of undirected motility. Therefore, we cannot exclude that GRN might have effects on directed migration (chemotaxis) or the degradation of extracellular matrix components required for invasion. However, in the DU145 prostate cancer cell line, siRNA-mediated knockdown of GRN expression severely impaired the ability to migrate in a wound-healing assay for undirected motility (Monami *et al.* 2009). In contrast to our experiments, this study was performed under serum-free conditions. Unfortunately, we were not able to perform migration assays under serum-free conditions since all the examined glioma cell lines did not migrate at all in the absence of serum.

In addition to proliferation, apoptosis-resistance and cell motility, GRN has been shown to promote anchorage-independent growth *in vitro* and tumor xenograft formation *in vivo*. Knockdown of endogenous GRN expression reduced the number of colonies formed in soft agar in the prostate cancer cell line DU145 and the ovarian cancer cell lines OVCAR3 and HeyA8 (Jones *et al.* 2003, Monami *et al.* 2009). Similar results were reported for a hepatocellular carcinoma cell line (Hep3B), which also formed less and smaller tumors after implantation into athymic mice when GRN expression was suppressed (Cheung *et al.* 2004, Jones *et al.* 2003, Monami *et al.* 2009). Reduced *in vitro* clonogenicity of a breast cancer cell line (MDA-MB-468) transfected with antisense GRN cDNA could be rescued by exogenous stimulation with recombinant GRN and this cell line also displayed a dramatic inhibition of tumor formation in nude mice as measured by tumor incidence and weight after knock down

of GRN expression (Lu & Serrero 2000). Conversely, overexpression of GRN was shown to enhance anchorage-independent growth and soft agar colony formation in a second breast cancer cell line (MCF-7) (Tangkeangsirisin & Serrero 2004). An influence of GRN on anchorage-independent growth and xenograft formation of glioma cells has not been described so far. In this study, we investigated the ability of the cell lines U87MG, SMA560, U251MG, and T98G for anchorage-independent growth in semi-solid agar with or without overexpression of GRN. All cell lines formed viable colonies within 14 days. However, overexpression of GRN had no promoting effect on survival and growth of any of the four cell lines. Colony formation in soft agar is widely used as surrogate readout to investigate the effects of substances or genetic alterations on the ability of cancer cells to form solid tumors. It is important to note that this *in vitro* assay can only detect direct effects on the tumor cells. *In vivo*, the microenvironment of tumors plays an important role in supporting tumor growth and progression. Cancer cells produce a range of growth factors and proteases that modify their stromal environment to form a permissive and supportive, so-called reactive tumor stroma. Normal tissue homeostasis is disrupted leading to the induction of an inflammatory response and angiogenesis. The secretion of growth factors and proteases by activated stromal cells further contributes to a tumor growth-promoting environment (Mueller & Fusenig 2004). In the case of gliomas, the stroma consists of non-transformed astrocytes, endothelial cells, pericytes, and immune cells. Microglia are the resident immune cells of the brain and, depending on the factors they secrete, can promote or inhibit tumor growth. Glioma cells can secrete chemo-attractants and anti-inflammatory factors to recruit microglia to the tumor environment and transform them to a pro-tumorigenic and immunosuppressive phenotype (Jones & Holland 2011). The importance of microglia cells for glioma formation was clearly demonstrated by *in vivo* studies in microglia-deficient glioma mouse models where tumor cell growth was inhibited (Daginakatte & Gutmann 2007, Markovic *et al.* 2009). Interestingly, GRN has recently been identified as a chemo-attractant for microglial cells, and anti-inflammatory actions have previously been attributed to this protein (He & Bateman 2003, Kessenbrock *et al.* 2008, Pickford *et al.* 2011). A paracrine effect of GRN secreted by tumor cells on microglia cells may thus be an alternative mechanism to promote glioma growth through a supportive tumor stroma. Therefore, we investigated the ability of GRN to enhance tumor formation *in vivo* using the murine glioma cell line SMA560 with doxycycline inducible overexpression of GRN (SMA560 Tet-On-GRN cells). To provide a cellular environment similar to that of developing gliomas, the cells were injected intracranially, and syngenic Vd/Mk mice were used to avoid the need for immunosuppression. Two groups of 14 animals each were injected with the cell line SMA560 Tet-On-GRN, and one group received drinking water supplemented with doxycycline to induce GRN overexpression. A third group was injected with a parental cell line that lacked the expression vector encoding for GRN. This

group also received doxycycline in the drinking water to control for potential effects of this compound, which has numerous biological activities. Unexpectedly, the incidence of tumor growth was low in both groups treated with doxycycline. Only 5 of 14 animals that had received the inducible cell line SMA560 Tet-On-GRN and doxycycline, and 8 of 14 animals that had received the control cell line and doxycycline developed tumors. Tumor volumes were measured by MR imaging in 4-5 animals per group 14 and 21 days after inoculation. At day 14, the glioma cell line with doxycycline-induced overexpression of GRN had formed approximately 40% larger tumors compared to the non-induced and the parental control cell line. At day 21, tumors formed by the induced cell line were significantly larger than tumors in both control groups. Unexpectedly, the control group that had received the parental cell line lacking the GRN expression vector but that was treated with doxycycline had formed larger tumors than the control group harbouring the SMA560 Tet-On-GRN cells without doxycycline induction. This could indicate a minor tumor growth promoting effect of doxycycline, although the difference between the control groups was not statistically significant. Two animals of each group were sacrificed after the second MRI analysis to examine the histology of the tumors. In H&E stainings, highly cellular, pleiomorph tumor masses were observed. Unlike diffusely infiltrating human gliomas, tumors formed by the murine SMA560 cells were well circumscribed, consistent with earlier transplantation studies with this cell line (Ashley *et al.* 1998) The cells had an epitheloid shape, hyperchromatic nuclei, and pale eosinophilic cytoplasm. We observed no obvious histological differences between the tumors of the three groups. In summary, we conclude from these transplantation studies that GRN has the ability to promote glioma growth *in vivo*. However, unlike previous findings in peripheral malignancies, our data do not support a direct autocrine effect of GRN in gliomas. Using the same SMA560 cells with inducible overexpression of GRN, no effects on cellular proliferation, sensitivity to apoptosis inducing agents, or the ability for anchorage-independent growth were observed in our functional *in vitro* assays. Hence, the fact that a growth promoting effect of GRN was exclusively found in the *in vivo* model of glioma development suggests that GRN secreted by the tumor cells acted on cells of the tumor stroma or the immune system. In future studies, a detailed immunohistochemical analysis of the xenografts with and without GRN overexpression may help to uncover the mechanism by which GRN exerts its growth promoting function in gliomas.

6 SUMMARY

High-grade gliomas of the brain belong to the most malignant human cancers. Despite substantial progress in the understanding of their molecular pathology, the prognosis of these tumors remains very poor with most glioblastoma patients dying within 1-2 years after diagnosis. Therefore, the characterization of novel therapeutic targets is urgently needed. Progranulin (GRN) is a secreted protein with growth factor-like properties that is upregulated in a variety of cancers and functions as an autocrine stimulant of tumor growth and invasive behavior. At the beginning of this thesis project, only minimal information was available about a potential role of GRN in human brain tumors. Two studies had suggested that GRN might be overexpressed in gliomas, and that peptides derived from GRN could have growth-promoting effects on glioma cells *in vitro*. However, these conclusions were based exclusively on RNA transcript analysis in a small number of gliomas and on very limited functional analysis.

In this study, overexpression of GRN was validated both on the transcript and the protein level in much larger collections of human gliomas. While GRN expression in normal brain samples was low and restricted to neurons and microglial cells, significant overexpression of GRN was demonstrated by quantitative RT-PCR and microarray gene expression analysis in both low and high-grade gliomas in two independents sets of tumor samples. Interestingly, the highest GRN mRNA expression levels were consistently found in primary glioblastomas. Overexpression of GRN was further confirmed on the protein level by Western blotting and screening of a tissue microarray, in which 55/56 glioma samples displayed GRN expression. Collectively, these data suggested that upregulation of GRN expression might be important rather early in glioma development, and particularly in primary glioblastomas, which develop without a prior history of lower grade gliomas and constitute a distinct genetic entity. As tools to enable functional studies, both human and murine glioma cell lines with inducible overexpression or stable miRNA-mediated knockdown of GRN expression were developed. Surprisingly, no differences in the cellular proliferation, migration, sensitivity to chemotherapeutic and apoptosis inducing agents, or in the anchorage-independent growth of these glioma cell lines with elevated or reduced GRN expression were observed. Importantly, *in vivo*, a murine glioblastoma cell line formed significantly larger tumors after intracranial injection into syngenic mice when GRN overexpression was induced by doxycycline treatment of the animals. Taken together, the presented work verifies that GRN is overexpressed in human gliomas. In contrast to previous studies in peripheral malignancies, functional assays did not provide evidence that GRN acts as an autocrine growth factor in gliomas. However, a growth promoting effect of GRN was observed in an intracranial glioma model *in vivo*, suggesting that GRN exerts its tumor promoting function in a non-cell autonomous fashion through effects on the tumor microenvironment.

7 REFERENCES

7.1 Literature

Ahmed, Z., Mackenzie, I. R., Hutton, M. L. and Dickson, D. W. (2007) Progranulin in frontotemporal lobar degeneration and neuroinflammation. *J Neuroinflammation,* **4,** 7.

Ahmed, Z., Sheng, H., Xu, Y. F. et al. (2010) Accelerated lipofuscinosis and ubiquitination in granulin knockout mice suggest a role for progranulin in successful aging. *Am J Pathol,* **177,** 311-324.

Albini, A. and Sporn, M. B. (2007) The tumour microenvironment as a target for chemoprevention. *Nat Rev Cancer,* **7,** 139-147.

Anderson, S. N., Towne, D. L., Burns, D. J. and Warrior, U. (2007) A high-throughput soft agar assay for identification of anticancer compound. *J Biomol Screen,* **12,** 938-945.

Ashley, D. M., Kong, F. M., Bigner, D. D. and Hale, L. P. (1998) Endogenous expression of transforming growth factor beta1 inhibits growth and tumorigenicity and enhances Fas-mediated apoptosis in a murine high-grade glioma model. *Cancer Res,* **58,** 302-309.

Baba, T., Hoff, H. B., 3rd, Nemoto, H., Lee, H., Orth, J., Arai, Y. and Gerton, G. L. (1993) Acrogranin, an acrosomal cysteine-rich glycoprotein, is the precursor of the growth-modulating peptides, granulins, and epithelins, and is expressed in somatic as well as male germ cells. *Mol Reprod Dev,* **34,** 233-243.

Baker, M., Mackenzie, I. R., Pickering-Brown, S. M. et al. (2006) Mutations in progranulin cause tau-negative frontotemporal dementia linked to chromosome 17. *Nature,* **442,** 916-919.

Balss, J., Meyer, J., Mueller, W., Korshunov, A., Hartmann, C. and von Deimling, A. (2008) Analysis of the IDH1 codon 132 mutation in brain tumors. *Acta Neuropathol,* **116,** 597-602.

Bartkowska, K., Turlejski, K. and Djavadian, R. L. (2011) Neurotrophins and their receptors in early development of the mammalian nervous system. *Acta Neurobiol Exp (Wars),* **70,** 454-467.

Bateman, A., Belcourt, D., Bennett, H., Lazure, C. and Solomon, S. (1990) Granulins, a novel class of peptide from leukocytes. *Biochem Biophys Res Commun,* **173,** 1161-1168.

Bateman, A. and Bennett, H. P. (2009) The granulin gene family: from cancer to dementia. *Bioessays,* **31,** 1245-1254.

Bhandari, V. and Bateman, A. (1992) Structure and chromosomal location of the human granulin gene. *Biochem Biophys Res Commun,* **188,** 57-63.

Bhandari, V., Daniel, R., Lim, P. S. and Bateman, A. (1996) Structural and functional analysis of a promoter of the human granulin/epithelin gene. *Biochem J,* **319 (Pt 2),** 441-447.

Bhandari, V., Giaid, A. and Bateman, A. (1993) The complementary deoxyribonucleic acid sequence, tissue distribution, and cellular localization of the rat granulin precursor. *Endocrinology,* **133,** 2682-2689.

Brat, D. and Perry, A. (2010) *Astrocytic and Oligodendroglial Tumors*: Practical Surgical Neuropathology - A Diagnostic Approach. Elsevier.

Carrasquillo, M. M., Nicholson, A. M., Finch, N. et al. (2011) Genome-wide screen identifies rs646776 near sortilin as a regulator of progranulin levels in human plasma. *Am J Hum Genet,* **87,** 890-897.

Charles, N. A., Holland, E. C., Gilbertson, R., Glass, R. and Kettenmann, H. (2012) The brain tumor microenvironment. *Glia,* **60,** 502-514.

Cheung, S. T., Cheung, P. F., Cheng, C. K., Wong, N. C. and Fan, S. T. (2011) Granulin-epithelin precursor and ATP-dependent binding cassette (ABC)B5 regulate liver cancer cell chemoresistance. *Gastroenterology,* **140,** 344-355.

Cheung, S. T., Wong, S. Y., Leung, K. L., Chen, X., So, S., Ng, I. O. and Fan, S. T. (2004) Granulin-epithelin precursor overexpression promotes growth and invasion of hepatocellular carcinoma. *Clin Cancer Res,* **10,** 7629-7636.

Cruts, M., Gijselinck, I., van der Zee, J. et al. (2006) Null mutations in progranulin cause ubiquitin-positive frontotemporal dementia linked to chromosome 17q21. *Nature,* **442,** 920-924.

Cruts, M. and Van Broeckhoven, C. (2008) Loss of progranulin function in frontotemporal lobar degeneration. *Trends Genet,* **24,** 186-194.

Cuevas-Antonio, R., Cancino, C., Arechavaleta-Velasco, F. et al. (2010) Expression of progranulin (Acrogranin/PCDGF/Granulin-Epithelin Precursor) in benign and malignant ovarian tumors and activation of MAPK signaling in ovarian cancer cell line. *Cancer Invest,* **28,** 452-458.

D'Alimonte, I., Ballerini, P., Nargi, E., Buccella, S., Giuliani, P., Di Iorio, P., Caciagli, F. and Ciccarelli, R. (2007) Staurosporine-induced apoptosis in astrocytes is prevented by A1 adenosine receptor activation. *Neurosci Lett,* **418,** 66-71.

Daginakatte, G. C. and Gutmann, D. H. (2007) Neurofibromatosis-1 (Nf1) heterozygous brain microglia elaborate paracrine factors that promote Nf1-deficient astrocyte and glioma growth. *Hum Mol Genet,* **16,** 1098-1112.

Daniel, R., Daniels, E., He, Z. and Bateman, A. (2003) Progranulin (acrogranin/PC cell-derived growth factor/granulin-epithelin precursor) is expressed in the placenta, epidermis, microvasculature, and brain during murine development. *Dev Dyn,* **227,** 593-599.

Daniel, R., He, Z., Carmichael, K. P., Halper, J. and Bateman, A. (2000) Cellular localization of gene expression for progranulin. *J Histochem Cytochem,* **48,** 999-1009.

De Witt Hamer, P. C., Van Tilborg, A. A., Eijk, P. P., Sminia, P., Troost, D., Van Noorden, C. J., Ylstra, B. and Leenstra, S. (2008) The genomic profile of human malignant glioma is altered early in primary cell culture and preserved in spheroids. *Oncogene,* **27,** 2091-2096.

Denmeade, S. R. and Isaacs, J. T. (2005) The SERCA pump as a therapeutic target: making a "smart bomb" for prostate cancer. *Cancer Biol Ther,* **4,** 14-22.

Diaz-Cueto, L., Stein, P., Jacobs, A., Schultz, R. M. and Gerton, G. L. (2000) Modulation of mouse preimplantation embryo development by acrogranin (epithelin/granulin precursor). *Dev Biol,* **217,** 406-418.

Egland, K. A., Vincent, J. J., Strausberg, R., Lee, B. and Pastan, I. (2003) Discovery of the breast cancer gene BASE using a molecular approach to enrich for genes encoding membrane and secreted proteins. *Proc Natl Acad Sci U S A,* **100,** 1099-1104.

El Andaloussi, A., Han, Y. and Lesniak, M. S. (2006) Prolongation of survival following depletion of CD4+CD25+ regulatory T cells in mice with experimental brain tumors. *J Neurosurg,* **105,** 430-437.

Eriksen, J. L. and Mackenzie, I. R. (2008) Progranulin: normal function and role in neurodegeneration. *J Neurochem,* **104,** 287-297.

Fael Al-Mayhani, T. M., Ball, S. L., Zhao, J. W., Fawcett, J., Ichimura, K., Collins, P. V. and Watts, C. (2009) An efficient method for derivation and propagation of glioblastoma cell lines that conserves the molecular profile of their original tumours. *J Neurosci Methods,* **176,** 192-199.

Gao, X., Joselin, A. P., Wang, L., Kar, A., Ray, P., Bateman, A., Goate, A. M. and Wu, J. Y. (2010) Progranulin promotes neurite outgrowth and neuronal differentiation by regulating GSK-3beta. *Protein Cell,* **1,** 552-562.

Grzmil, M. and Hemmings, B. A. (2010) Deregulated signalling networks in human brain tumours. *Biochim Biophys Acta,* **1804,** 476-483.

Hanahan, D. and Weinberg, R. A. (2000) The hallmarks of cancer. *Cell,* **100,** 57-70.

Hau, P., Jachimczak, P., Schlingensiepen, R. et al. (2007) Inhibition of TGF-beta2 with AP 12009 in recurrent malignant gliomas: from preclinical to phase I/II studies. *Oligonucleotides,* **17,** 201-212.

He, Z. and Bateman, A. (1999) Progranulin gene expression regulates epithelial cell growth and promotes tumor growth in vivo. *Cancer Res,* **59,** 3222-3229.

He, Z. and Bateman, A. (2003) Progranulin (granulin-epithelin precursor, PC-cell-derived growth factor, acrogranin) mediates tissue repair and tumorigenesis. *J Mol Med,* **81,** 600-612.

He, Z., Ismail, A., Kriazhev, L., Sadvakassova, G. and Bateman, A. (2002) Progranulin (PC-cell-derived growth factor/acrogranin) regulates invasion and cell survival. *Cancer Res,* **62,** 5590-5596.

Hermanson, M., Funa, K., Hartman, M., Claesson-Welsh, L., Heldin, C. H., Westermark, B. and Nister, M. (1992) Platelet-derived growth factor and its receptors in human glioma tissue: expression of messenger RNA and protein suggests the presence of autocrine and paracrine loops. *Cancer Res,* **52,** 3213-3219.

Himes, R. H., Kersey, R. N., Heller-Bettinger, I. and Samson, F. E. (1976) Action of the vinca alkaloids vincristine, vinblastine, and desacetyl vinblastine amide on microtubules in vitro. *Cancer Res,* **36,** 3798-3802.

Ho, J. C., Ip, Y. C., Cheung, S. T., Lee, Y. T., Chan, K. F., Wong, S. Y. and Fan, S. T. (2008) Granulin-epithelin precursor as a therapeutic target for hepatocellular carcinoma. *Hepatology,* **47,** 1524-1532.

Hoelzinger, D. B., Demuth, T. and Berens, M. E. (2007) Autocrine factors that sustain glioma invasion and paracrine biology in the brain microenvironment. *J Natl Cancer Inst,* **99,** 1583-1593.

Hrabal, R., Chen, Z., James, S., Bennett, H. P. and Ni, F. (1996) The hairpin stack fold, a novel protein architecture for a new family of protein growth factors. *Nat Struct Biol,* **3,** 747-752.

Hu, F., Padukkavidana, T., Vaegter, C. B., Brady, O. A., Zheng, Y., Mackenzie, I. R., Feldman, H. H., Nykjaer, A. and Strittmatter, S. M. (2010) Sortilin-mediated endocytosis determines levels of the frontotemporal dementia protein, progranulin. *Neuron,* **68,** 654-667.

Ichimura, K., Bolin, M. B., Goike, H. M., Schmidt, E. E., Moshref, A. and Collins, V. P. (2000) Deregulation of the p14ARF/MDM2/p53 pathway is a prerequisite for human astrocytic gliomas with G1-S transition control gene abnormalities. *Cancer Res,* **60,** 417-424.

Ishii, N., Maier, D., Merlo, A., Tada, M., Sawamura, Y., Diserens, A. C. and Van Meir, E. G. (1999) Frequent co-alterations of TP53, p16/CDKN2A, p14ARF, PTEN tumor suppressor genes in human glioma cell lines. *Brain Pathol,* **9,** 469-479.

Jones, M. B., Michener, C. M., Blanchette, J. O. et al. (2003) The granulin-epithelin precursor/PC-cell-derived growth factor is a growth factor for epithelial ovarian cancer. *Clin Cancer Res,* **9,** 44-51.

Jones, T. S. and Holland, E. C. (2011) Standard of care therapy for malignant glioma and its effect on tumor and stromal cells. *Oncogene*.

Kayasuga, Y., Chiba, S., Suzuki, M. et al. (2007) Alteration of behavioural phenotype in mice by targeted disruption of the progranulin gene. *Behav Brain Res,* **185,** 110-118.

Kessenbrock, K., Frohlich, L., Sixt, M. et al. (2008) Proteinase 3 and neutrophil elastase enhance inflammation in mice by inactivating antiinflammatory progranulin. *J Clin Invest,* **118,** 2438-2447.

Kim, C. H., Cheong, J. H. and Kim, J. M. (2010) Correlation of granulin expression in intracranial meningiomas to clinical parameters. *Experimental and Therapeutic Medicine,* **1,** 493-496.

Kleinberger, G., Wils, H., Ponsaerts, P., Joris, G., Timmermans, J. P., Van Broeckhoven, C. and Kumar-Singh, S. (2010) Increased caspase activation and decreased TDP-43 solubility in progranulin knockout cortical cultures. *J Neurochem,* **115,** 735-747.

Krakstad, C. and Chekenya, M. (2010) Survival signalling and apoptosis resistance in glioblastomas: opportunities for targeted therapeutics. *Mol Cancer,* **9,** 135.

Lai, A., Tran, A., Nghiemphu, P. L. et al. (2011) Phase II study of bevacizumab plus temozolomide during and after radiation therapy for patients with newly diagnosed glioblastoma multiforme. *J Clin Oncol,* **29,** 142-148.

Le, D. M., Besson, A., Fogg, D. K., Choi, K. S., Waisman, D. M., Goodyer, C. G., Rewcastle, B. and Yong, V. W. (2003) Exploitation of astrocytes by glioma cells to facilitate invasiveness: a mechanism involving matrix metalloproteinase-2 and the urokinase-type plasminogen activator-plasmin cascade. *J Neurosci,* **23,** 4034-4043.

Lee, J., Kotliarova, S., Kotliarov, Y. et al. (2006) Tumor stem cells derived from glioblastomas cultured in bFGF and EGF more closely mirror the phenotype and genotype of primary tumors than do serum-cultured cell lines. *Cancer Cell,* **9,** 391-403.

Leerkes, M. R., Caballero, O. L., Mackay, A., Torloni, H., O'Hare, M. J., Simpson, A. J. and de Souza, S. J. (2002) In silico comparison of the transcriptome derived from purified normal breast cells and breast tumor cell lines reveals candidate upregulated genes in breast tumor cells. *Genomics,* **79,** 257-265.

Liau, L. M., Lallone, R. L., Seitz, R. S., Buznikov, A., Gregg, J. P., Kornblum, H. I., Nelson, S. F. and Bronstein, J. M. (2000) Identification of a human glioma-associated growth factor gene, granulin, using differential immuno-absorption. *Cancer Res,* **60,** 1353-1360.

Liu, Y., Xi, L., Liao, G. et al. (2007) Inhibition of PC cell-derived growth factor (PCDGF)/granulin-epithelin precursor (GEP) decreased cell proliferation and invasion through downregulation of cyclin D and CDK4 and inactivation of MMP-2. *BMC Cancer,* **7,** 22.

Lohr, J., Ratliff, T., Huppertz, A. et al. (2011) Effector T-cell infiltration positively impacts survival of glioblastoma patients and is impaired by tumor-derived TGF-beta. *Clin Cancer Res,* **17,** 4296-4308.

Lorger, M. (2012) Tumor Microenvironment in the Brain. *Cancers,* **4,** 218-243.

Louis, D. N., Ohgaki, H., Wiestler, O. D., Cavenee, W. K., Burger, P. C., Jouvet, A., Scheithauer, B. W. and Kleihues, P. (2007) The 2007 WHO classification of tumours of the central nervous system. *Acta Neuropathol,* **114,** 97-109.

Lu, R. and Serrero, G. (2000) Inhibition of PC cell-derived growth factor (PCDGF, epithelin/granulin precursor) expression by antisense PCDGF cDNA transfection inhibits tumorigenicity of the human breast carcinoma cell line MDA-MB-468. *Proc Natl Acad Sci U S A,* **97,** 3993-3998.

Lu, R. and Serrero, G. (2001) Mediation of estrogen mitogenic effect in human breast cancer MCF-7 cells by PC-cell-derived growth factor (PCDGF/granulin precursor). *Proc Natl Acad Sci U S A,* **98,** 142-147.

Mackenzie, I. R., Baker, M., Pickering-Brown, S. et al. (2006) The neuropathology of frontotemporal lobar degeneration caused by mutations in the progranulin gene. *Brain,* **129,** 3081-3090.

Markert, J. M., Fuller, C. M., Gillespie, G. Y. et al. (2001) Differential gene expression profiling in human brain tumors. *Physiol Genomics,* **5,** 21-33.

Markovic, D. S., Vinnakota, K., Chirasani, S. et al. (2009) Gliomas induce and exploit microglial MT1-MMP expression for tumor expansion. *Proc Natl Acad Sci U S A,* **106,** 12530-12535.

Matsumura, N., Mandai, M., Miyanishi, M., Fukuhara, K., Baba, T., Higuchi, T., Kariya, M., Takakura, K. and Fujii, S. (2006) Oncogenic property of acrogranin in human uterine leiomyosarcoma: direct evidence of genetic contribution in in vivo tumorigenesis. *Clin Cancer Res,* **12,** 1402-1411.

Matsuwaki, T., Asakura, R., Suzuki, M., Yamanouchi, K. and Nishihara, M. (2011) Age-dependent changes in progranulin expression in the mouse brain. *J Reprod Dev,* **57,** 113-119.

Moisse, K., Volkening, K., Leystra-Lantz, C., Welch, I., Hill, T. and Strong, M. J. (2009) Divergent patterns of cytosolic TDP-43 and neuronal progranulin expression following axotomy: implications for TDP-43 in the physiological response to neuronal injury. *Brain Res,* **1249,** 202-211.

Monami, G., Emiliozzi, V., Bitto, A. et al. (2009) Proepithelin regulates prostate cancer cell biology by promoting cell growth, migration, and anchorage-independent growth. *Am J Pathol,* **174,** 1037-1047.

Monami, G., Gonzalez, E. M., Hellman, M., Gomella, L. G., Baffa, R., Iozzo, R. V. and Morrione, A. (2006) Proepithelin promotes migration and invasion of 5637 bladder cancer cells through the activation of ERK1/2 and the formation of a paxillin/FAK/ERK complex. *Cancer Res,* **66,** 7103-7110.

Mueller, M. M. and Fusenig, N. E. (2004) Friends or foes - bipolar effects of the tumour stroma in cancer. *Nat Rev Cancer,* **4,** 839-849.
Mukherjee, O., Pastor, P., Cairns, N. J. et al. (2006) HDDD2 is a familial frontotemporal lobar degeneration with ubiquitin-positive, tau-negative inclusions caused by a missense mutation in the signal peptide of progranulin. *Ann Neurol,* **60,** 314-322.
Naphade, S. B., Kigerl, K. A., Jakeman, L. B., Kostyk, S. K., Popovich, P. G. and Kuret, J. (2010) Progranulin expression is upregulated after spinal contusion in mice. *Acta Neuropathol,* **119,** 123-133.
Nedachi, T., Kawai, T., Matsuwaki, T., Yamanouchi, K. and Nishihara, M. (2011) Progranulin enhances neural progenitor cell proliferation through glycogen synthase kinase 3beta phosphorylation. *Neuroscience,* **185,** 106-115.
Norden, A. D. and Wen, P. Y. (2006) Glioma therapy in adults. *Neurologist,* **12,** 279-292.
Parnell, P. G., Wunderlich, J., Carter, B. and Halper, J. (1992) Transforming growth factor e: amino acid analysis and partial amino acid sequence. *Growth Factors,* **7,** 65-72.
Petkau, T. L., Neal, S. J., Orban, P. C., MacDonald, J. L., Hill, A. M., Lu, G., Feldman, H. H., Mackenzie, I. R. and Leavitt, B. R. (2010) Progranulin expression in the developing and adult murine brain. *J Comp Neurol,* **518,** 3931-3947.
Pickford, F., Marcus, J., Camargo, L. M. et al. (2011) Progranulin is a chemoattractant for microglia and stimulates their endocytic activity. *Am J Pathol,* **178,** 284-295.
Pizarro, G. O., Zhou, X. C., Koch, A., Gharib, M., Raval, S., Bible, K. and Jones, M. B. (2007) Prosurvival function of the granulin-epithelin precursor is important in tumor progression and chemoresponse. *Int J Cancer,* **120,** 2339-2343.
Plowman, G. D., Green, J. M., Neubauer, M. G., Buckley, S. D., McDonald, V. L., Todaro, G. J. and Shoyab, M. (1992) The epithelin precursor encodes two proteins with opposing activities on epithelial cell growth. *J Biol Chem,* **267,** 13073-13078.
Raguz, S. and Yague, E. (2008) Resistance to chemotherapy: new treatments and novel insights into an old problem. *Br J Cancer,* **99,** 387-391.
Reifenberger, G. and Collins, V. P. (2004) Pathology and molecular genetics of astrocytic gliomas. *J Mol Med,* **82,** 656-670.
Reifenberger, G., Reifenberger, J., Ichimura, K., Meltzer, P. S. and Collins, V. P. (1994) Amplification of multiple genes from chromosomal region 12q13-14 in human malignant gliomas: preliminary mapping of the amplicons shows preferential involvement of CDK4, SAS, and MDM2. *Cancer Res,* **54,** 4299-4303.
Reitman, Z. J. and Yan, H. (2010) Isocitrate dehydrogenase 1 and 2 mutations in cancer: alterations at a crossroads of cellular metabolism. *J Natl Cancer Inst,* **102,** 932-941.
Riemenschneider, M. J., Hegi, M. E. and Reifenberger, G. MGMT promoter methylation in malignant gliomas. *Target Oncol,* **5,** 161-165.
Riemenschneider, M. J., Jeuken, J. W., Wesseling, P. and Reifenberger, G. (2010) Molecular diagnostics of gliomas: state of the art. *Acta Neuropathol,* **120,** 567-584.
Riemenschneider, M. J. and Reifenberger, G. (2009a) Astrocytic tumors. *Recent Results Cancer Res,* **171,** 3-24.
Riemenschneider, M. J. and Reifenberger, G. (2009b) Molecular neuropathology of gliomas. *Int J Mol Sci,* **10,** 184-212.
Roth, P., Junker, M., Tritschler, I. et al. (2010) GDF-15 contributes to proliferation and immune escape of malignant gliomas. *Clin Cancer Res,* **16,** 3851-3859.
Ryan, C. L., Baranowski, D. C., Chitramuthu, B. P. et al. (2009) Progranulin is expressed within motor neurons and promotes neuronal cell survival. *BMC Neurosci,* **10,** 130.
Schneider, T., Mawrin, C., Scherlach, C., Skalej, M. and Firsching, R. (2010) Gliomas in adults. *Dtsch Arztebl Int,* **107,** 799-807; quiz 808.
Shoyab, M., McDonald, V. L., Byles, C., Todaro, G. J. and Plowman, G. D. (1990) Epithelins 1 and 2: isolation and characterization of two cysteine-rich growth-modulating proteins. *Proc Natl Acad Sci U S A,* **87,** 7912-7916.
Siddik, Z. H. (2003) Cisplatin: mode of cytotoxic action and molecular basis of resistance. *Oncogene,* **22,** 7265-7279.
Stupp, R., Hegi, M. E., Neyns, B. et al. (2010) Phase I/IIa study of cilengitide and temozolomide with concomitant radiotherapy followed by cilengitide and

temozolomide maintenance therapy in patients with newly diagnosed glioblastoma. *J Clin Oncol,* **28,** 2712-2718.

Suzuki, M. and Nishiahara, M. (2002) Granulin precursor gene: a sex steroid-inducible gene involved in sexual differentiation of the rat brain. *Mol Genet Metab,* **75,** 31-37.

Tang, W., Lu, Y., Tian, Q. Y. et al. (2011) The growth factor progranulin binds to TNF receptors and is therapeutic against inflammatory arthritis in mice. *Science,* **332,** 478-484.

Tangkeangsirisin, W. and Serrero, G. (2004) PC cell-derived growth factor (PCDGF/GP88, progranulin) stimulates migration, invasiveness and VEGF expression in breast cancer cells. *Carcinogenesis,* **25,** 1587-1592.

Toh, H., Chitramuthu, B. P., Bennett, H. P. and Bateman, A. (2011) Structure, Function, and Mechanism of Progranulin; the Brain and Beyond. *J Mol Neurosci*.

Tolkatchev, D., Malik, S., Vinogradova, A., Wang, P., Chen, Z., Xu, P., Bennett, H. P., Bateman, A. and Ni, F. (2008) Structure dissection of human progranulin identifies well-folded granulin/epithelin modules with unique functional activities. *Protein Sci,* **17,** 711-724.

Wang, M., Li, G., Yin, J., Lin, T. and Zhang, J. (2011) Progranulin overexpression predicts overall survival in patients with glioblastoma. *Med Oncol*.

Wang, W., Hayashi, J., Kim, W. E. and Serrero, G. (2003) PC cell-derived growth factor (granulin precursor) expression and action in human multiple myeloma. *Clin Cancer Res,* **9,** 2221-2228.

Watanabe, T., Katayama, Y., Yoshino, A., Yachi, K., Ohta, T., Ogino, A., Komine, C. and Fukushima, T. (2007) Aberrant hypermethylation of p14ARF and O6-methylguanine-DNA methyltransferase genes in astrocytoma progression. *Brain Pathol,* **17,** 5-10.

Weller, M. (2011) Novel diagnostic and therapeutic approaches to malignant glioma. *Swiss Med Wkly,* **141,** w13210.

Willnow, T. E., Petersen, C. M. and Nykjaer, A. (2008) VPS10P-domain receptors - regulators of neuronal viability and function. *Nat Rev Neurosci,* **9,** 899-909.

Witkiewicz, A. K., Casimiro, M. C., Dasgupta, A. et al. (2009) Towards a new "stromal-based" classification system for human breast cancer prognosis and therapy. *Cell Cycle,* **8,** 1654-1658.

Yin, F., Banerjee, R., Thomas, B. et al. (2010a) Exaggerated inflammation, impaired host defense, and neuropathology in progranulin-deficient mice. *J Exp Med,* **207,** 117-128, S111-114.

Yin, F., Dumont, M., Banerjee, R. et al. (2010b) Behavioral deficits and progressive neuropathology in progranulin-deficient mice: a mouse model of frontotemporal dementia. *FASEB J,* **24,** 4639-4647.

Zanocco-Marani, T., Bateman, A., Romano, G., Valentinis, B., He, Z. H. and Baserga, R. (1999) Biological activities and signaling pathways of the granulin/epithelin precursor. *Cancer Res,* **59,** 5331-5340.

Zhang, H. and Serrero, G. (1998) Inhibition of tumorigenicity of the teratoma PC cell line by transfection with antisense cDNA for PC cell-derived growth factor (PCDGF, epithelin/granulin precursor). *Proc Natl Acad Sci U S A,* **95,** 14202-14207.

Zhou, J., Gao, G., Crabb, J. W. and Serrero, G. (1993) Purification of an autocrine growth factor homologous with mouse epithelin precursor from a highly tumorigenic cell line. *J Biol Chem,* **268,** 10863-10869.

Zhu, J., Nathan, C., Jin, W. et al. (2002) Conversion of proepithelin to epithelins: roles of SLPI and elastase in host defense and wound repair. *Cell,* **111,** 867-878.

7.2 References - Figures

Figure 1 Reprinted from Cruts, M. and Van Broeckhoven, C. (2008) Loss of progranulin function in frontotemporal lobar degeneration. *Trends Genet,* **24,** 186-194, with permission from Elsevier Ltd.

Figure 2 Reprinted from He, Z. and Bateman, A. (2003) Progranulin (granulin-epithelin precursor, PC-cell-derived growth factor, acrogranin) mediates tissue repair and tumorigenesis. *J Mol Med,* **81,** 600-612, with permission from SPRINGER Verlag Berlin/Heidelberg.

Figure 3 Reprinted from Brat, D. and Perry, A. (2010) *Astrocytic and Oligodendroglial Tumors*: Practical Surgical Neuropathology - A Diagnostic Approach. Elsevier Books, with permission from Elsevier.

Figure 4 Schneider, T., Mawrin, C., Scherlach, C., Skalej, M. and Firsching, R. (2010) Gliomas in adults. *Dtsch Arztebl Int,* **107,** 799-807; quiz 808

Figure 5 Reprinted from Riemenschneider, M. J., Jeuken, J. W., Wesseling, P. and Reifenberger, G. (2010) Molecular diagnostics of gliomas: state of the art. *Acta Neuropathol,* **120,** 567-584, with permission from SPRINGER-Verlag.

Figure 6 Reprinted from Grzmil, M. and Hemmings, B. A. (2010) Deregulated signalling networks in human brain tumours. *Biochim Biophys Acta,* **1804,** 476-483, with permission from Elsevier.

8 APPENDIX

8.1 Zusammenfassung

Maligne Gliome sind die häufigsten primären Tumore des zentralen Nervensystems. Obwohl das Verständnis der molekularen Ursachen der Pathologie dieser Tumore stetig zunimmt, konnte die Prognose für Patienten bislang nicht verbessert werden. Die meisten Patienten mit Glioblastomen versterben innerhalb der ersten 1-2 Jahre nach der Diagnose. Neue therapeutische Ansätze sind daher von dringender Notwendigkeit. Progranulin (GRN) ist ein sekretiertes Protein mit Wachstumsfaktor ähnlichen Eigenschaften. Eine Überexpression dieses Proteins wurde bereits in vielen Tumorarten beschrieben, wo es Wachstum und Invasivität der Tumorzellen autokrin stimulieren soll. Für gliale Hirntumore wurde eine Überexpression von GRN bislang in zwei Studien beschrieben, wobei nur eine sehr geringe Anzahl von Tumorproben ausschließlich auf RNA-Ebene analysiert wurde.

In der vorliegenden Arbeit wurde die Überexpression von GRN in glialen Hirntumoren in einer größeren Anzahl von Proben, sowohl auf RNA- als auch auf Proteinebene, bestätigt. Während die Expression in normalem Hirngewebe sehr gering und auf Neurone und Mikroglia beschränkt war, konnte eine signifikante Überexpression in den Tumorproben mittels quantitativer RT-PCR (48 Proben) und Genexpressionsanalyse (74 Proben) gezeigt werden. Zusätzlich wurden erhöhte Expressionslevel per Western Blot und Immunhistochemie auch auf Proteinebene festgestellt. Die höchsten Expressionswerte wurden übereinstimmend in primären Glioblastomen, die sich *de novo* entwickeln gefunden, wohingegen die Progression von Astrozytomen zu sekundären Glioblastomen nicht mit steigenden Expressionswerten korrelierte. Um funktionelle Studien zu ermöglichen wurden Gliom-Zelllinien mit induzierbarer Überexpression oder stabilem knockdown von GRN hergestellt. Überraschenderweise konnten jedoch abhängig vom Expressionslevel keine Unterschiede in Zellproliferation, Migration, Sensitivität gegenüber chemotherapeutischen und Apoptose induzierenden Substanzen oder der Fähigkeit zu Adhäsions-unabhängigem Wachstum gefunden werden. Die Tumorigenität einer murinen Glioblastom-Zelllinie nach intracranialer Injektion in syngenen Mäusen war dagegen signifikant erhöht, wenn die operierten Tiere mit Doxycyclin behandelt wurden um die Überexpression von GRN in den injizierten Zellen zu induzieren.

Zusammenfassend konnte diese Studie die Überexpression von GRN in humanen Gliomen bestätigen. Anders als bereits für verschiedene periphere Tumorarten beschrieben, wurden in funktionellen Studien dieser Arbeit allerdings keine Hinweise auf einen autokrinen, Wachstum stimulierenden Effekt von GRN auf Gliomzellen gefunden. Im Gegensatz dazu wurde das Tumorwachstum nach intracranialer Transplantation von Zellen durch GRN-Überexpression stark erhöht. Wechselwirkungen des Proteins mit dem umliegenden Gewebe sind daher ein wahrscheinlicher, alternativer Mechanismus mit dem GRN das Tumorwachstum fördert.

8.2 Abbreviations

°C	Degree Celsius
µg	Microgram
µl	Microliter
µm	Micrometer
AKT	v-akt murine thymoma viral oncogene homolog 1
ATP	Adenosintriphosphate
BDNF	Brain-derived neurotrophic factor
BSA	Bovine serum albumin
CCD	Charge-coupled device
CDK	Cyclin-dependent kinase
CDKN2A	CDK inhibitor 2A
cDNA	Complementary DNA
CNS	Central nervous system
CREB	Cyclic AMP response element binding protein
DAB	3,3'-Diaminobenzidine
DNA	Deoxyribonucleic acid
dNTP	Deoxyribonucleoside-triphosphate
DTT	Dithiothreitol
E2F	E2F transcription factor
EDTA	Ethylendiamin-tetraacetate
EGFR	Epidermal growth factor receptor
EMP3	Epithelial membrane protein 3
ERK	Extracellular signal-regulated kinase
FAK	Focal adhesion kinase
FTLD-U	Frontotemporal dementia with ubiquitin-positive inclusions
g	Gram
GBM	Glioblastoma multiforme
GRN	Progranulin
GSK-3β	Glycogen synthase kinase-3β
h	Hour
HCC	Hepatocellular carcinoma
HIF1α	Hypoxia inducible factor 1 alpha
HRP	Horse reddish peroxidise
hTERT	Human telomerase reverse transcriptase
IC	Immune complex

IDH1	Isocitrate dehydrogenase 1/2
IGF-IR	Insulin-like growth factor I receptor
IkB	Inhibitor of NFκB
IL10	Interleukin-10
kDa	Kilo Dalton
LB	Lysogeny Broth
LMP	Low malignant potential
M	Molar
mA	Milli-Ampere
MDM2	Murine double minute 2
MES	2-(N-morpholino)ethanesulfonic acid
mg	Milligram
MGMT	O-6-methylguanine-DNA methyltransferase
min	Minute
ml	Milliliter
MM	Multiple myeloma
mM	Millimolar
MRI	Magnetic resonance imaging
mRNA	Messenger RNA
mTOR	Mechanistic target of rapamycin
MYC	v-myc myelocytomatosis viral oncogene homolog
NaN_3	Sodiumazide
NE	Neutrophil elastase
NFκB	Nuclear factor of kappa light polypeptide gene enhancer in B-cells
NGF	Nerve growth factor
nm	Nanometer
NPCs	Neural progenitor cells
PBS	Phosphate buffered saline
PCR	Polymerase chain reaction
PCR	Polymerase chain reaction
PCV	Procarbazine/lomustine/vincristine
$pd(N)_6$	Random hexamer primer
PDGF	Platelet-derived growth factor
PDGFR	PDGF receptor
PI3K	Phosphoinositide 3-kinase
PIP_2	Phosphatidylinositol-4,5 bisphosphate
PIP_3	Phosphatidylinositol-3,4,5 triphosphate

PR3	Proteinase 3
pRb	Retinoblastoma tumor suppressor protein
PTEN	Phosphate and tensin homologue
PVDF	Polyvinylidene fluoride
RB1	Retinoblastoma gene
rcf	Relative centrifugal force
RNA	Ribonucleic acid
RNAi	RNA interference
ROS	Reactive oxygen species
RT	Room temperature
RTK	Receptor tyrosine kinase
RT-PCR	Reverse transcription PCR
SDS	Sodium dodecyl sulphate
SDS-PAGE	SDS - polyacrylamide gel electrophoresis
sec	Seconds
siRNA	Small interfering RNA
SLPI	Secretory leukocyte protease inhibitor
SOB	Super Optimal Broth
SOC	SOB supplemented with glucose
SORT1	Sortilin
SV40ER	SV40 early region
TBS	Tris-buffered saline
TBST	TBS supplemented with Tween20
TGF-β2	Transforming growth factor beta 2
TNFR	TNF receptor
TNF	Tumor necrosis factor
UV	Ultraviolet light
V	Volt
VPS10P	Vacuole protein sorting 10 protein
WHO	World Health Organization

8.3 Curriculum vitae

PERSONAL INFORMATION

Name:	Julia Neß
Address:	Geistenstraße 2, 40476 Düsseldorf
Date of Birth:	January 28, 1982
Place of Birth:	Mainz
Nationality:	German
Family status:	unmarried

EDUCATION AND TRAINING

07/07 - 06/12	**Ph.D. in biology**, Institute of Neuropathology, Heinrich-Heine-University Düsseldorf Titel: *„Expression and functional analysis of progranulin (GRN) in glial brain tumors“* Supervisor: Prof. Dr. Sascha Weggen
07/09 - 06/12	associated student of the Research Training Group 1033 „Molecular Targets of the Aging Process and Strategies for the Prevention of Aging“
07/07 - 03/10	associated student of the European Marie Curie Ph.D. Graduate School „Neurodegeneration in Alzheimer’s Disease“
09/01 - 11/06	**Diploma in biology**, Johannes-Gutenberg-University Mainz Diplomathesis: Institute of Physiological Chemistry and Pathobiochemistry, Johannes-Gutenberg-University Mainz Titel: *„Modulation of endogenous Aβ42-production in primary neurons by non-steroidal anti-inflammatory drugs (NSAIDs) and GTPases of the Rho-family"* Supervisor: Prof. Dr. Sascha Weggen
06/01	**Abitur**, Wilhelm-Leuschner-School, Mainz-Kastel
05/99	**High School Diploma**, West Point High School, West Point, MS, USA

8.4 Publications

Leuchtenberger S, Maler J, Czirr E, **Ness J**, Lichtenthaler SF, Esselmann H, Pietrzik CU, Wiltfang J, Weggen S. *Nonsteroidal anti-inflammatory drugs and ectodomain shedding of the amyloid precursor protein*. **Neurodegener Dis**. 2009; 6:1-8.

Hieke M, **Ness J**, Steri R, Dittrich M, Greiner C, Werz O, Baumann K, Schubert-Zsilavecz M, Weggen S, Zettl H. *Design, synthesis, and biological evaluation of a novel class of gamma-secretase modulators with PPARgamma activity.* **J Med Chem**. 2010; 53:4691-700.

Richter L, Munter LM, **Ness J**, Hildebrand PW, Dasari M, Unterreitmeier S, Bulic B, Beyermann M, Gust R, Reif B, Weggen S, Langosch D, Multhaup G. *Amyloid beta 42 peptide (Abeta42)-lowering compounds directly bind to Abeta and interfere with amyloid precursor protein (APP) transmembrane dimerization.* **Proc Natl Acad Sci U S A**. 2010; 107:14597-602.

Hahn S, Brüning T, **Ness J**, Czirr E, Baches S, Gijsen H, Korth C, Pietrzik CU, Bulic B, Weggen S. *Presenilin-1 but not amyloid precursor protein mutations present in mouse models of Alzheimer's disease attenuate the response of cultured cells to γ-secretase modulators regardless of their potency and structure.* **J Neurochem**. 2011; 116:385-95.

Hieke M, **Ness J**, Steri R, Greiner C, Werz O, Schubert-Zsilavecz M, Weggen S, Zettl H. *SAR studies of acidic dual γ-secretase/PPARγ modulators.* **Bioorg Med Chem**. 2011 Aug 6. [Epub ahead of print]

Bulic B, **Ness J**, Hahn S, Rennhack A, Jumpertz T, Weggen S. *Chemical biology, molecular mechanism and clinical perspective of γ-secretase modulators in Alzheimer's disease.* **Current Neuropharmacology**. 2011; 598-622(25).

Jumpertz T, Rennhack A, **Ness J**, Baches S, Sisodia SS, Pietrzik CU, Bulic B, Weggen S. *Presenilin is the molecular target of acidic γ-secretase modulators in living cells.* **PLos ONE** 7(1): e30484; 2012.

Zettl H, **Ness J**, Hähnke V, Beher D, Jumpertz T, Saric A, Baumann KH, Pietrzik CU, Bulic B, Schneider G, Weggen S. *Discovery of γ-Secretase Modulators with a Novel Activity Profile by Text-Based Virtual Screening.* **ACS Cem Biol**. 2012; In press.

8.5 Acknowledgements

I thank Prof. Dr. Sascha Weggen and all current and former members of his lab, especially Sandra Baches, Julia Seegel, Thorsten Jumpertz, Isabella Ogorek, Vanessa Kurth, Tanja Brüning, Eva Czirr, and Stefanie Leuchtenberger, for many years of support and a great working atmosphere! I also want to thank Prof. Dr. Dieter Willbold for agreeing to be the co-referee for my Ph.D. thesis, Dr. Philipp Pfenning and Prof. Dr. Wolfgang Wick for animal experiments, and Dr. Sebastian Barbus and Prof. Dr. Peter Lichter for Glioma Core Collection microarray data. I am grateful for technical support I received from my colleagues at the Institute of Neuropathology and, more than that, for all the good times we shared. Finally, I thank my family and friends, especially Nadine, Julia, Anne, Sabrina, Attila, Sepp, Britta, Thorsten, Irene, Uwe, Natascha, Sandra, and Jochen for carrying me through the hard times and just for being part of my life!

Eidesstattliche Erklärung

Hiermit erkläre ich, die vorliegende Arbeit selbständig und ohne unerlaubte Hilfe angefertigt und alle Hilfsmittel und Inhalte aus anderen Quellen als solche kenntlich gemacht zu haben.

Düsseldorf, 07.05.2012 _____

(Julia Neß)

Aus dem Institut für Neuropathologie
der Heinrich-Heine-Universität Düsseldorf

Gedruckt mit der Genehmigung der
Mathematisch-Naturwissenschaftlichen Fakultät der
Heinrich-Heine-Universität Düsseldorf

Referent: Prof. Dr. Sascha Weggen

Ko-Referent: Prof. Dr. Dieter Willbold

Tag der mündlichen Prüfung: 19. Juni 2012